MASTER THESIS

LOG-FACIES AND LOG-CORRELATION OF CENOMANIAN SEDIMENTS IN THE MOLASSE BASIN (UPPER AUSTRIA)

LEOBEN, 2011

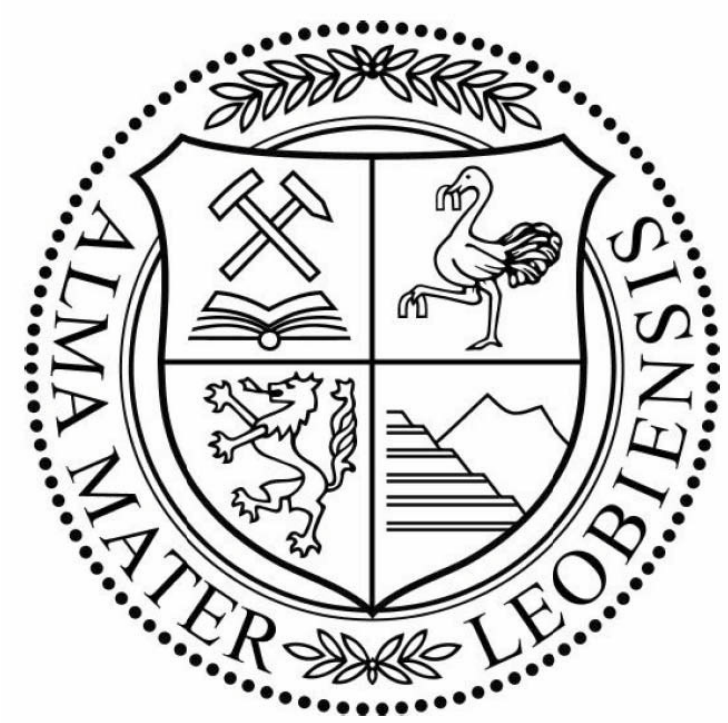

Author:

Arno Rech, BSc

Advisor of the chair of Petroleum Geology

Univ.-Prof. Mag. rer. nat. Dr. mont. Reinhard F. Sachsenhofer

I declare in lieu of oath, that I wrote this thesis and performed the associated research myself, using only literature cited in this volume.

Leoben, October 2011

Arno Rech

Acknowledgements

First of all I thank my supervisor Professor Sachsenhofer for the support, his helpful constructive remarks and critical review of the thesis.

I am grateful to Rohöl-Aufsuchungs AG (RAG) for kindly providing relevant well log data, reports and support on related questions.

I also want to thank all colleagues of the Chair for Petroleum Geology for their support and encouragement.

I extend my thanks to the members of the Chair for Applied Geophysics for providing the Software Interactive Petrophysics.

In addition I thank the team of Joanneum Research for technical questions referring to the handling of the software Interactive Petrophysics.

Special thanks are given to my family and friends for their outstanding support and patience.

List of contents

Abbreviations

Abstract

Kurzfassung

1 INTRODUCTION 7

1.1 SCOPE AND OBJECTIVE 7

1.2 STUDY AREA 8

1.3 GEOLOGICAL SETTING 9

1.3.1 Tectonic Evolution 10

1.3.2 Stratigraphic elements 14

2 DATA 21

2.1 WELL LOGS 23

2.1.1 GR Log 24

2.1.2 DT Log 25

2.1.3 Resistivity Logs 26

2.2 CORE REPORTS 29

2.3 GEOLOGICAL SHORT PROFILES 30

3 METHODS 31

3.1 ADJUSTMENT OF LOG DEPTHS 31

3.2 CORE GAMMA RAY MEASUREMENTS 31

3.3 CORE GAMMA RAY DEPTH SHIFT AND RESCALE 33

4 RESULTS AND INTERPRETATION 35

4.1 CORE GAMMA RAY AND SPECTRAL CORE GAMMA RAY 35

4.2 WELL LOG CORRELATION PROFILES 83

4.3 FACIES GROUPS OF THE STUDY AREA 97

4.4 THICKNESS MAPS 106

5 CONCLUSION 109

6 REFERENCES 111
6.1 LIST OF REFERENCES 111
6.2 LIST OF FIGURES 116
6.3 LIST OF TABLES 119

Abbreviations

API	American Petroleum Institute
CE	Cenomanian
CC	Correlative Conformity
CGR	Core Gamma Ray
CPS	Counts per second
EO	Eocene
IAEA	International Atomic Energy Agency
JU	Jurassic
K	Potassium
LLS	Latero Log Shallow
MD	Measured Depth
MFS	Maximum flooding surface
MINV	Microinverse Log
MLL	Microlatero Log
MSFL	Microspherically Focused Log
DT	Sonic Log
GR	Gamma Ray
ILD	Induction Log Deep
OMV	Österreichische Mineralölverwaltungs Aktiengesellschaft
PCE	Pre-Cenomanian
RAG	Rohöl-Aufsuchungs Aktiengesellschaft

ROI	Region of Interest
R_t	Resistivity of the uninvaded zone (true resistivity)
R_{xo}	Resistivity of the invaded zone (resistivity of the flushed zone)
SB	Sequence Boundary
SGR	Spectral Gamma Ray
SCGR	Spectral Core Gamma Ray
Th	Thorium
TU	Turonian
U	Uranium
Δt	slowness (reciprocal of the transit time)

Abstract

The Cenomanian in the Upper Austrian part of the Molasse Basin is an important clastic reservoir horizon for oil. In the present thesis this formation is characterized on the basis of geophysical well logs. For this purpose log facies and well log correlation profiles have been interpreted.

The thesis mainly concentrates on well log data for 58 wells kindly provided by Rohöl-Aufsuchungs AG. In addition, spectral core gamma measurements have been performed using cores representing Cenomanian units from 30 wells.

In a first step, base and top of the Cenomanian sandstones ("Regensburg Formation sensu Niebuhr et al., 2009) as, well as a maximum flooding surface within overlying Upper Cenomanian to Turonian marls (Eibrunn Formation sensu Niebuhr et al., 2009) have been defined and laterally correlated. Considerably varying log patterns of the Cenomian sandstones from west to east indicate lateral facies changes.

Based on the detailed correlation between well gamma log and core gamma data, cores together with measured total and spectral core gamma logs were exactly depth shifted. Thus, changes in lithology observed in the cores could be directly related to their well log response. This allows an interpretation of lithology and subunits in boreholes where log data, but no cores are available.

The Cenomanian of the Upper Austrian Molasse Basin overlies different geological units. In the easternmost area the Cenomanian sediments overlie crystalline basement units of the Bohemian Massif, whereas in the western area they overlie Upper Jurassic carbonates. Locally terrestrial sediments, partly representing karst deposits (Schutzfels Formation), are intercalated between the Jurassic carbonates and the Cenomanian sandstones.

Correlation panels and thickness maps demonstrate a basinward (SW-ward) increase in thickness of the oldest Cenomanian units ("Saal Member" sensu Niebuhr et al., 2009). Within the study area the thickness of the Saal Member ranges generally between 10 and 30 m. Within the Saal Member the gamma log is a poor tool for the estimation of shale contents. This is because the gamma response is

strongly influenced by varying glauconite contents of the near shoreline marine sandstones. Moreover detailed investigations of spectral gamma logs suggest that the total gamma values are often dominated by increased thorium and uranium contents. On the basis of sonic and resistivity logs the Saal Member correlates with the informal units CE3 and CE2 of Rohöl-Aufsuchungs AG, at least in the Trattnach and Voitsdorf fields.

The Saal Member is overlain by lower energetic sandy-silty, often carbonate cemented sandstones (Bad Abbach Member sensu Niebuhr et al., 2009). Its base is defined by a characteristic marker bed in the area of the Trattnach Field. So far it has also been called “red layer”, due to colorful red shaded gravels. The exact correlation of core and well gamma logs shows that the red layer may be part of the marker bed, but does not necessarily define it. The Bad Abbach Member is characterized by high sonic velocity, high resistivity and in most wells by gamma log values, which are significantly lower than those from the Saal Member. The thickness of the Bad Abbach Member reaches a maximum (12-15 m) along a SE-NW trending zone and decreases towards the basin (SW-ward) and towards the paleo-shore line (NE-ward).

The overlying Eibrunn Formation represents the uppermost Cenomanian to Lower Turonian units and comprises a maximum flooding surface. It is located 4 to 15 m above the Cenomanian sandstones of the Regensburg Formation. The sediment package between Top Regensburg Formation and maximum flooding surface shows, for the most parts of the study area, a remarkable increase in thickness from SW to NE.

Kurzfassung

Das Cenoman im oberösterreichischen Teil des Molassebeckens ist ein wichtiger klastischer Speicherhorizont für Erdöl. In der vorliegenden Diplomarbeit wird dieser Horizont anhand von Bohrlochmessdaten charakterisiert. Dazu wurde die Logfazies bestimmt und Log–Korrelationsprofile erstellt.

Die Arbeit basiert im Wesentlichen auf digitalen Bohrlochmessdaten von 58 Bohrungen der Rohöl-Aufsuchungs AG. Diese wurden im Rahmen der Arbeit mit totalen und spektralen Kern Gamma Messungen an 30 Bohrungen ergänzt.

In einem ersten Schritt wurden Basis und Top des Cenoman-Sandsteins (Regensburg-Formation sensu Niebuhr et al., 2009), sowie eine „Maximum Flooding Surface“ in den überlagernden cenomanen bis turonen Tonsteinen (Eibrunn-Formation sensu Niebuhr et al., 2009) definiert und lateral für sämtliche Bohrungen korreliert.

Als Folge von Faziesänderungen, variiert die Signatur der Bohrlochmessdaten in Ost-West-Richtung erheblich. Durch die detaillierte Korrelation von Bohrungs und Kern Gamma Messungen konnten die Bohrkerne und deren gemessene spektralen Gamma Logs exakt tiefenverschoben werden. Damit können Kernaufnahmen direkt mit den Bohrlochlogs verknüpft werden und in Folge Formationswechsel und Subeinheiten auch anhand der Bohrlochlogs alleine interpretiert werden.

Das Cenoman überlagert unterschiedliche Gesteinseinheiten. Im Osten lagert es kristallinen Einheiten der Böhmischen Masse auf, im Westen hingegen oberjurassischen Karbonaten. Lokal schalten sich zwischen die Jurakalke und die cenomanen Sandsteine terrestrische Sedimente ein, die mitunter als Karstfüllungen vorliegen (Schutzfels-Formation).

Korrelationsprofile und Mächtigkeitskarten verdeutlichen eine beckenwärtige Mächtigkeitszunahme der ältesten Cenomanen Einheiten („Saal-Member“ sensu Niebuhr et al., 2009) Richtung SW von ca. 10 m auf ca. 30 Meter. Das Gamma Log erweist sich als ungeeigneter Korngrößenanzeiger, da es zum einen durch den

variierenden Glaukonitgehalt der küstennahen Sandsteine beeinflusst und zum anderen von erhöht auftretendem Thorium und Uran dominiert wird. Anhand des Sonic und Widerstand Logs ist die Korrelation des Saal Members mit den informellen Einheiten CE3 und CE2 der Rohöl-Aufsuchungs AG zumindest im Bereich des Trattnach und Voitsdorf Feldes wahrscheinlich.

Das Saal Member wird von niedriger-energetischen sandig bis siltigen, häufig karbonatisch zementierten Sandsteinen überlagert (Bad Abbach-Member sensu Niebuhr et al., 2009). Deren Basis wird im Bereich Trattnach durch ein charakteristisches „Marker Bed“ definiert. Dieses ist zumindest im Bereich Trattnach eindeutig im Sonic und Widerstand Log identifizierbar. Bislang wurde es aufgrund seiner charakteristischen bunten Kiese als „Rote Lage“ bezeichnet. Durch die exakte Korrelation des gemessenen Kern Gamma Logs zum Bohrungs Gamma Log wird deutlich, dass die „Rote Lage“ Teil des „Marker Bed“ sein kann, diese allerdings nicht zwingend definiert. Das Bad Abbach-Member ist durch hohe Geschwindigkeiten, hohen Widerstand und meist niedere Gamma Werte charakterisiert. Die Mächtigkeit des Bad Abbach-Members erreicht entlang eines SE – NW streichenden Streifens ein Maximum (12 – 15 m) und nimmt sowohl beckenwärts (SW) als auch küstenwärts (NE) ab. Im Unterschied zum Saal Member weist das Bad Abbach-Member sowohl im totalem als auch im spektralen Gamma Log relativ niedrige Werte auf.

Die überlagernde Eibrunn Formation repräsentiert die jüngsten cenomanen bis unterturonen Einheiten und beinhaltet eine gut korrelierbare „Maximum Flooding Surface“. Diese befindet sich 4 bis 15 m über dem Top der cenomanen Sandsteine (Top Regensburg-Formation). Die Mächtigkeit des Sedimentpaketes zwischen dem Top der cenomanen Sandsteine und der „Maximum Flooding Surface“ zeigt im Großteil des Untersuchungsgebietes einen bemerkenswerten Anstieg von SW nach NE.

1 Introduction

1.1 Scope and Objective

Cenomanian sediments in the Upper Austrian Molasse Basin form an important reservoir horizon for oil. The main objective of the present thesis is to investigate the log facies of key reservoir members and to study their lateral distribution.

The study area is located in Upper Austria and covers an area of approximately 4000 km^2. The thesis is based on well log data from 58 wells kindly provided by Rohöl–Aufsuchungs AG (RAG). In addition core reports and geological short profiles complete the framework. The geological evolution of the area has been summarized by Nachtmann & Wagner (1987).

Well logs and well log correlation profiles illustrate how the Boundaries between different stratigraphic units and facies successions change vertically and laterally.

The thesis also comprises the results of spectral core gamma measurements of cores from 30 wells, which were obtained within the frame of the present study. These data were used together with gamma ray (GR) logs to determine the exact (log-) depth of the cores.

Incorporating these investigations helped to clarify uncertainties referring to formation top and base. Furthermore new spectral gamma data helped for a better understanding and characterization of the Upper Cretaceous in Upper Austria.

Based on the established well log correlation profiles new thickness maps of the main reservoir members were constructed and interpreted.

1.2 Study area

The study area (Figure 1) is located in the Upper Austria Austrian part of the Molasse Basin, the northern Alpine Foreland Basin. It covers an area of approximately 4000 km^2 (between -28000 and 76000, 5316000 and 5352000 UTM coordinates). 58 wells that penetrated the Cenomanian in the Upper Austrian Molasse Basin were provided by RAG and integrated in this study.

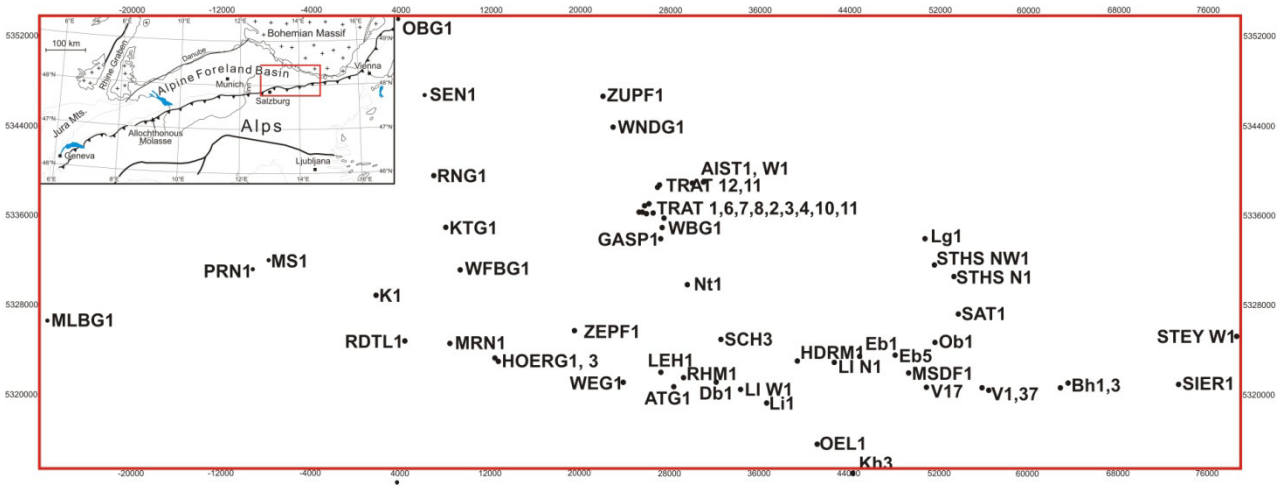

Figure 1: Geographic overview of the study area indicating position of the investigated wells.

1.3 Geological Setting

The Upper Austrian Molasse Basin (Figure 2) is an east–west trending foreland basin, which resulted from the subduction of the southern margin of the European plate beneath the Adriatic plate (Ziegler, 1987).The asymmetrical foredeep in Austria is bordered in the north by the crystalline basement of the Bohemian Massif and in the south by the main overthrust of the Alpine orogenic front (Figure 2).

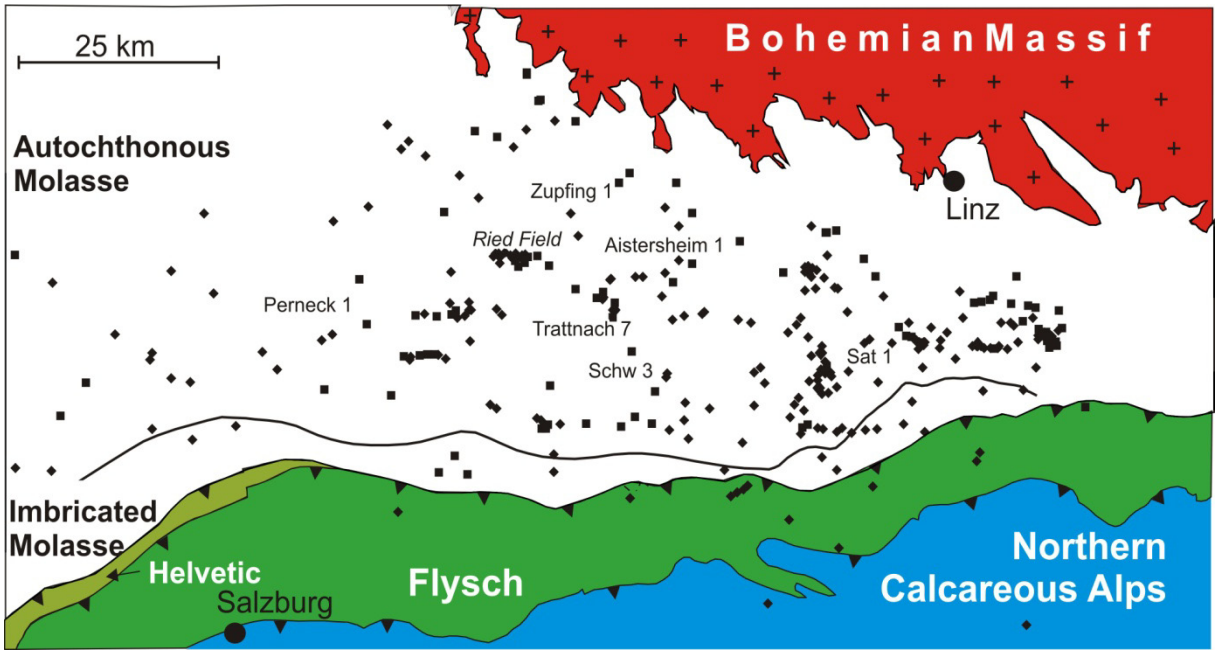

Figure 2: Geologic map of the Molasse Basin in upper Austria indicating well positions (black squares) (modified after Sachsenhofer et al., 2010).

The northern foreland basin of the Alps extends from French Savoie (Haute-Savoie) in the west, Switzerland, southern Germany (Bavaria) to Lower Austria in the east (Sissingh, 1997). The Austrian part of the Molasse Basin shows strong lateral changes in shape with a decrease in width from approximately 150 km in the German Molasse Basin to less than 10 km at the spur of the Bohemian Massif (Genser, 2007). The principal features of the foreland basin in Austria are generally well known due to the exploration and production activities of the Austrian oil companies RAG and OMV. The thesis concentrates on Cenomanian facies well log patterns and their lateral distribution in the Upper Austrian Molasse Basin, thus especially the Mesozoic geologic and tectonic evolution is highlighted.

1.3.1 Tectonic Evolution

The Molasse Basin and its substratum passed through four major evolutionary stages. According to Veron (2005) basin evolution can be divided into a Permo-Carboniferous syn-rift, a Mesozoic epicontinental and passive margin and a Cenozoic foredeep stage.

In Permo-Carboniferous times (syn-rift phase) troughs were formed along ENE-WSW and WNW-ESE trends of the Variscian wrench faults. From that time on marine development started to progress. Epicontinental deposits of Triassic – middle Jurassic age almost completely overlie the crystalline basement (Veron, 2005). The passive margin stage was accompanied by transpressional and transtensional movements in middle Jurassic to early Cretaceous time (Nachtmann & Wagner, 1987). The shift from the epicontinental to the passive margin setting is correlated with Jurassic extensional events (Roeder & Bachmann, 1996), obviously falling into the period of middle Jurassic crustal separation in the western Tethys (Ziegler, 1990). From that time on subsidence rates increased and clastic sedimentation was replaced by the deposition of a massif Upper Jurassic carbonate platform. Sea-floor spreading in the central Atlantic in the Late Jurassic established sinistral translation between Africa and Europe forming consequently the opening of the Alboran-Ligurian-Penninic Ocean (Ziegler, 1987).

The Early Cretaceous was marked by transpressional wrench deformation and differential uplift of individual fault blocks, which consequently induced erosion and karstification of Jurassic carbonates (Bachmann et al., 1987). Starting with a first tectonic event in Berriasian to Hauterivian, a second followed in Aptian time. These deformation events are correlated to rift and wrench tectonics in NW-Europe as a consequence of crustal extension in the N-Atlantic and Norwegian-Greenland sea areas (Nachtmann & Wagner, 1987). Due to the opening of the Atlantic-Indian Ocean, Africa drifted northwards causing progressive subduction of the South Penninic-Piedmont Ocean (Ziegler, 1987). After the closure of the Penninic Ocean between Albian and Turonian times, the Alpine subduction unit started to collide with the passive margin of the European craton (Ziegler, 1987).

The Late Cretaceous to Paleogene tectonic evolution of the Molasse basin was primarily dominated by strike–slip movements along NW-SE trending faults. It is

characterized by the deposition of shallow marine sands and shales. Glauconitic marine sandstones transgressed in the Cenomanian from south and west to north and east initiating the development of the Upper Austrian Cretaceous Basin.

During Turonian to Early Senonian time the orogenic front reached the passive margin of the Helvetic shelf of the Eastern Alps and the Carpathians. This caused (1) reactivation of intra-plate discontinuities in the Alpine Foreland, (2) reactivation of Permo-Carboniferous fracture zones, which transsected the Bohemian Massif, and (3) the uplift of major basement blocks along wrench and steep reverse faults.

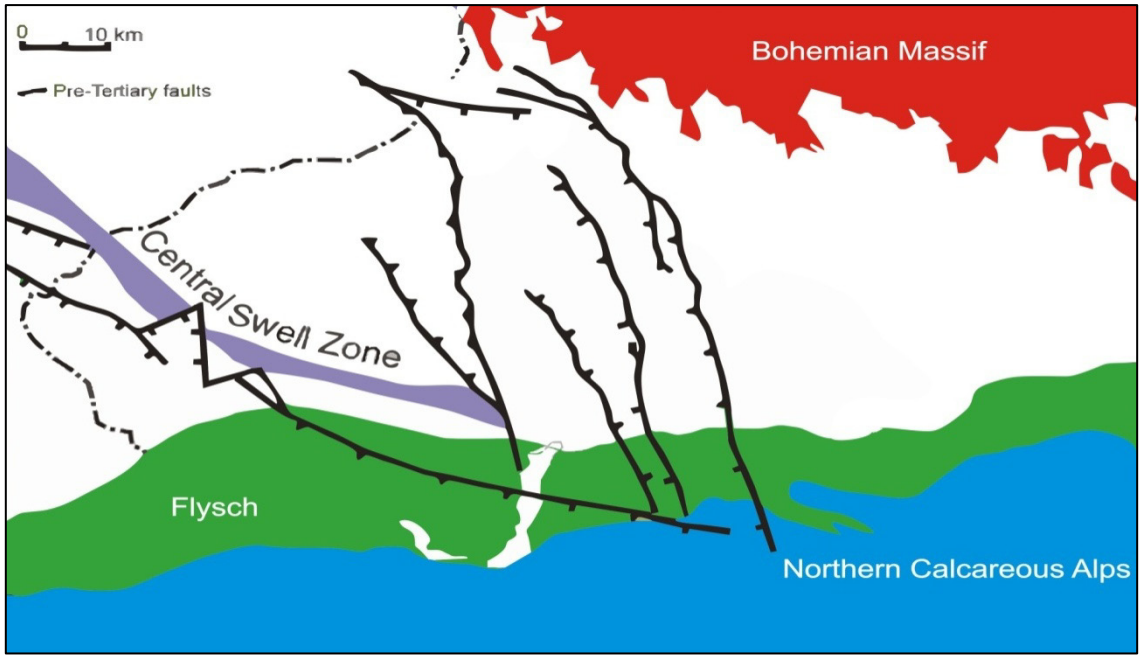

Figure 3: Geologic map of the Molasse Basin in Upper Austria indicating pre-Tertiary faults and the Central Swell Zone (modified after Nachtmann & Wagner, 1987)

The faults bordering the Central Swell Zone (Figure 3) became reactivated. The Central Swell Zone sharply uplifted with erosion cutting down through its Cretaceous and locally even its Jurassic cover into the basement (Nachtmann & Wagner, 1987). According to Ziegler et al. (1995) Late Cretaceous and Early Paleocene processes result from the collision of the Alpine-Carpathian orogen with Europe's southern margin. In contrast, recent investigations by Kley and Voigt (2008) relate Late Cretaceous deformation with the onset of Africa-Iberia-Europe convergence. Similarly mechanical coupling of the Alps and Europe was largely accomplished during the Cenozoic era. A schematic sketch illustrating major tectonic events during Late

Mesozoic and Cenozoic time for Central Europe, the Pyrenees and the Alps after Kley and Voigt (2008) is shown in Figure 4.

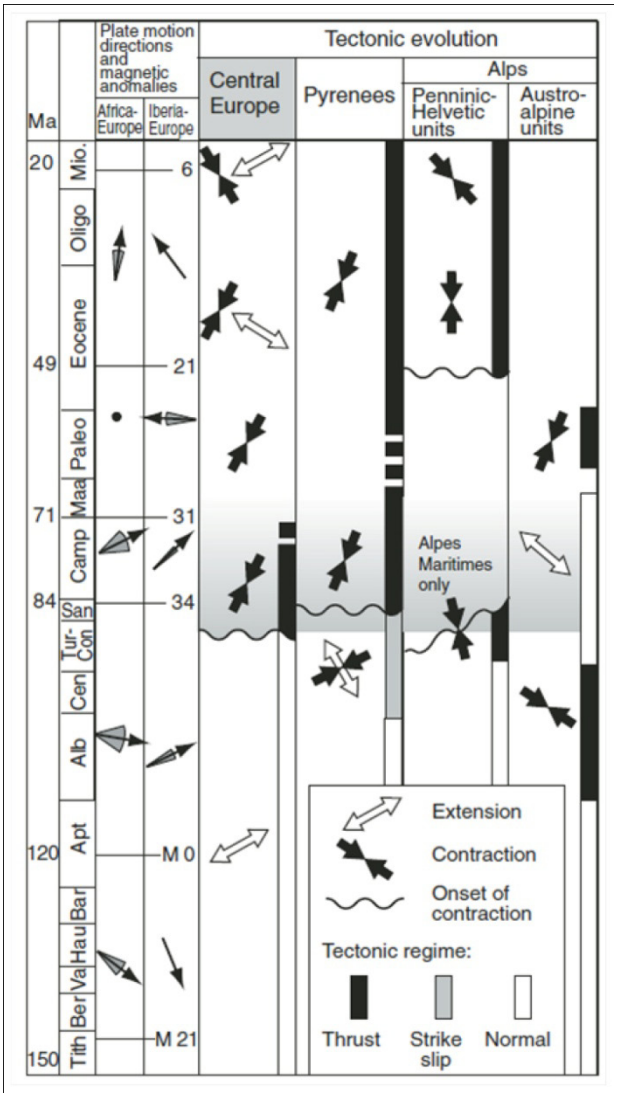

Figure 4: Kinematic evolution in central Europe from Upper Cretaceous to Neogene times (after Kley & Voigt, 2008).

In the late Eocene and early Oligocene thrust loading by the advancing Alpine nappes caused flexural downbending of the European margin, resulting in a deepening of the Molasse Basin. Consequently a dense network of synthetic and antithetic normal faults was formed and older fault systems reactivated (Andeweg & Cloetingh, 1998).

The Molasse Basin is mainly filled with clastic sediments of Oligocene – Miocene age, with thicknesses up to 4500 m (De Ruig, 2003). The basin was formed due to the collision between the Apulian continental microplate and the North European

Craton (Ziegler, 1990; Sissingh, 1997). Clastic sediments derived from the rising Alps started to fill the deep-marine sediment-starved Molasse Basin from the Mid-Oligocene onwards (De Ruig 2003). Sediments were mainly derived from the south, during Miocene times onward, onlapping progressively to northwest. During Eggenburgian to Ottnangian times rapid tectonic subsidence started in the E-part of the Austrian Molasse Basin accompanied by increasing sediment accumulation rates (Genser et al. 2007).

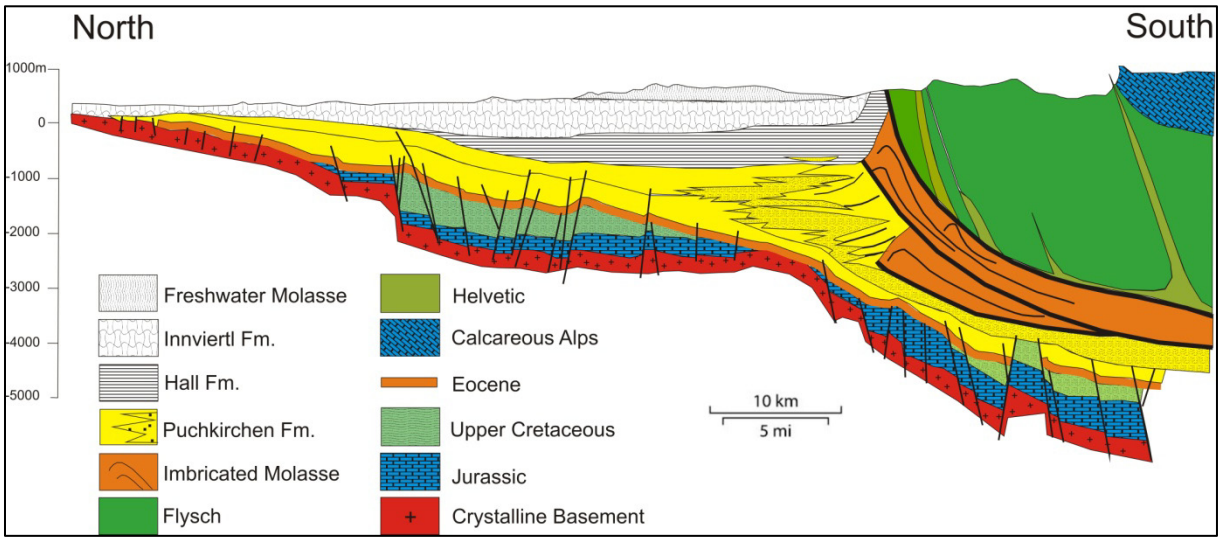

Figure 5: Geological cross-section indicating tectonic elements through the Austrian Molasse Basin (modified after Wagner 1996, De Ruig, 2006).

After initially deep marine sedimentation, clastic detritus from the rising Alps started to fill the Molasse Basin from mid Oligocene time onwards (Wagner, 1996). The deep marine trough relates to the Puchkirchen Basin, characterized by thick successions of gravity flow deposits, including the Oligocene – Early Miocene Puchkirchen Formation (Figure 5) and the basal parts of the Miocene Hall Formation (De Ruig, 2003).

Two geologically and geomorphologically differing units can be distinguished in the Molasse Basin (Figure 5): the mainly undeformed part (autochthonous), including more than ninty percent of the basin and the deformed part, the folded and thrusted imbricated (allochthonous) Molasse, that forms the southernmost parts of the basin area. In the studied Upper Austria area of the basin the imbricated Molasse is overridden by the Alpine thrusts (Flysch, Helvetic, Calcareous Alps).

1.3.2 Stratigraphic elements

Crystalline basement

The Bohemian Massif (Figure 6) is transected by a system of conjugate NW-SE and NE-SW trending faults (Wagner, 1996). The shear zones of the southern Bohemian Massif are interpreted as strike-slip zones, which have their origin in the crust below the brittle-ductile transition zone (Wallbrecher et al., 1996). The crystalline basement of the Bohemian Massif in Austria consists of medium to high grade metamorphic Precambrian to Palaeozoic rocks and Variscian granitic plutonites (Fuchs & Matura, 1980). It forms the northern border of the Molasse Basin (Figure 2) and has also been encountered by numerous wells beneath the Molasse sediments.

Paleozoic deposits

Permo-Carboniferous sediments formed along major Variscian NW-SE trending faults (Ziegler, 1990; Wagner, 1998). These sediments are exposed at the surface in Bavaria. In Upper Austria, Upper Paleozoic sediments are limited to graben structures along the south-western margin of the Central Swell Zone.

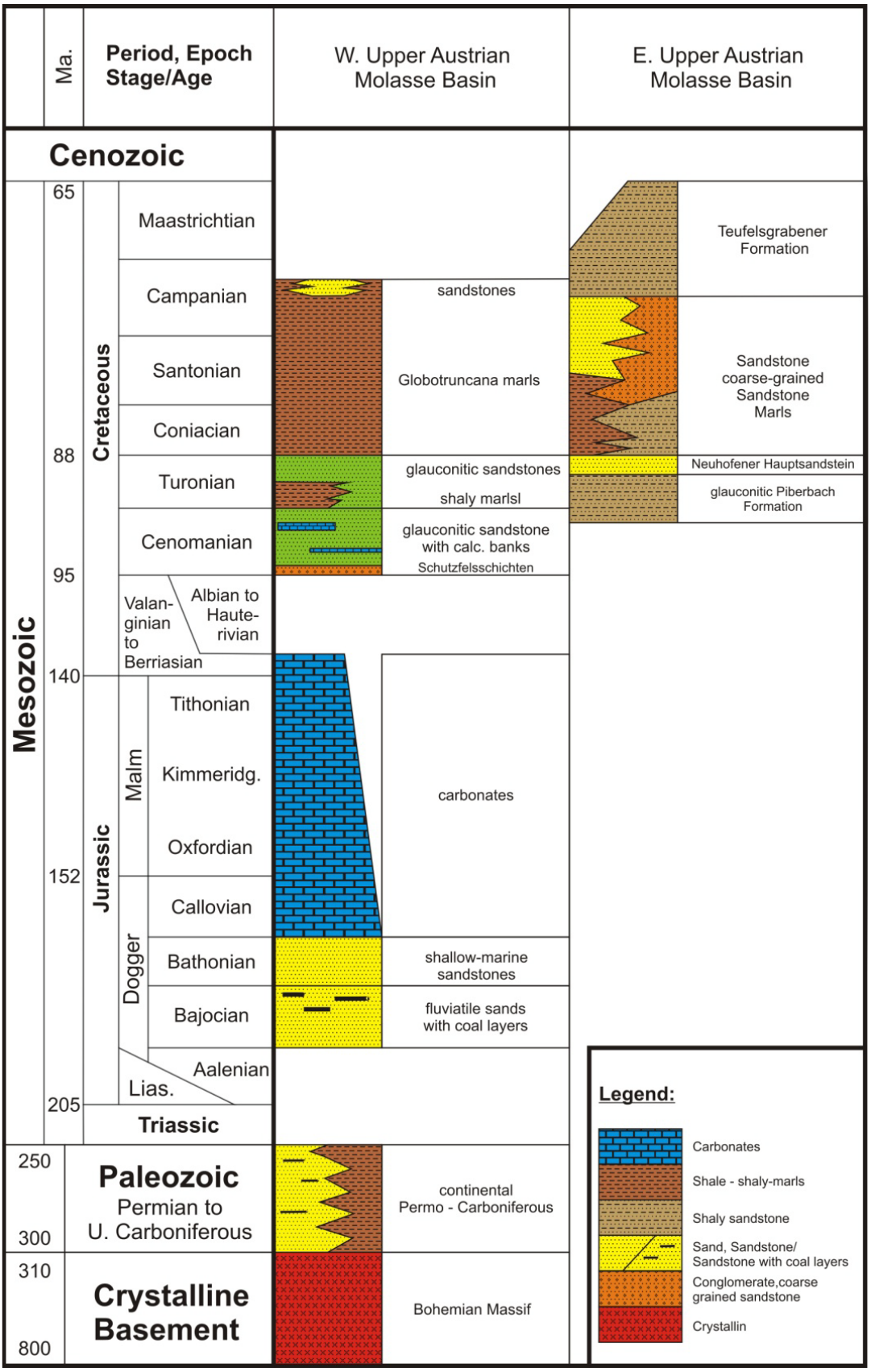

Figure 6: Schematic stratigraphic column illustrating the Mesozoic and Paleozoic sedimentary record of the western and eastern Upper Austrian Molasse Basin (modified after Malzer, 1993).

Mesozoic deposits

The oldest Mesozoic sediments in the Upper Austrian Molasse Basin are of Middle Jurassic (Doggerian) age (Figure 6) (Wagner, 1998).

Jurassic deposits

The Jurassic sedimentary record in the Upper Austrian part of the Molasse Basin is divided into three different facies zones: the facies north and south of the Central Swell Zone and the facies below the thrust sheets of the Imbricated Molasse (Wagner, 1996).

The Middle Jurassic (Figure 6) consists mainly of fluvial to shallow marine sandstones, containing local coal seams. From Callovian to Malmian times and into Early Cretaceous time, carbonates were produced on the tropical shelf along the Bohemian landmass. The Upper Jurassic facies indicates a progressive shallowing from the southwest below the thrust sheets to the Bohemian Massif. The carbonates start with dark brown arenaceous nodular micrites containing lumachelles, ammonites, belemnites and sponge spicules with abundant chert nodules. They grade upwards into biostromal limestones. Oxfordian and Kimmeridgian algal and sponge banks are capped by coral reefs and their debris, surrounded by the high energy environment with oolites and grainstones (Wagner, 1998).

Cretaceous deposits

The unconformity separating Jurassic carbonates from the overlying Upper Cretaceous deposits, reflects the Early Cretaceous phase of basin inversion. This tectonic deformation event accompanied uplift along a system of NW-SE striking wrench and reverse faults causing erosion of rocks up to 600 m thick (Nachtmann & Wagner, 1987).

The oldest Cretaceous sediments are locally developed and consist of light grey, white, red or green non-fossiliferous, coarse grained fluvial sands. These beds relate to the Schutzfels Formation and fill the Jurassic karst relief to depths up to 100 m below the Jurassic surface (Wagner, 1998). The Schutzfels Formation represents terrestrial sediments and its deposition took place in a peri-continental setting (Figure 8) at the northern margin of the Neotethys (Wilmsen et al., 2010).

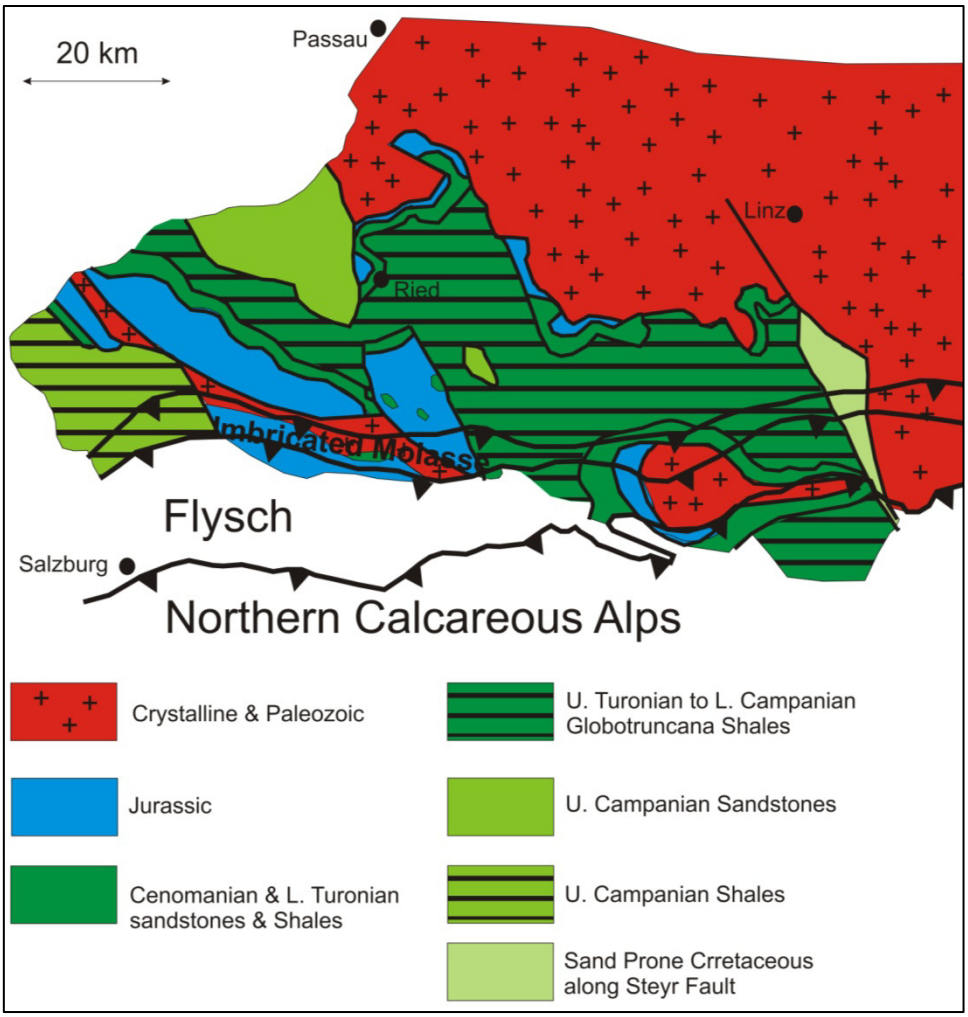

Figure 7: Pre-Cenozoic subcrop map in the Alpine Foredeep (modified after Wagner, 1998).

Marine conditions commenced in the Early Cenomanian and persist until the Coniacian (Wilmsen et al., 2010). Marine units include transgressive glauconitic sandstones corresponding to the Regensburg Formation. The Regensburg Formation overlies various older rock units; in the western part of the study area mainly Upper Jurassic carbonates or the terrestrial Schutzfels Formation, and in the eastern part the substrate is formed by the Variscian basement of the Bohemian Massif. The Regensburg Formation is characterized by strong terrigenous input containing mixed glauconitic-bioclastic sediments. It can be subdivided into a Lower Saal Member comprising thickly bedded glauconitic sandstones and an Upper Bad Abbach Member intercalated with sandy-silty marls and siliceous limestones (Wilmsen et al., 2010).

The Cenomanian sandstones in the Upper Austrian Molasse basin reach a thickness of up to 60 m and consist of fine to coarse grained sandstones. The sandstones are

often intensively bioturbated representing fine weather conditions (Nachtmann, 1995). The shallow marine glauconitic sandstones were deposited on a broad shelf, below the normal wave base (Wagner, 1998). The Cenomanian sandstones of the Regensburg Formation are conformably overlain by Turonian shaly marlstones termed Eibrunn Formation (Wilmsen et al., 2010), containing glauconitic storm-deposits in the upper parts. The complete succession documents a trans- / regressive megacycle with a maximum flooding interval during the late Middle to early Late Turonian (Wilmsen et al., 2010). The top of the Cretaceous succession in the Upper Austrian Molasse Basin is formed by a regional unconformity called “base Eocene unconformity” (Figure 7).

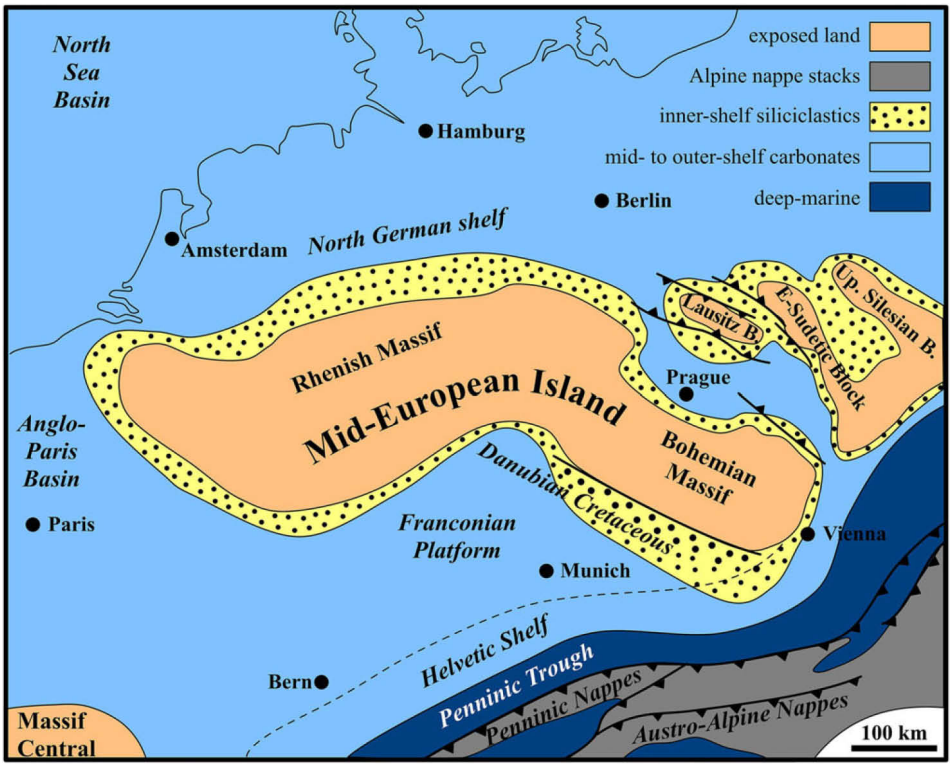

Figure 8: Paleogeography of the Cenomanian - Turonian in Central Europe (after Ziegler, 1990) with indication of the depositional area.

Cenozoic deposits

In the Eocene the Molasse stage started with the deposition of fluvial and shallow marine sandstones, shales and carbonates (Figure 9). Rapid erosion of the structural relief formed by the latest Cretaceous to Paleocene inversion movements led to the progression of the Tethys Sea during the Eocene. Tectonic loading of the European

foreland crust by the advancing nappe systems caused the subsidence of the Alpine foredeep (Nachtmann & Wagner, 1987). With a gradually rising sea level, sands were covered by the Upper Eocene Lithothamnium Limestone.

During the latest Eocene and Early Oligocene the basin deepened rapidly. Consequently the Lithothamnium carbonate platform became drowned and covered by organic matter-rich Lower Oligocene “fish shale” (Schöneck Formation), an important source rock for oil generation (Bachmann et al., 1987; Schulz et al., 2002). The Schöneck Formation has mainly been deposited on the northern paleo-slope of the Molasse Basin and is up to 30 m thick (Wagner, 1996). At the same time Globigerina marls was deposited in the south. The Schöneck Formation is overlain by the Dynow Formation, which corresponds to a pure nanofossil chalk, deposited in a basin with reduced salinity (Schulz et al., 2004).

The Dynow Formation grades upwards into the Eggerding Formation, which comprises dark grey laminated pelites with thin white layers of nannoplankton. According to Sachsenhofer et al. (2010) it was deposited under outer slope conditions. The Eggerding Formation is overlain by the Zupfing Formation consisting of distal turbidites and hemipelagites (Wagner, 1998)

The overlying sandstones of Rupelian age consist of fine to medium grained sandstones intercalated by mudstones and refer to the start of coarse clastic sedimentation in the deep-marine basin. The complete succession of gravity flow deposits includes the Lower Puchkirchen Formation, the Upper Puchkirchen Formation and basal parts of the Hall Formation. The Puchkirchen depositional system is interpreted as W-E trending deep water channel belt indicating a variety of gravity flow processes, slurry flows, submarine slides and slumps (De Ruig & Hubbard, 2006).

An unconformity separates the Puchkirchen Formation from the overlying Hall Formation. The depositional system of the basal Hall Formation is characterized by deep water deposits containing NW prograding muddy prodelta sediments (De Ruig, 2003).

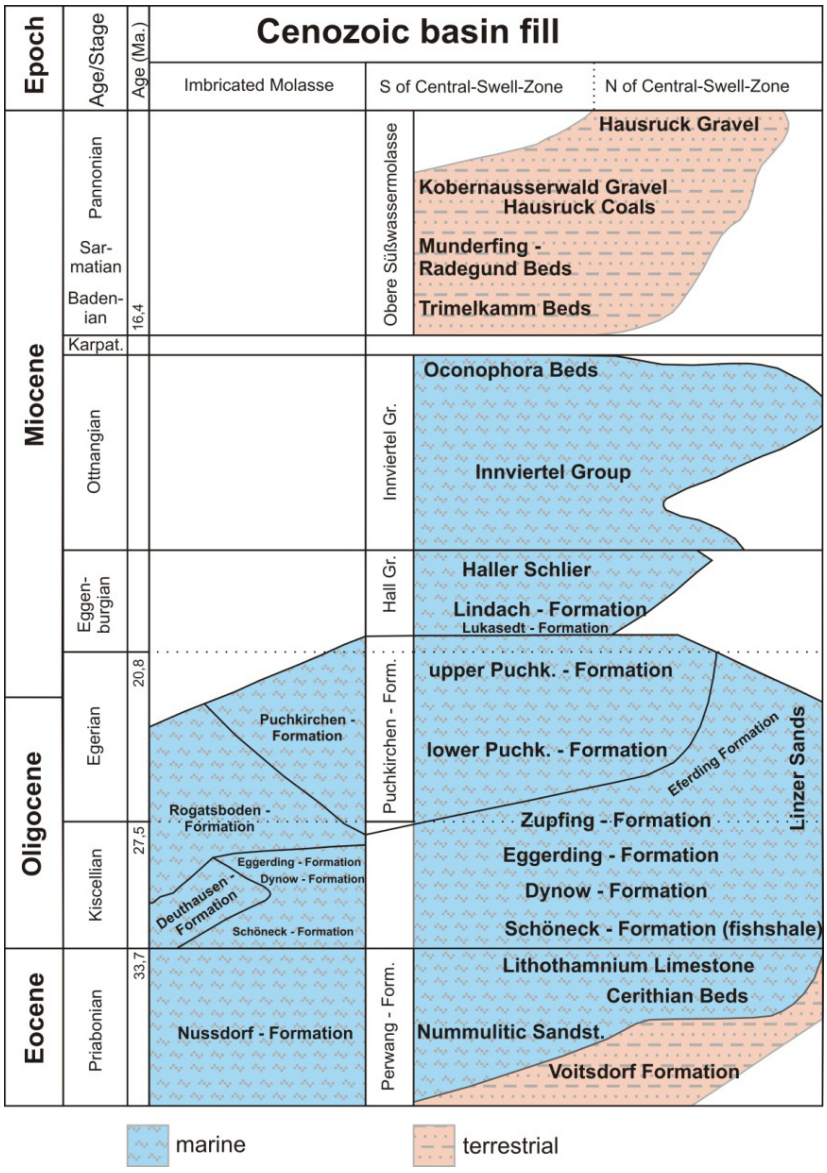

Figure 9: Stratigraphy of the Cenozoic sedimentary record in the Upper Austrian Molasse (modified after Wagner, 1998).

2 Data

A large suite of well logs was provided for 58 wells in the Upper Cretaceous succession of the Upper Austrian Molasse Basin. These wells also include some prominent oil (and gas) fields such as Trattnach, Voitsdorf or Sattledt. The standard log suite, available for all wells, includes a gamma ray log, sonic log, microlatero log and / or microinverse log. For some wells, porosity logs (neutron, density or sonic) were additionally provided. Both composite logs and traces of individual logging runs were provided. A summary of the availability of the most important well logs for correlation and interpretation is given in Table 1.

Core data (porosity, permeability, density) were available for wells Trattnach 1, 6, 7, 8 and 12. Core reports were provided for most wells (except Aistersheim 1 and Aistersheim W1). Additionally, geological short profiles have been obtained for some of the wells.

The quality of the log data is generally good and provides an excellent basis for the determination of well log correlation profiles and geological interpretation. Unfortunately for some of the well logs only short sections (apparently the Cenomanian) have been provided. Especially for well log correlation it is essential that the well log trace spans over several identifiable formations or zones in order to prevent misinterpretations. Well logs were obtained as LAS and ASCII files, which facilitates interpretation with commercial software, such as Petrel or Interactive Petrophysics and contains important information about the well, the log and the logging operation itself.

Table 1: List of the most important well logs available for the study area. Stated depths refer to measured depth in meters. Boxes marked with x document, that the log trace is not limited to the Upper Cretaceous.

Well	DT	GR	MLL	MINV	MNOR	(M)SFL
Aistersheim1	x	x	x	x	x	
Aistersheim W1	x	x	x	x	x	x
Attnang1	x	x				x
Bad Hall1		2199-2228		2199-2233	2199-2233	
Bad Hall3	x	x		x	x	
Desselbrunn1	-2873	-2873	-2873	-2873	-2873	
Eberstalzell1	x			x	x	
Eberstalzell5	2143-2177	2143-2158				
Gaspoldshofen1	x	-1780	x	x	x	
Haidermoos1	x	x				
Hoergersteig1		2517-2550				
Hoergersteig3	2222-2250	2222-2250	2222-2250	2222-2250	2222-2250	
Kemating1	x	x				x
Kirchham3	2960-3001	2960-3001		2960-3001	2960-3001	2960-3001
Kohleck1	x			x	x	
Lehen1	x	x		x	x	
Lichtenegg2	1303-1325	1303-1325		1303-1325	1303-1325	1303-1325
Lindach1	-2890			-2890	-2890	
Lindach N1	-2411	-2411	-2411	-2411	-2411	
Lindach W1	-2870	-2870		-2870	-2870	-2870
Maria Schmolln1	-2261		-2261	-2261	-2261	
Mauern1	x	x		x	x	
Mayersdorf1	x	2210-2258	2210-2258	2210-2258	2210-2258	2210-2258
Muehlberg1	-2964	-2999		x	x	x
Nieder-Thalheim1	x			x	x	
Oberaustall1	1940-1976	1940-1976	1940-1976	1940-1976	1940-1976	
Obernberg1	-1676		x	x	x	
Oelling1	2978-2303	2978-2303		2978-2303	2978-2303	2978-2303
Perneck1	2331-2349!			x	x	
Redlham1	x	x	x	x	x	x
Redltal1		x	x	x	x	
Renging1	-2427	-2427		-2427	-2427	-2427
Sattledt1	1792-1821	1792-1821	1792-1821	1792-1821	1792-1821	
Schwanenstadt3	2310-2344	2310-2344		2310-2344	2310-2344	
Senftenbach1	-1984	-1984	-1984	-1984	-1984	
Sierning1	x					
Steinhaus N1	1546-1562	1546-1562				1546-1562
Steinhaus NW1	1540-1558	1540-1558		1540-1558	1540-1558	1540-1558
Steyr West1	x	x				x
Trattnach1		x	x	x	x	
Trattnach10	x	-1608	-1608	-1608	-1608	-1608
Trattnach11	x	x		x	x	x
Trattnach12	x	x		x	x	
Trattnach2	x	x	x	x	x	

Trattnach3	x	x	x	x	x	
Trattnach4	x	x				
Trattnach6	x	-1637	-1641	-1641	-1641	
Trattnach7	x	x	x	x	x	
Trattnach8	x	-1625	-1624	-1624	-1624	
Trattnach9		x				
Voitsdorf1	x	2102-2137		2102-2137	2102-2137	
Voitsdorf17	2109-2137	2109-2137		2109-2137	2109-2137	
Voitsdorf37	x	x		x	x	x
Wegscheid1				x	x	
Weinberg1	-1653		x	x	x	
Wendling1	-1389					
Wolfersberg1	x	x		x	x	x
Zell am Pettenfirst1	2458-2487	2458-2487	2458-2487	2458-2487	2458-2487	2458-2487
Zupfing	x	x				x

2.1 Well Logs

“Well logs represent geophysical recordings of various rock properties in boreholes, and can be used for geological interpretations” (Serra, 2004).

Well logs have both advantages and disadvantages relative to what outcrops have to offer in terms of facies data. One major advantage of geophysical logs is that they provide continuous information from relatively thick successions, often in a range of kilometers. Log curves allow the interpreter to see trends at various scales, from the size of individual depositional elements within a depositional system, up to entire basin fills (Cant, 1992; Serra 2004). For this reason, data provided by well logs may be considered more complete relative to the discontinuous information that may be extracted from the study of outcrops. Therefore, the subsurface investigations of facies relationships and stratigraphic correlations can usually be accomplished at scales much larger than the ones possible from the study of outcrops. On the other hand, nothing can replace the study of rocks, hence the wealth of details that can be obtained from outcrop facies analysis cannot be matched by well-log analysis, no matter how closely spaced the boreholes may be (Cant, 1992; Serra 2004).

The most common applied well logs for the study area are discussed in the following sections.

2.1.1 GR Log

The GR log is a measurement of the natural radioactivity of the formation. In sedimentary formations the log normally reflects the shale content of the formation. This is a consequence of the fact that radioactive elements tend to concentrate in clays and shales. Clean (without shale) formations have a very low level of radioactivity, unless radioactive contaminent such as volcanic ash, or granite wash or the formation water contains dissolved radioactive salts. The GR log can be recorded also in cased holes (Schlumberger, 1996).

Properties of gamma rays

Gamma rays are bursts of high-energy electromagnetic waves that are emitted spontaneously by some radioactive elements. Nearly all the natural gamma radiation that occurs in the earth is emitted by the radioactive isotope of K^{40} and by the radioactive elements of the Uranium and Thorium series. Each of these elements emits gamma rays, while number and energies are distinctive for each element. Figure 10 illustrates the energies of the emitted gamma rays; K^{40} emits gamma rays of a single energy at 1.46 MeV, whereas the Uranium and Thorium series emit gamma rays of various energies.

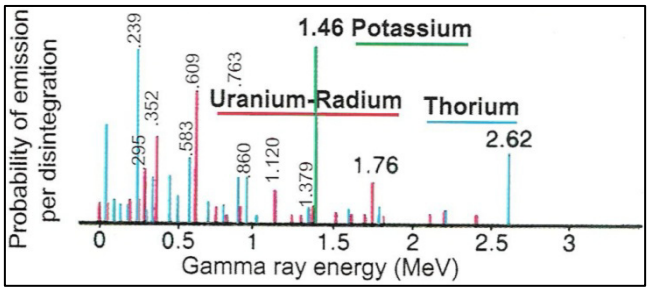

Figure 10: Gamma ray emission spectra of radioactive elements (after Serra 2004)

In passing through matter, gamma rays experience successive Compton-scattering collisions with atoms of the formation material, losing energy with each collision. After the gamma rays have lost enough energy, it is absorbed, by means of photoelectric effect, by an atom of the formation. Thus, natural gamma rays are gradually absorbed and their energies degraded (reduced) as they pass through the formation (Schlumberger, 1996).

Usage

(1) Definition of shale beds

(2) Indicator of shale content

(3) Detection of radioactive and non-radioactive content

(4) Identification of formation tops, log correlation

Geological factors influencing the GR log

Well logs provide information on physical rock properties, but not a direct indication of lithology. Gamma ray logs are commonly used for the interpretation of siliciclastic successions in lithological terms, but the interpreter must be always aware of the potential pitfalls that may occur in interpreting log signatures of GR logs. They are often interpreted in grading terms (fining- and coarsening-upward), or worse, as it adds another degree of unconstrained interpretation, in bathymetric terms (deepening- and shallowing-upward trends). In reality, gamma ray logs simply indicate the degree of strata radioactivity, which is generally proportional to the shaliness of the rocks and/or the amount of organic matter.

Zones of high gamma ray response may correspond to a variety of depositional settings, from shelf and deeper-marine to coastal plains, backshore marshes and lacustrine environments (Serra, 2004). Besides sections may also be marked by a variety of chemical and biochemical precipitates formed during times of sediment starvation (e.g., siderite, glauconite, carbonate hardgrounds, etc.), thus exhibiting a wide range of log motifs which may not necessarily fit the classic high peaks on gamma ray logs (Posamentier & Allen, 1999).

2.1.2 DT Log

A sonic tool (Figure 11) consists of a transmitter that emits a sound pulse and a receiver that picks up and records the pulse as it passes the receiver. The sound emanated from the transmitter impinges on the borehole wall. This establishes compressional and shear waves along the borehole wall and guided waves in the fluid column.

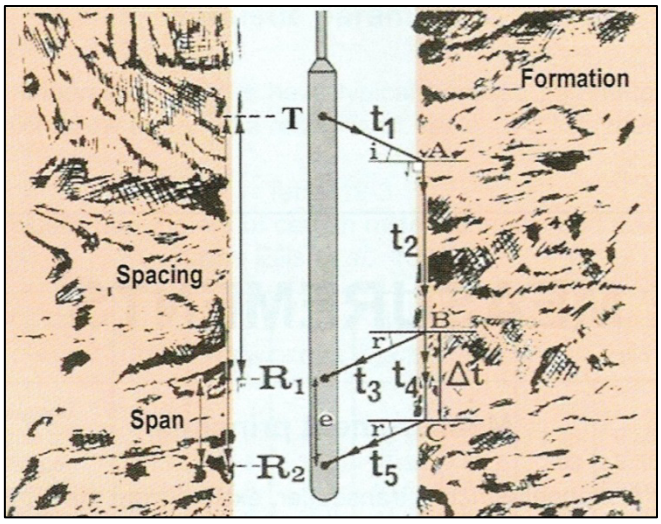

Figure 11: Sonic log device (tool with two receivers), illustrating the principle for measuring the interval time (after Serra, 2004)

The sonic log is simply a recording versus depth of time, required for a compressional sound wave to traverse one meter of formation. Known as the interval transit time, transit time, Δt or slowness is the reciprocal of the sound wave. The interval transit time for a given formation depends upon its lithology and porosity. This porosity dependence, if the lithology is known, makes the sonic log useful for a porosity log. Integrated sonic transit times are also helpful in interpreting seismic records.

Borehole Compensated Log - BHC

The borehole-compensated (BHC) tool transmitters are pulsed alternately, and Δt values are read on alternate pairs of receivers. The Δt values from the two sets of receivers are averaged by a computer automatically at the surface for borehole compensation.

2.1.3 Resistivity Logs

The electrical resistivity of a substance is its ability to impede the flow of electrical current through it. The unit is ohm-m. It is a fundamental inherent property of substance (metal, fluid, mineral or rock).

According to the number of electrodes and the spacing between them resistivity can be measured either:

(1) at great depths (up to several feet beyond the borehole) allowing a measurement inside the uninvaded zone of the reservoir (called true resistivity, R_t) not too much affected by the invasion of the mud filtrate.
(2) or close to the borehole (called invaded or flushed zone resistivity, R_{xo}), where mud filtrate has largely replaced the original pore fluid

There are several techniques in use for measurement of the resistivity. Generally all are variations of a common basic system: one (or several) emitter (electrode) sends a signal (electrical current) into the formation and one (or several) receiver (electrodes) measure the response of the formation to this signal to a certain distance from the emitter. Basically an increase in the distance between emitter and receiver (called spacing) results in an improved depth of investigation (and a reading close to R_t), at the expense of vertical resolution (Serra, 2004).

In this study mainly short spacing devices or micro- devices / tools were applied for correlation and interpretation. They are characterized with a high vertical resolution (2 – 5 cm) and a shallow radial reading (3 – 5 cm) and are mounted on pads which are applied against the borehole wall by spring. They are designed to read $R_{xo,}$ by virtue of their short spacing and their very shallow depth of investigation. Borehole fluid effect is very low, but the mud-cake contributes a small signal (Fricke & Schön, 1999).

Principle

Three electrode buttons, spaced one inch are mounted in line on the face of an oil-filled rubber pad. With these electrodes a one inch by one inch micro-inverse and a two inch micro-normal are recorded simultaneously. The pad-face is pressed against the borehole wall, either by a hydraulic controlled spring pressure system in the oldest tools, or by a micro-focused device such as microlaterolog (Figure 12) (Serra, 2004).

Environmental effects

If the pad is in perfect contact with the borehole wall, the borehole fluid has no effect on the log response. However, shallow resistivity measurements are very sensitive to the mud-cake. The vertical resolution is very fine and adjacent beds will only affect the response, if bed thickness is less than a few inches (Serra, 2004).

Geological factors influencing the resistivity

Generally the solid part of the rock indicating solid grains and cement are infinitely resistive. However some clays are more or less conductive and additionally some minerals (graphite, hematite, metals and sulphides) can considerably decrease the resistivity reading. Hydrocarbons are infinitely resistive. The resistance of water depends on the amount and occurrence of dissolved salts. The amount of conductive fluids depends mainly on the porosity and the hydrocarbon saturation in the zone of investigation.

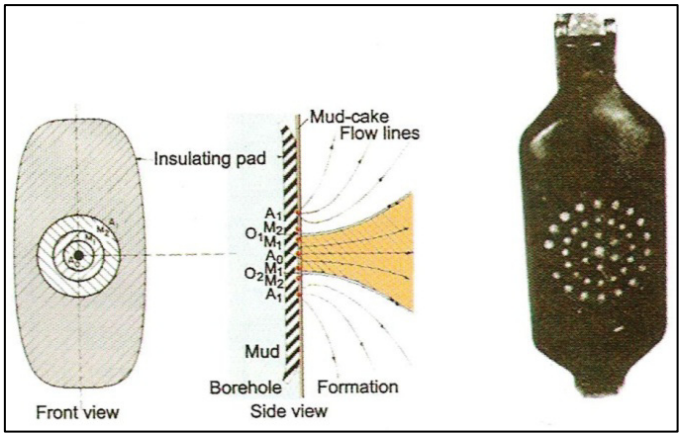

Figure 12: Microlaterolog measurement principle (left) and hydraulic pad (right) (after Schlumberger, Serra, 2004)

Microlaterolog-MLL

The operation mode is roughly explained at Principles. The electrode array is mounted of an oil-filled rubber pad (Figure 12). Borehole effects are considerably reduced on shallow depth of investigation if the pad contact is good. Though the mud-cake can simulate a wrong reading and be corrected with appropriate log charts. The uninvaded zone does not affect the MLL log, if invasion is deeper than a few inches (Serra, 2004).

Microsperically Focused Log-MSFL

The MSFL (Figure 13) tool is a pad mounted, spherically-focused logging device that has replaced the microlaterolog. It has two distinct advantages over the other R_{xo} devices. First, it is compatible with other logging tools. This eliminates the need for a separate logging run to obtain R_{xo} information. The second improvement is in the

tool's response to shallow R_{xo} zones in the presence of mud-cakes (which was the main limitation of the MLL log) (Schlumberger, 1996).

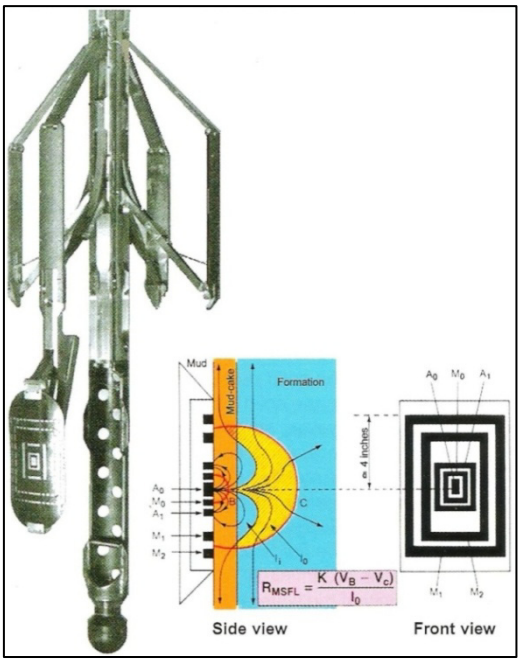

Figure 13: Microspherically focused logsonde (left) including pad and caliper arms, distribution (middle) and electrode arrangement device (right) (after Serra, 2004)

2.2 Core reports

Core reports were provided for all cores with Cenomanian rocks in wells used in this study. Additionally, lithologs (Figure 14) of cores mapped by Stephan Schnitzer (Montanuniversität Leoben) have been incorporated in the study.

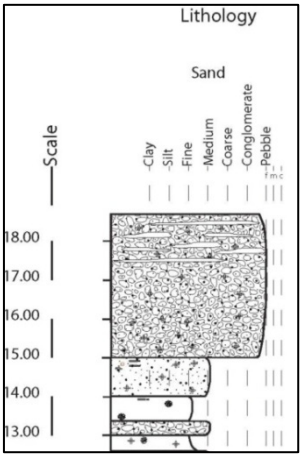

Figure 14: Example of a lithology recorded by S. Schnitzer.

2.3 Geological short profiles

Geological short profiles and/or completion logs were provided for the wells listed in Table 2

Table 2: Wells for which RAG provided geological short profiles and/or completion logs

Bad Hall 1
Eberstalzell 1
Hoergersteig 1
Kirchham 3
Kohleck 1
Lindach 1
Maria Schmolln 1
Mauern 1
Mayersdorf 1
Muehlberg 1
Oberaustall 1
Oelling 1
Perneck 1
Redltal 1
Renging 1
Sattledt 1
Schwanenstadt 3
Senftenbach 1
Sierning 1
Steinhaus N1
Steyr W1
Trattnach (all)
Voitsdorf 1
Voitsdorf 17
Wolfersberg 1

3 Methods

3.1 Adjustment of Log depths

Reservoir properties are estimated from calculations that involve more than one log trace, or a single log trace that has been calibrated using readings from multiple logs. Such estimates assume that the log traces are correctly aligned so that the responses from different tools all represent a single depth interval in the well. Unfortunately, it may not be possible to assemble all tools needed for a logging program into a single sonde, so multiple wire-line runs may be necessary. In drilling deep holes, it is common practice to log the well at successive times to obtain information on the progress of the well through the stratigraphic section and on the condition of the hole.

Most logging sondes include a gamma ray tool, so a GR trace should be available for each logging run. When well log files are placed in a log analysis program such as Senergy's Interactive Petrophysics, it is relatively simple to adjust the various files to a common depth. The gamma ray traces from the different runs are examined and peaks, shoulders, and other distinctive features that are common to all the gamma ray traces are identified. If they do not match at the same depths, they are adjusted until the features align.

3.2 Core gamma ray measurements

The total and spectral core gamma ray measurements have been accomplished with the instrument Gamma Surveyor (Figure 15). Like the GR log, the natural gamma ray spectrometer tool measures the natural radioactivity of the formation. In addition, the Gamma Surveyor measures both the number and energy level of gamma rays and permits the determination of the concentration of radioactive potassium, thorium and uranium.

Figure 15: Gamma Surveyor (GF Instruments)

The Gamma Surveyor offers three basic measuring modes. The methodology is based on the recommendation of IAEA (International Atomic Energy Agency). The factory calibration is done on high-volume standards for K, U, and Th. The general purpose calibration is based on homogenous half space geometry. This half space geometry is not realized in the case of the investigations of drill cores. Therefore, the concentrations cannot be determined quantitatively. For each measuring point a standard time configuration of two minutes was selected.

The instrument always measures the complete spectrum, from which it evaluates the [cps] values in ROIs (region of interest) and calculates the concentrations of elements K, U and Th. The concentration of K is determined directly. The U and Th concentrations are based on detection of radioisotopes 214Bi and 208Tl that are parts of the related disintegration series (the balance of individual daughter products in the frame of measuring conditions is supposed). The natural dose rate value (in nGy/h) is calculated from measured concentrations of K, U, and Th. This value refers to the output of the instrument and does not relate to real [ppm] or [%] values, due to the fact, that we do not have a half space geometry.

Physical Principle

Most of the gamma ray radiation in the earth originates from the decay of three radioactive isotopes. Potassium (K^{40}), Uranium (U^{238}) anf Thorium (Th^{232}). Potassium decays directly to the stable Ar^{40} with the emission of a 1.46 MeV gamma ray. Uranium and Thorium decay sequentially through a long sequence of various daughter isotopes before arriving s stable lead isotope. As a result, gamma ray of

many different energies are emitted and fairly complex energy spectra are obtained (Serra, 2004).

3.3 Core gamma ray depth shift and rescale

(1) In a first step the output data of the gamma surveyor has been rescaled to find a visual fit (Figure 16) with the API values of the measured GR well log data. This was accomplished using the curve rescaling function of the software Interactive Petropysics by Senergy (Figure 17).

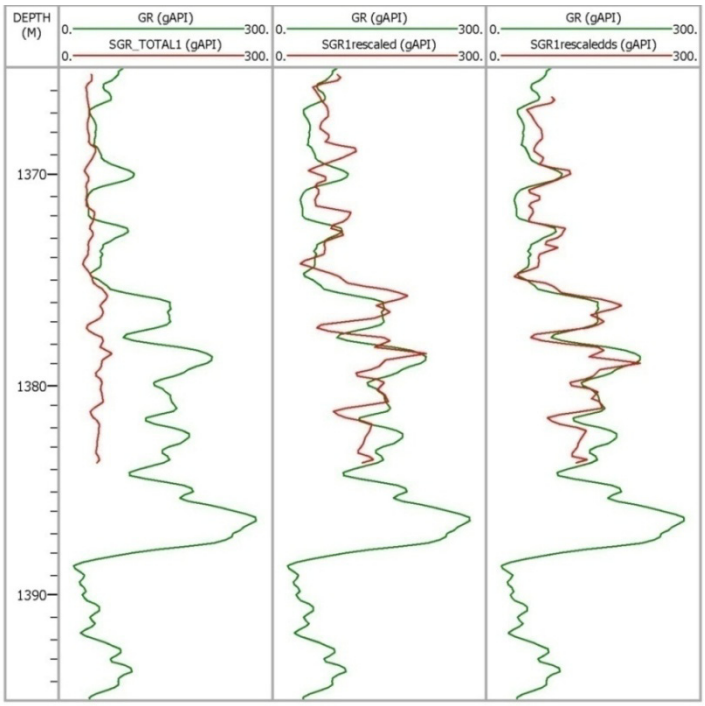

Figure 16: Example of rescaled and depth shifted core gamma log (Wendling 1). Red line: core gamma log (CGR); green line: well gamma log (GR). First column: original CGR and GR log, second column: CGR log after rescaling, third column: rescaled and depth shifted (squeezed) CGR log.

Maximum and Minimum GR Log values are the reference for rescaling the original data measured with the Gamma Surveyor. Within the software, the interpreter has to insert the maximum and minimum values of the measured core gamma log (SGR_total_meas), as well as the maximum and minimal of the GR well log data of the cored section. The output is a new curve (GR-rescaled) which fits with the GR log.

(2) In a second step the rescaled core gamma log had to be depth shifted (Figure 17) to the reference GR well log. This step was also performed with Interactive Petrophysics, which allows the interpreter to shift the whole measured CGR curve, as well as single intervals of the curve (block shift).

All rescaled and depth shifted core gamma ray (CGR) and spectral core gamma ray (SCGR) logs are presented in the “Results and Interpretation” section. Information on the depth shift for all wells is provided in table format. In these tables, MD refers to the core depth and “shift” refers to the core shift in meters. A negative shift means that the core gamma ray log had to be shifted upwards; a positive one, that it had to be shifted downwards. Partly, different core intervals had to be shift by different distances.

Detailed core descriptions have been provided by S. Schnitzer (Montanuniversität Leoben). His descriptions have been shifted together with the SCGR logs.

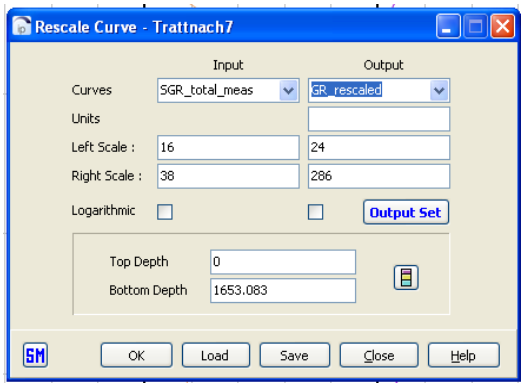

Figure 17: Example for SGR log rescaling for well Trattnach 7.

4 Results and Interpretation

4.1 Core Gamma Ray and Spectral Core Gamma Ray

Overall cores from thirty wells (Figure 18) have been measured with the Gamma Surveyor in order to get an idea of the spectral gamma distribution of the study area. The cores for the wells Kohleck 1 and Bad Hall 1 were too short (less than one m) for a correlation with the GR log.

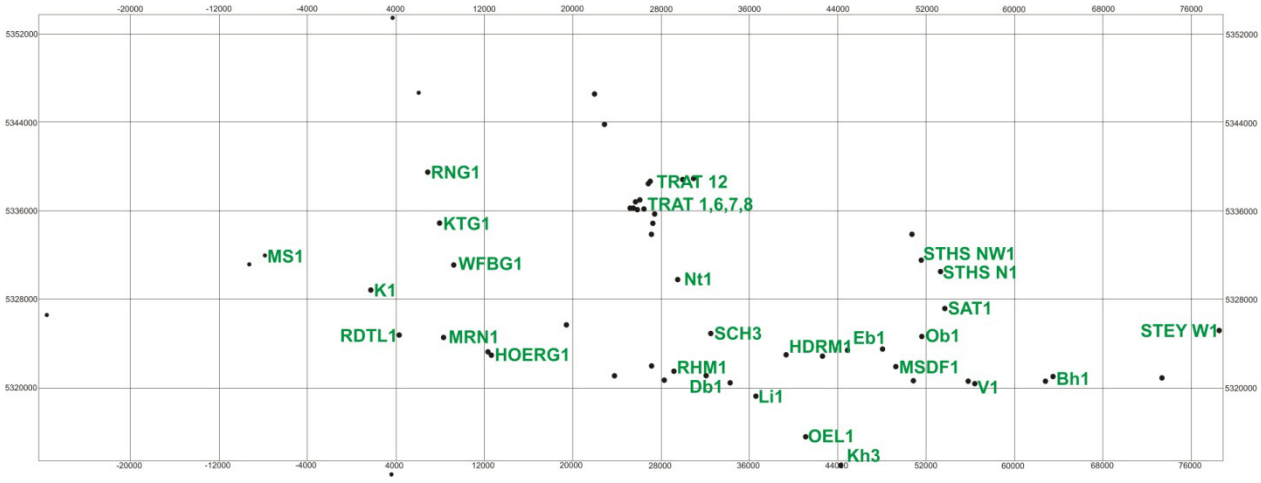

Figure 18: Base map indicating wells (marked in green) that have been measured with the Gamma Surveyor.

The Trattnach Field is represented by a high number of cores, which represent the entire Cenomanian succession. Moreover, these cores have been studied in great detail using sedimentological techniques and CGR measurements. Therefore, the following section starts with correlation profiles of the Trattnach Field. The following illustrated wells are alphabetically ranked.

The Upper Jurassic limestones in the Trattnach Field are characterized by high velocities (low DT) and low GR responses. The transition to the overlying Cenomanian sandstones referring to the log signature is sharp and well-defined. Only in Trattnach 6 the Upper Jurassic carbonates are overlain by terrestrial Lower Cretaceous sandstones (Schutzfels Formation).

The Cenomanian in the Trattnach Field has been subdivided from bottom to top into the informal units CET3, CET2, and CET1. The lower units CE3 and CE2 correspond to the glauconitic sandstones of the Saal Member.

In contrast to the Saal Member the overlying Bad Abbach Member (CE1 unit) relates to sediments with lower radioactivity. It is characterized by a low DT reading (high velocity) and high resistivity in the shallow MLL or MINV log. The so-called marker bed (Nachtmann, 1995) separates the CE1 unit from the underlying CE2 unit. It is characterized by a prominent peak both in the sonic and in the resistivity log. A red-coloured layer ("Rote Lage") corresponds to the marker bed according to Nachtmann (1995). Detailed core to log gamma correlations show that the red layer may be part of the marker bed, but does not necessarily define it. In some wells even two red layers occur. Generally the thickness of the red layer varies between one and two meters.

In the following section the characteristics of the total and spectral core gamma and the lithological associations are illustrated and discussed. In each well the first column indicates the stratigraphic unit and the measured log depth in m. The second column refers to the gamma ray (green) and depth shifted core gamma ray log (red).The lithologs in the third column have been provided by Stephan Schnitzer. For the Trattnach Field they are shown together with porosity and permeability data. The fourth column corresponds to the depth shifted spectral logs potassium (green), uranium (blue) and thorium (black) and the last column represents the sonic and a shallow resistivity log.

Trattnach 6

The Trattnach 6 well logs (Figure 19) illustrate the typical well log character of the transgressive Cenomanian sandstones. Obtained well logs start within whitish sediments forming part of the pre-Cenomanian sandstones. Those are characterized by an upward decrease in sonic velocity and resistivity. A sharp DT and MLL peak separates the CE3 unit from pre-Cenomanian (PCE) sandstones. Referring to the core interpretation this can be related to the conglomeratic interval at the base of CE3. Note also the low K contents in the PCE. The logged and measured core intervals from CE3 to CE1 are characterized by the typical log response of the glauconitic sandstones showing a high GR response especially in the lower intervals.

Also Th and K contents are relatively high in the lower part of CE3. The marker bed defines the base of the subunit CE1. The sharp contact to the Turonian marls suggests that the top of the Cenomanian is formed by a fault. Fine grained, conductive sediments with low velocity characterize the overlying Turonian marlstones. CGR and SCGR data have been shifted (Table 3) with the listed values.

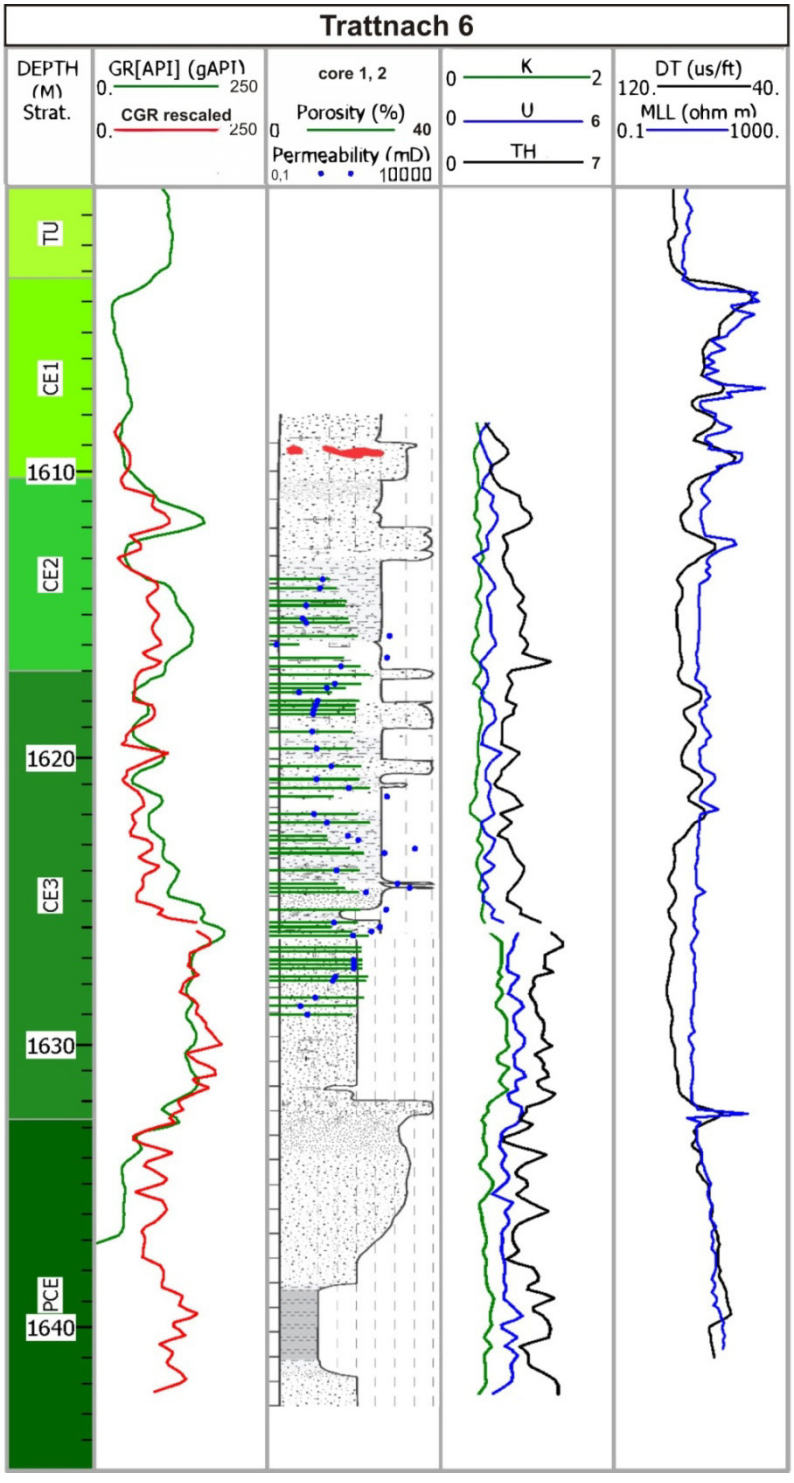

Figure 19: Trattnach 6 well logs and shifted CGR, SCGR logs and core interpretation. Porosity (green) and permeability (blue) data overlie in the third column the core interpretation (Schnitzer).

Table 3: CGR, SCGR and core log depth shift of well Trattnach 6 core 1 and 2.

Core 1 1605-1623 Core recovery 18 m		Core 2 1623-1641 Core recovery 18 m	
MD [m]	Shift [m]	MD [m]	Shift [m]
1608.277	2.999	1623.67	2.515
1609.801	3.158	1624.127	2.855
1615.288	3.123	1624.279	3.134
1616.507	3.362	1625.346	2.591
1618.031	3.553	1625.956	2.378
1619.707	3.401	1627.48	2.595
1620.164	3.354	1630.223	1.899
1621.384	3.337	1631.594	1.243
1621.536	3.441	1632.814	1.048
1621.841	3.597		
1622.603	3.117		

Trattnach 7

Figure 20 illustrates the facies well log successions of the well Trattnach 7. Core 1 and 2 were measured and depth shifted (Table 4) to the current position. The fit between the CGR to the GR log is very good.

Both, the K and Th responses show a general upward decrease. A closer look reveals two cycles with upward decreasing K and Th contents (1623.5 – 1611 and 1611 – 1602 m MD). The general Th trend is overlain by Th maxima at 1623.5 and 1611m MD. The similarity of the total GR and Th concentration curves suggests that the total GR is mainly controlled by Th content. Apart from this K-rich glauconite in the greenish sandstones may influence the log pattern.

The DT response looks completely different compared to the GR log. The third column of the well log plot is overlain with depth shifted porosity (green) and permeability (blue) data.

Apparently there's a connection between grain size and porosity, especially in the upper parts. The red layer is characterized by a slightly increased K reading and seems to be at least part of the marker bed (at base CE1).

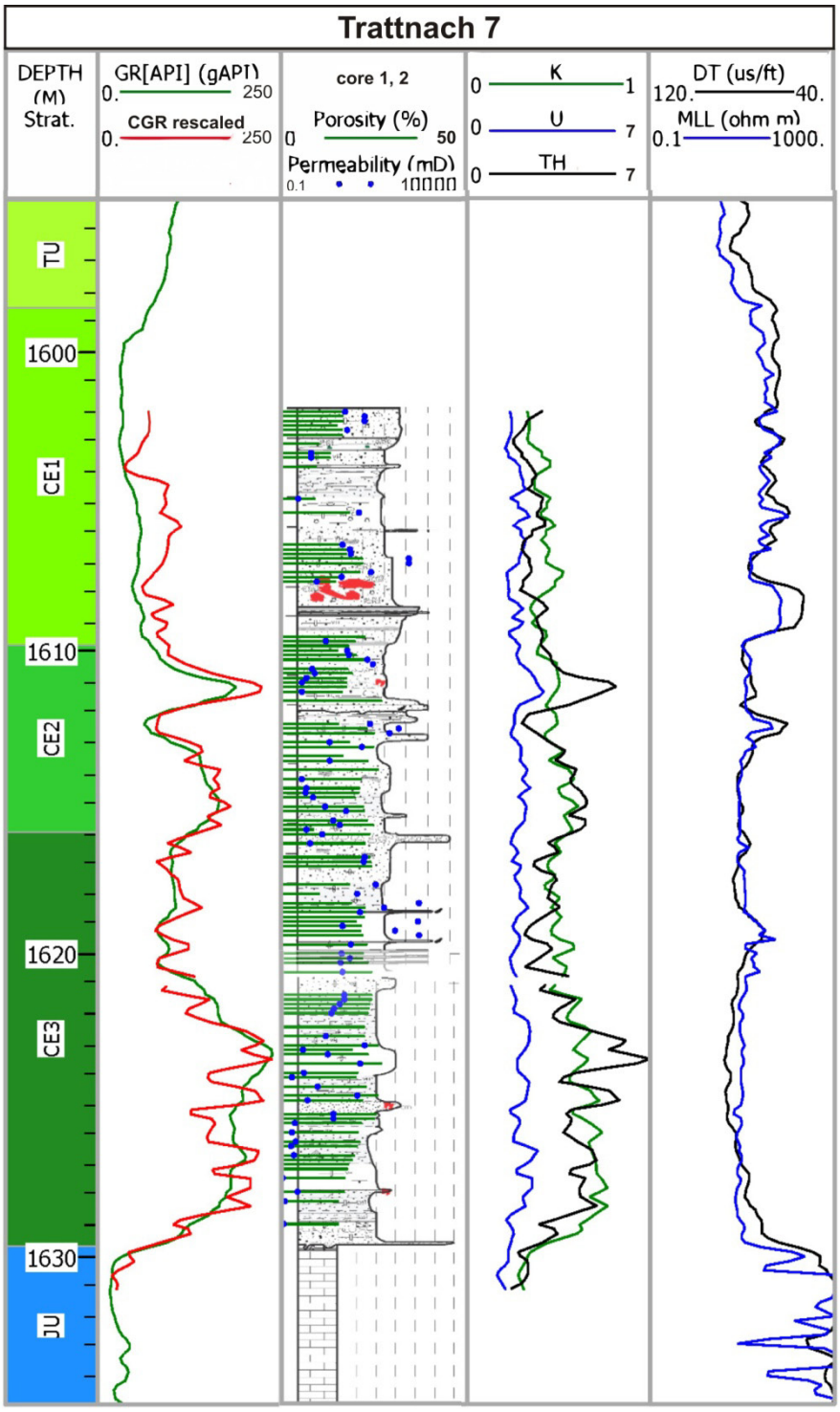

Figure 20: Trattnach 7 well logs and shifted CGR, SCGR logs and core interpretation. Porosity (green) and permeability (blue) data overlay in the third column the core interpretation (Schnitzer).

Table 4: CGR, SCGR and core log depth shift of well Trattnach 7 core 1 and 2.

Core 1 1600-1618 Core recovery 18 m		Core 2 1618-1636 Core recovery 18 m	
MD [m]	Shift [m]	1619.402	2.876
1601.267	1.838	1623.517	2.856
1605.229	2.686	1627.327	2.475
1610.258	2.591	1628.242	2.098
1614.221	2.083		
1618.793	1.918		

Trattnach 8

For the well Trattnach 8 (Figure 23) core 1 and 2 have been measured, depth shifted (Table 5) and a sedimentological log has been provided by S. Schnitzer.

Both, obtained well logs and available cores start in the Cenomanian subunit CE3. The match between the measured CGR log and the GR log is satisfactory. Similarly to the other Trattnach wells, the K and particularly the Th content slightly decrease from base to top of the cored section.

The total core gamma ray log is mainly dominated by the response of the K and Th log. Two red layers occur in the CE1 subunit. Only the lower one (at approximately 1614 m MD) is part of the marker bed.

The illustration of porosity, permeability and core interpretation clarifies the connection between the reservoir specific parameters. Like in the other Trattnach wells, grain size and porosity in Cenomanian strata are directly linked.

The fine grained Turonian marlstones are characterized by high K and Th values. Even top CE1 illustrates an upward increased K response that apparently relate to the increased clay mineral content.

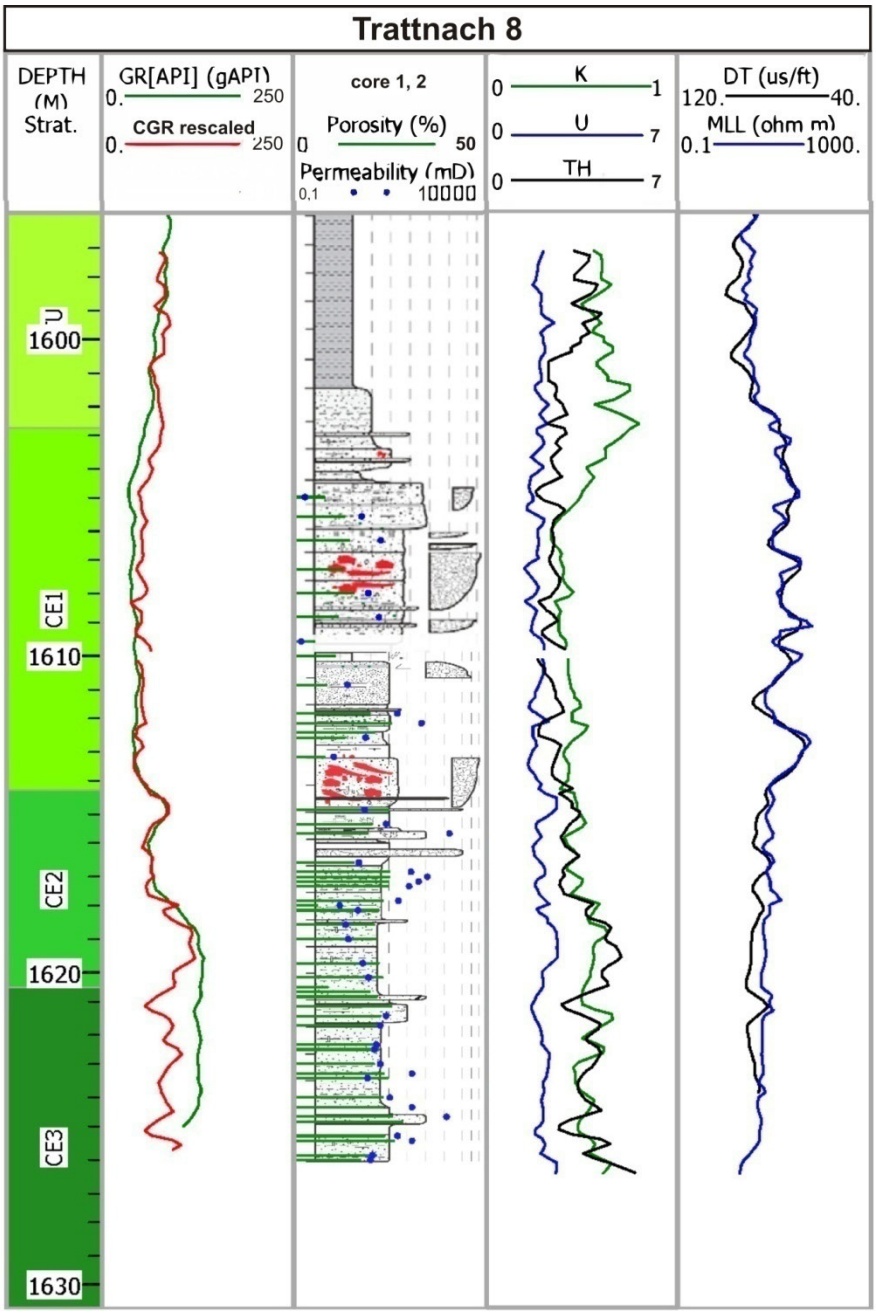

Figure 21: Trattnach 8 well logs and shifted CGR, SCGR logs and core interpretation. Porosity (green) and permeability (blue) data overlay in the third column the core interpretation (Schnitzer).

Table 5: CGR, SCGR and core log depth shift of well Trattnach 8 core 1 and 2.

Core 1 1591-1609 Core recovery 18.8 m		Core 2 1609-1627 Core recovery 18.5 m	
MD [m]	Shift [m]	MD [m]	Shift [m]
1595.524	1.897	1609.698	0.435
1596.744	1.701	1610.764	0.750
1597.81	1.633	1612.288	0.377
1598.268	1.534	1613.66	0.234
1598.877	1.896	1614.574	-0.297
1599.182	2.078	1615.184	-0.625
1602.535	1.463	1615.641	-0.391
1604.211	1.578	1615.946	-0.414
1606.497	1.365	1618.232	-0.576
1607.259	1.089	1620.67	-1.275
		1622.194	-0.982
		1625.852	-1.418

Trattnach 1

Figure 22 illustrates the depth shifted (Table 6) CGR and SCGR logs of the well Trattnach 1 together with the DT and MLL logs and the depth shifted porosity and permeability data.

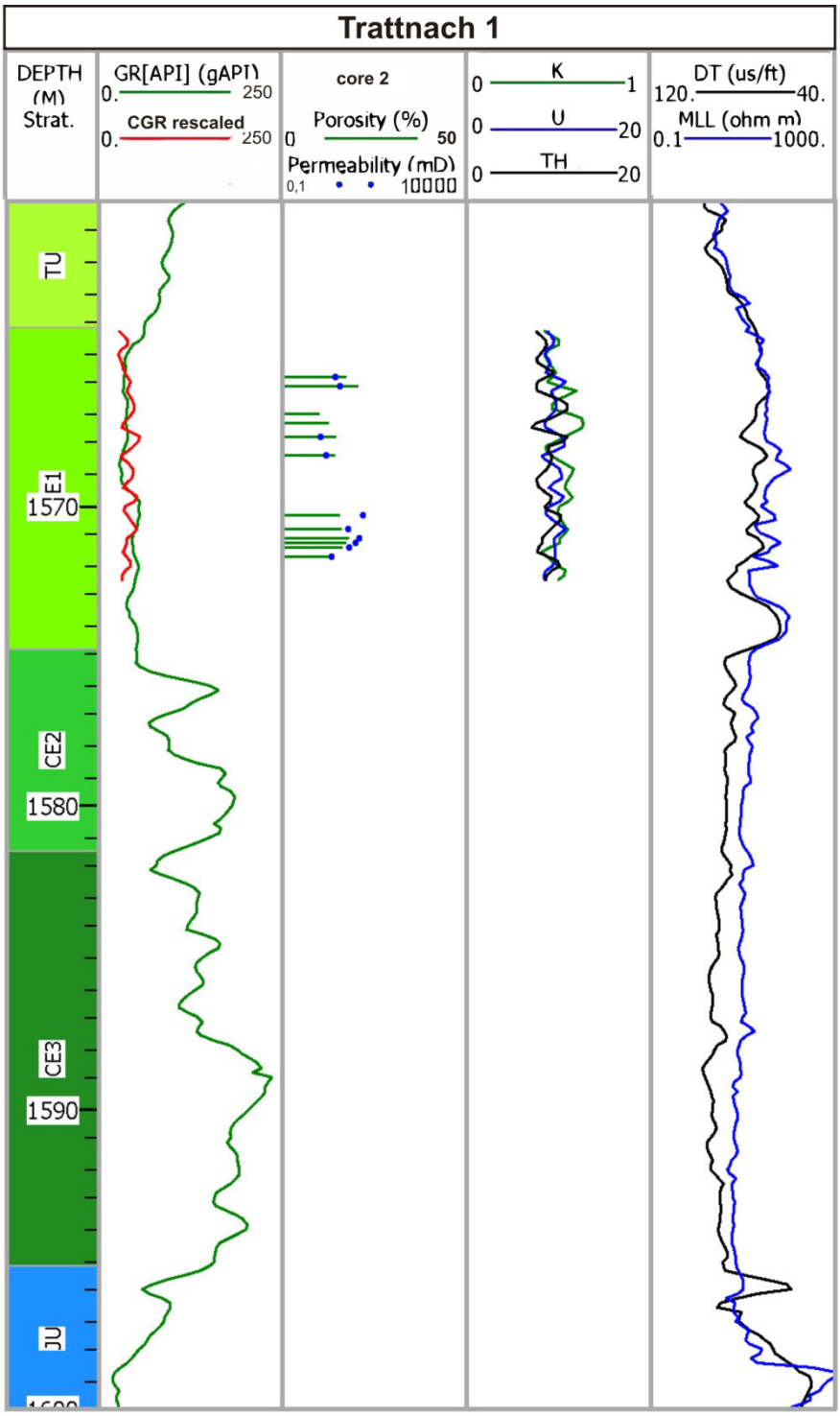

Figure 22: Trattnach 1well logs and shifted CGR, SCGR logs and porosity and permeability data. Porosity (green) and permeability (blue) data are illustrated in the third column.

Table 6: CGR and SCGR log depth shift of well Trattnach 1 core2.

Core 2 1565-1574.5 Core recovery 8.1 m	
MD [m]	Shift [m]
1568.245	-1.448
1569.007	-1.365
1572.207	-1.342
1573.122	-1.181

Trattnach 12

Figure 23 illustrates the depth shifted (Table 7) data of core 1 of well Trattnach 12. The fit of the total core gamma ray log to the GR log is very good, allowing a reliable correlation to the core interpretation.

In the CE2 unit the total GR is mainly controlled by Th contents, whereas in CE1, it is controlled by both Th and K. U plays a minor role. A red layer (~1626 m) occurs within CE1.

Based on DT and resistivity logs, no distinct marker bed exists in Trattnach 12. However, a sharp step at the sonic and resistivity log suggests the boundary between CE2 and the apparently compacted and well cemented CE1.

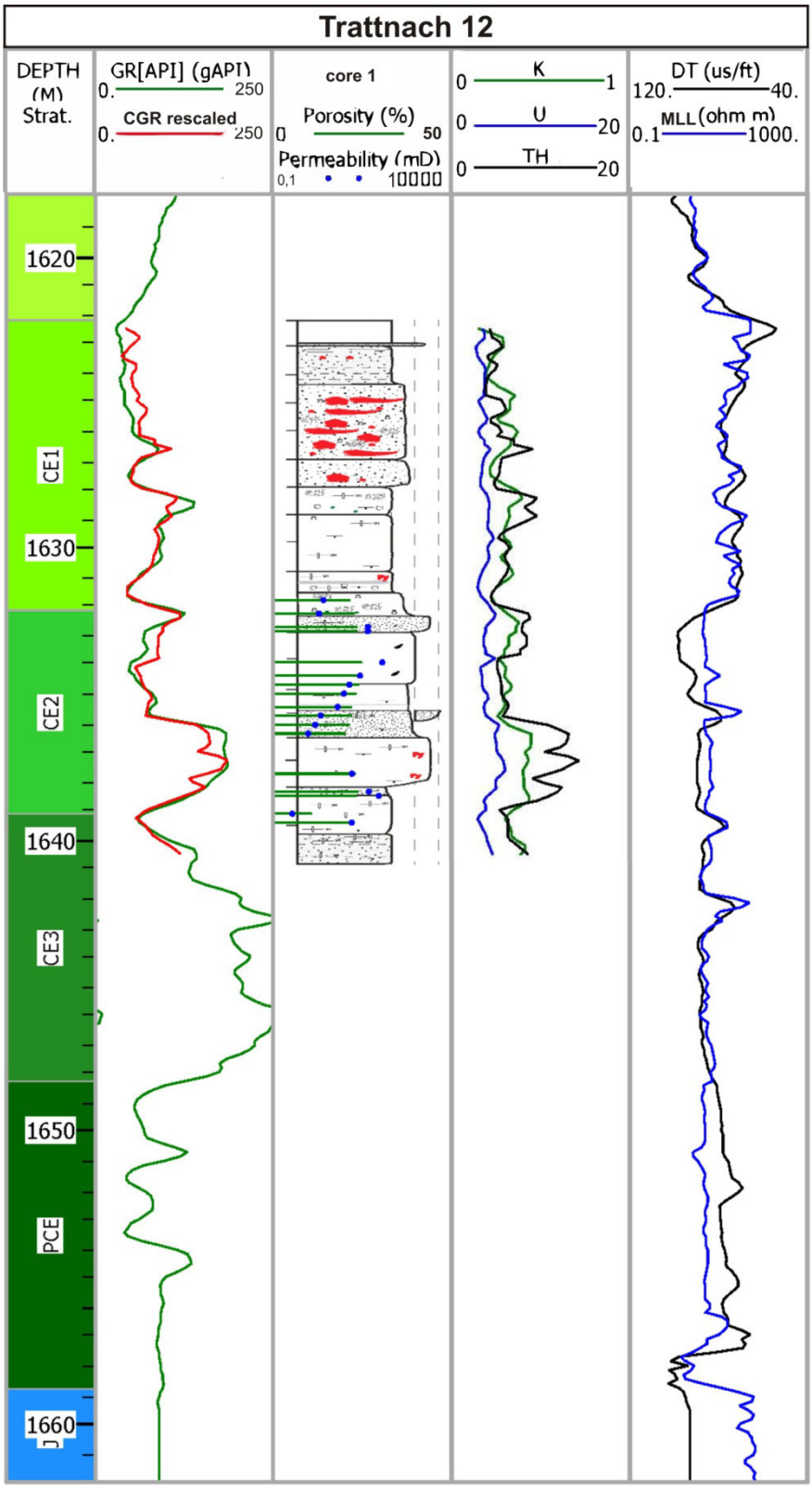

Figure 23: Trattnach 12 well logs and shifted CGR, SCGR logs and core interpretation. Porosity (green lines) and permeability (blue points) data overlay in the third column the core interpretation (Schnitzer).

Table 7: CGR, SCGR and core log depth shift of well Trattnach 12 core 1.

Core 1 1621-1639 Core recovery 18 m	
MD [m]	Shift [m]
1622.194	1.217
1623.871	1.134
1625.242	0.970
1626.309	1.182
1627.681	1.092
1630.576	1.091
1631.643	1.048
1631.948	1.644
1631.948	1.644
1632.558	1.516
1634.234	1.528
1637.892	1.300

Desselbrunn 1

Figure 24 illustrates the detailed measured section of core 3 (2874 – 2887 m) from well Desselbrunn 1 together with well logs. Obviously the latter ends at 2873 m MD. Thus a log-to-core shift was not possible. Furthermore, the CGR data are given in [cps] and cannot be directly compared to [API] units.

Based on core data, Top Jurassic was interpreted at 2887.5 m MD. Both CGR as well as K decrease considerably downwards in the Upper Jurassic limestones.

The K log seems to decrease upwards from Base to Top of the cored interval. This feature is not uncommon for the Upper Austrian Cenomanian sandstones and might result from increasing glauconite contents or an increased Th or U response. Further mineralogical investigations will give more reliable information to this topic.

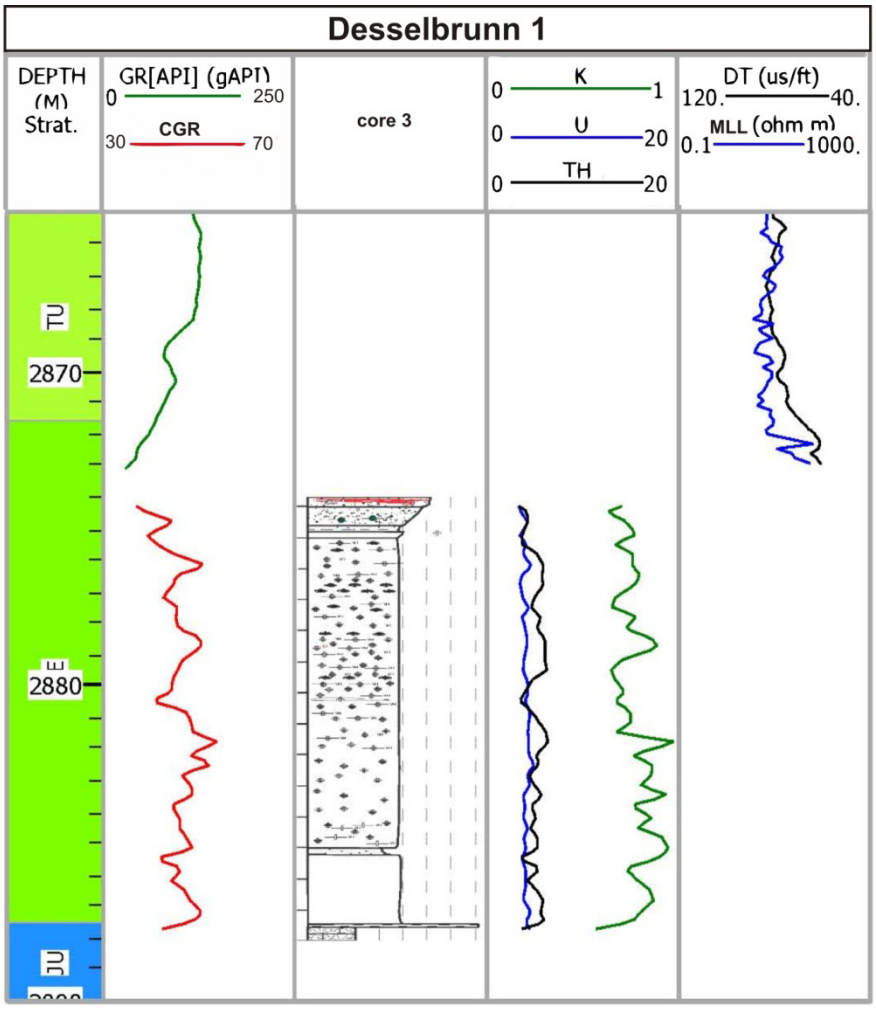

Figure 24: Desselbrunn 1 well logs and core interpretation (Schnitzer).

Eberstalzell 1

For the well Eberstalzell 1 (Figure 25) the resistivity log has apparently been cut at Top Cenomanian. Furthermore, no GR log has been available. Therefore, the CGR log has been shifted using the flipped DT log (Table 8). Nevertheless a more or less good match had been realized. Core 5 includes the boundary between Jurassic limestone and Cenomanian sandstone. This helped to connect the CGR and DT logs. While the DT increases significantly downwards the GR log decreases downwards in the Jurassic limestones. Note also the upward decrease of the K log from Base to Top Cenomanian. Furthermore the Th log has significant peaks especially at the fine grained sections of both, core 5 and 4. The marker bed defining the base of CE1 is clearly visible in the DT log. Obviously, it is not represented by the red layer. The empty interval between core 4 and core 5 indicates almost five meters of core loss?!

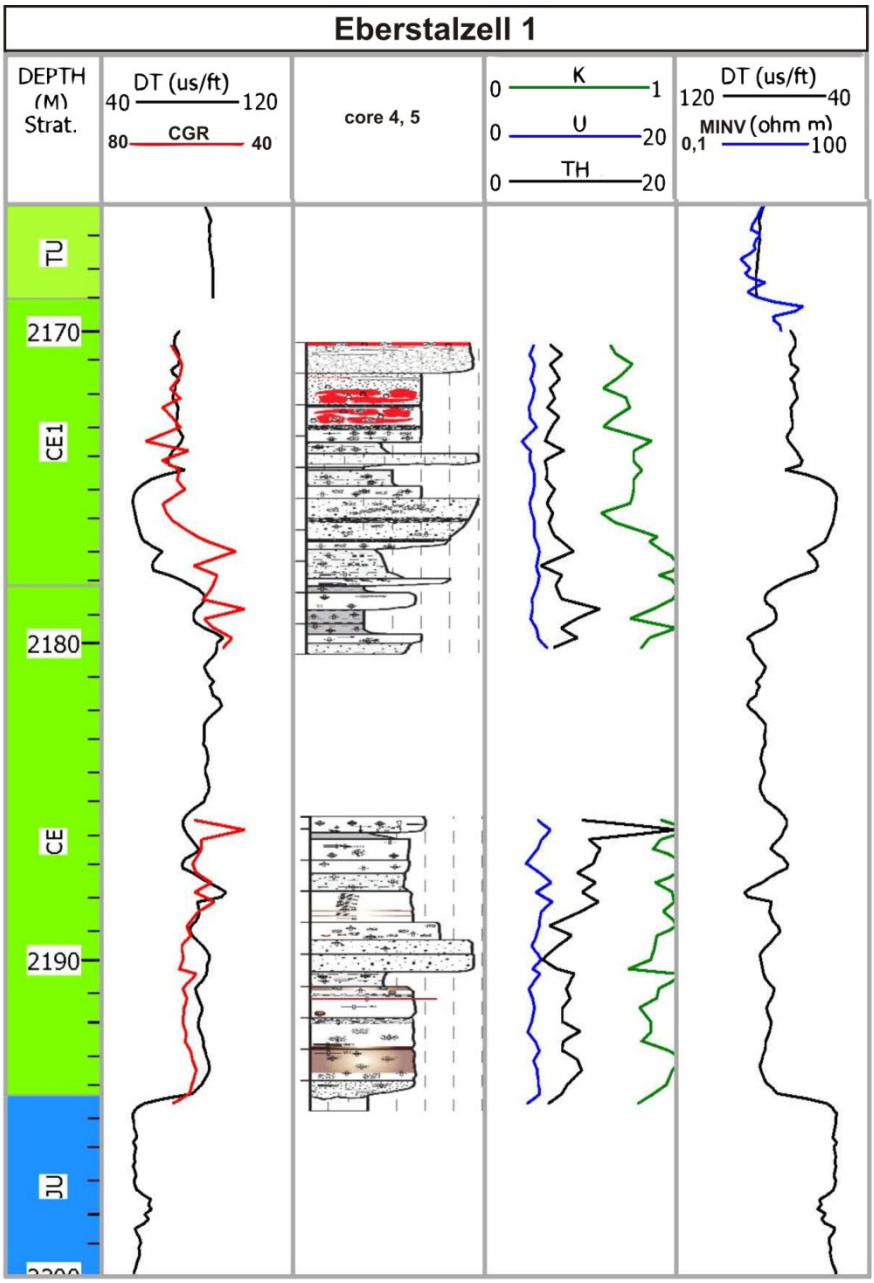

Figure 25: Eberstalzell 1 well logs and shifted CGR, SCGR and core interpretation (Schnitzer).

Table 8: CGR, SCGR and core log depth shift for well Eberstalzell 1 core 4 and 5.

Core 4 2170.0-2183.5 Core recovery: 10 m		Core 5 2183.5-2193.0 Core recovery: 9.5 m	
MD [m]	Shift [m]	MD [m]	Shift [m]
2175.967	0.327	2189.378	1.216

Haidermoos 1

The well log sketch of the well Haidermoos 1 (Figure 26) illustrates a very good fit between CGR and GR logs. Hence cores 5 and 6 could be exactly depth shifted (Table 9).

The Jurassic succession is characterized by high sonic velocities and a low gamma ray reading. The boundary between Upper Jurassic and Cenomanian sediments is very sharp in its log characteristic.

Similar to other wells, K and Th decrease upwards within the cored interval. The red layer has an extraordinarily large thickness, but does not show any characteristic log signature.

The “marker bed” is either absent or its thickness considerably reduced. Thin limestone beds above the red layer are characterized by low K, U and Th responses. Apparently the GR log as well as the CGR response seem to increase continuously from top core 5 to base core 6. Note that the high GR response is not related to fine grained sediments. Except the thin shaly–silty layer at approximately 2318 m MD the whole cored section includes sandstones intercalated with coarse grained to almost conglomeratic intervals (2307 – 2308 m MD). Note also the completely different log signature of the sonic log, especially at the deeper parts of the Cenomanian compared to the GR log.

The Cenomanian sandstones are overlain by Turonian marlstones. These are characterized by upward decreasing sonic velocities and upward increasing GR values.

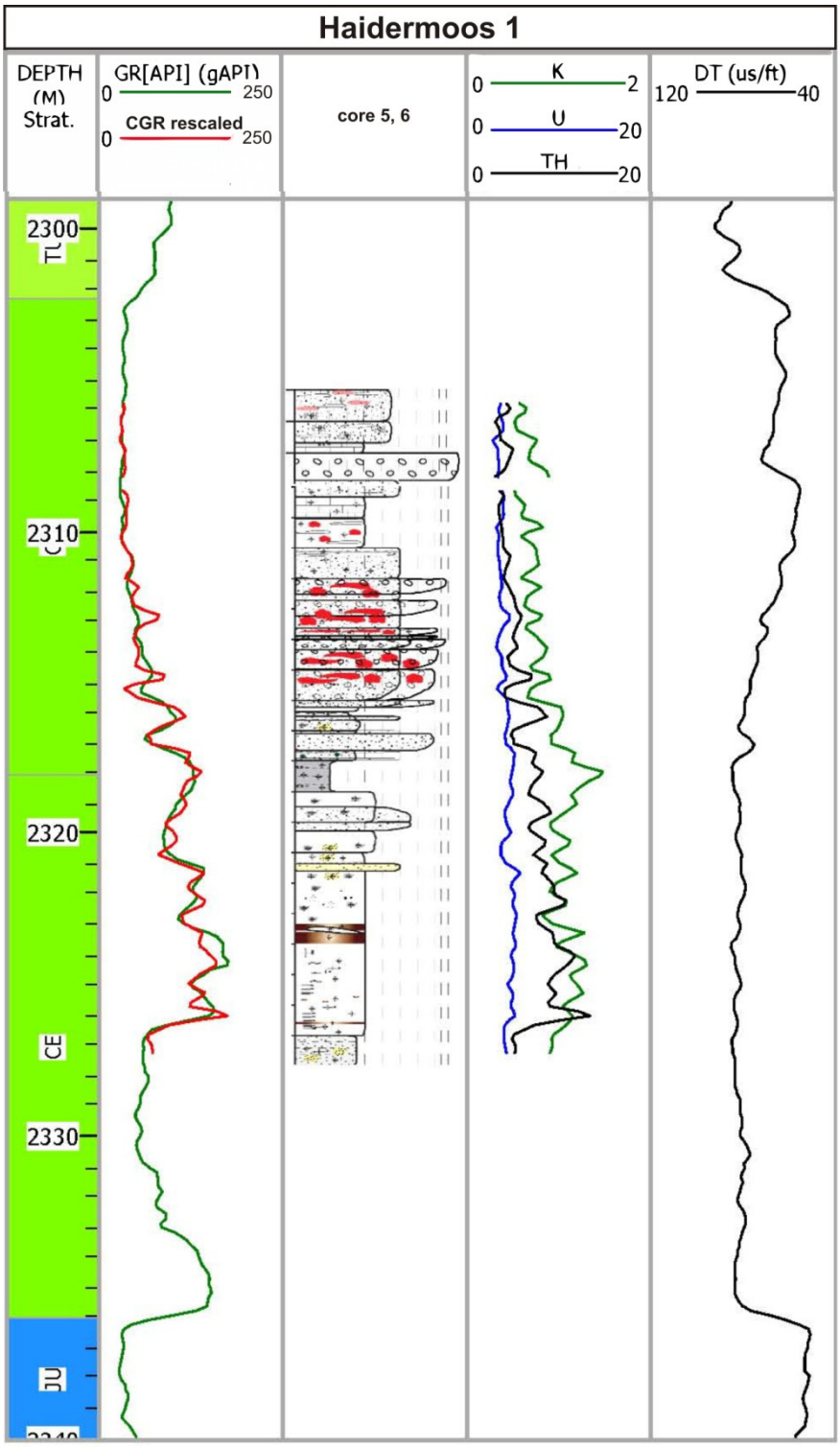

Figure 26: Haidermoos 1 well logs and shifted CGR, SCGR and core interpretation (Schnitzer).

Table 9: CGR, SCGR and core log depth shift for well Haidermoos 1 core 5 and 6.

Core 5 2306-2309 Core recovery 3.0 m		Core 6 2309-2327.5 Core recovery 18.5 m	
MD [m]	Shift [m]	MD [m]	Shift [m]
2307.452	-0.394	2315.834	-0.542
2307.909	-0.422	2316.748	-0.612
		2317.815	-0.502
		2321.473	-0.423
		2321.778	-0.472
		2323.149	-0.385
		2326.502	-0.411

Hoergersteig 1

Because of the low variability of the GR log (and its unusal low API values), it is difficult to depth shift the CGR log of cores 2, 3, 4 from well Hoergersteig 1 (Figure 27). Finally, using the border with the overlying Eocene sediments, the CGR and SCGR logs could be successfully depth shifted (Table 10). The core interpretation is still in progress.

Base Cenomanian (=Top PCE) has been defined following the core report provided by RAG. It is difficult (impossible?) to define base Cenomanian with the help of limited received well log data.

Both U and Th logs are rather uniform. Note the high K reading over the whole cored section. It is questionable if the GR reading is correct for this well, due to the high K log response, which refer according to core reports and personal core interpretation to glauconitic sandstones. There has been no sonic log obtained and the ILD is not really satisfying.

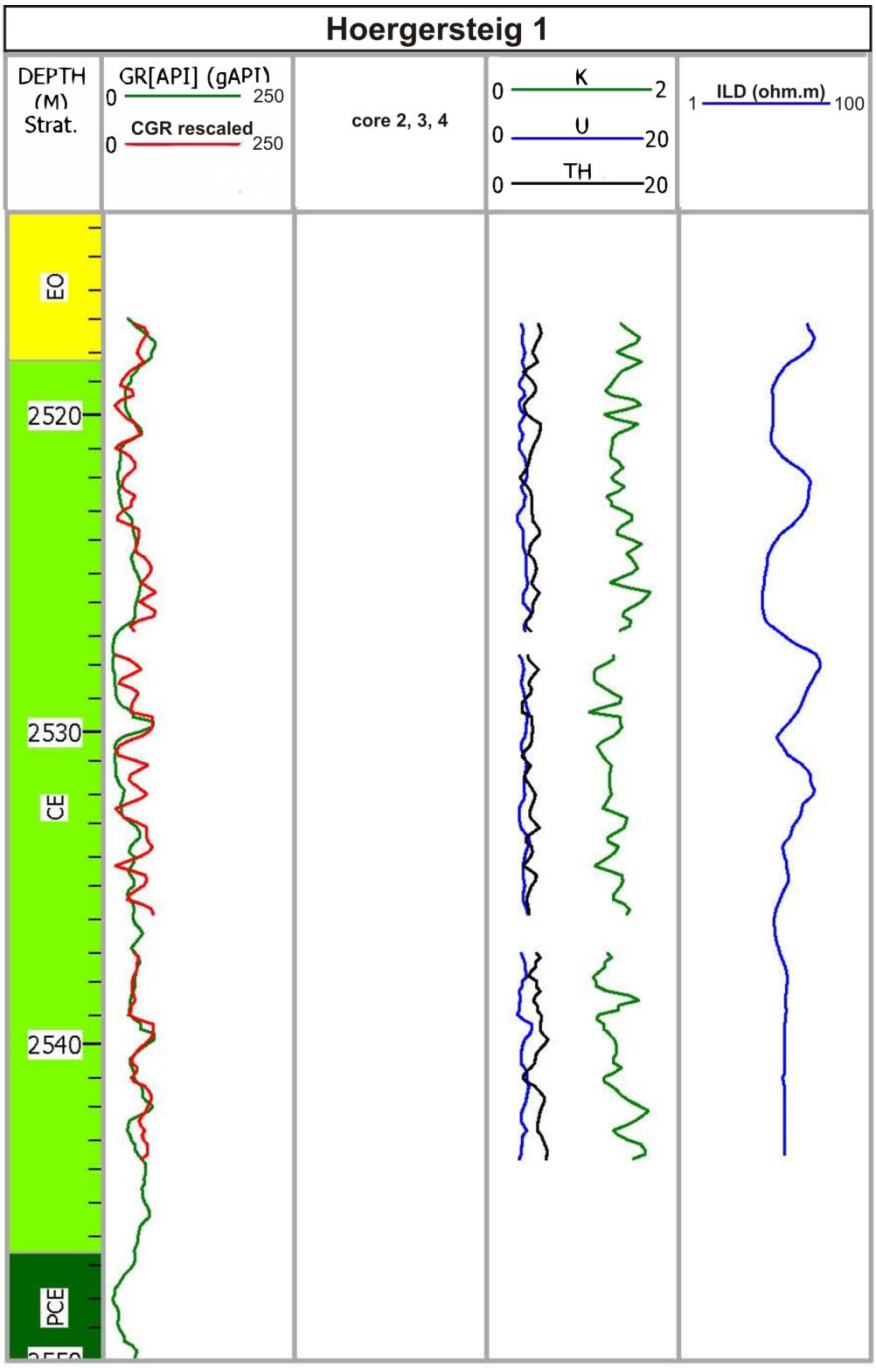

Figure 27: Hoergersteig 1 well logs and shifted CGR and SCGR logs.

Table 10: CGR and SCGR log depth shift for well Hoergersteig 1 core 2, 3 and 4.

Core 2 2516-2526.5 Core recovery 10 m		Core 3 2526.5-2538.5 Core recovery 8.8 m		Core 4 2538.5-2547 Core recovery 6.7 m	
MD [m]	Shift [m]	MD [m]	Shift [m]	MD [m]	Shift [m]
2521.685	0.905	2527.476	1.337	2539.211	-1.949
2522.6	1.347	2528.238	1.292	2540.735	-1.503
2523.514	1.251	2531.134	1.416	2541.497	-1.292
		2534.03	1.156	2541.954	-1.391
				2542.564	-1.540
				2543.936	-1.442
				2544.85	-1.728
				2545.002	-1.598

Kemating 1

Cores 5 and 6 of the well Kemating 1 (Figure 28) have been shifted at listed depths (Table 11) as well as CGR and SCGR log. Note the good match between measured CGR and GR log.

The boundary between Upper Jurassic and Cenomanian sediments is sharp in the well logs.

The log signature of the Th and K log looks very similar to the GR log. This suggests, that the GR log is mainly controlled by Th and K contents. U plays a minor role in the cored section.

Top Cenomanian is characterized by a downward decrease in sonic velocity and an increase in the GR log.

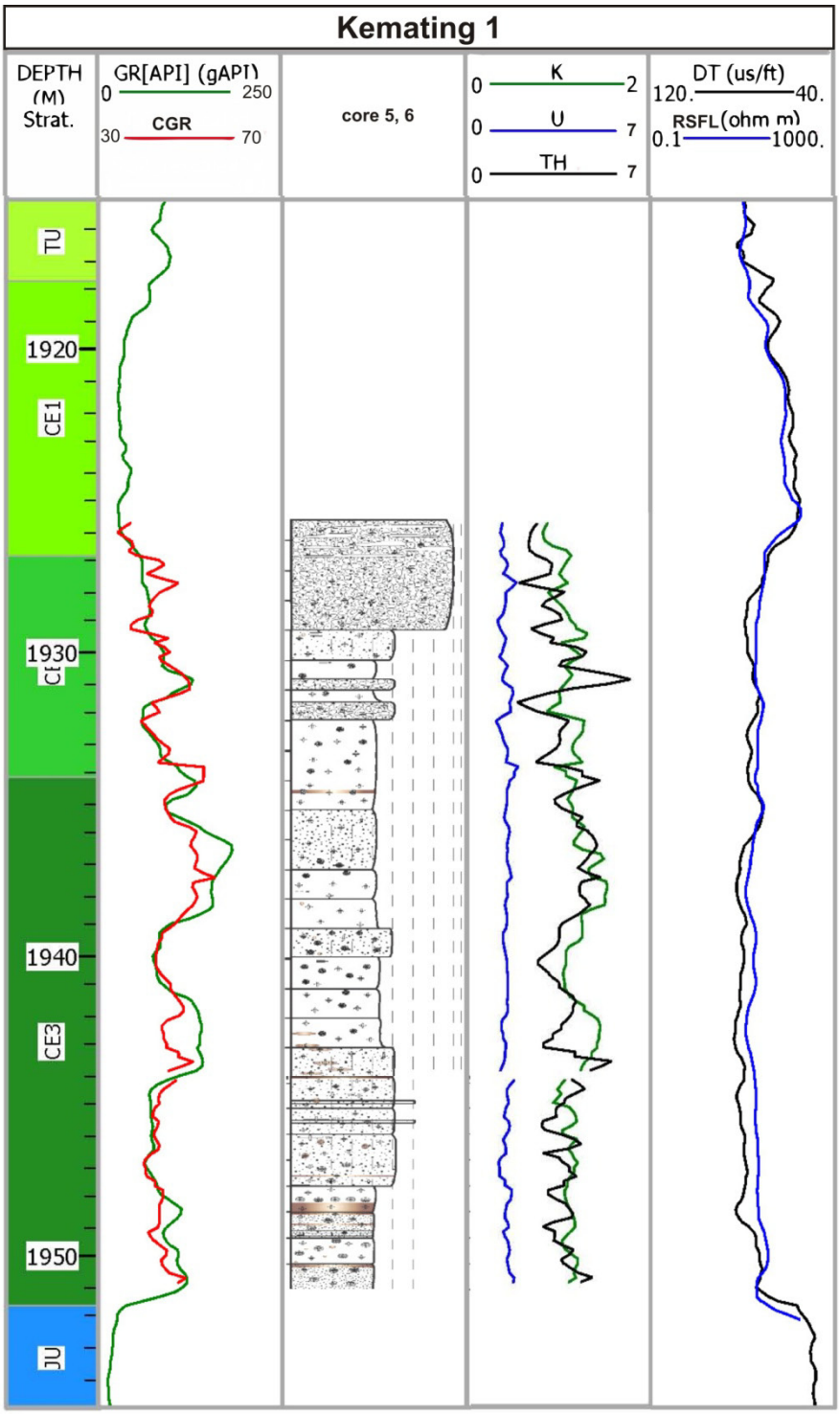

Figure 28: Kemating 1 well logs and shifted CGR, SCGR logs and core interpretation (Schnitzer).

Table 11: CGR, SCGR and core log depth shift for well Kemating 1 core 5 and 6.

Core 5 1924-1942.5 Core recovery 18.5 m		Core 6 1942.5-1950.5 Core recovery 8 m	
MD [m]	Shift [m]	MD [m]	Shift [m]
1927.86	1.145	1943.557	0.797
1929.536	0.672	1946.453	0.025
1930.756	0.440	1947.367	-0.582
1933.651	0.375	1947.977	-0.040
1933.956	0.454	1950.11	-0.101
1937.461	-0.073	1951.177	-0.272
1939.29	-0.120		
1941.728	0.451		
1942.49	1.071		

Kirchham 3

In Figure 29 rescaled and depth shifted CGR and SCGR logs, as well as the interpretation of cores 2 and 3 of well Kirchham 3 are illustrated. The CGR log matches perfectly to the GR log. CGR, SCGR and the core interpretation have been shifted with the values listed in Table 12. A gap between cores 2 and 3 (~1 m) is probably due to lost core.

Well logs are obviously cut off at top and base Cenomanian. According to the completion log, top Jurassic is at approximately 3001 m MD.

Sonic and GR logs look completely different compared to well logs of most neighboring wells. This reflects major differences in lithology.

The red layer is intercalated with thin coarse grained (conglomeratic) sediments. Neither sonic nor resistivity log, which differ considerably indicate a characteristic pattern for the marker bed.

The Turonian marlstone is absent due to erosion. Thus, Cenomanian sandstones are directly overlain by Eocene sandstones and conglomerates at approximately 2960 m MD. The Eocene sandstones are characterized by a remarkable high CGR response. Both K as well as Th reading increase upwards.

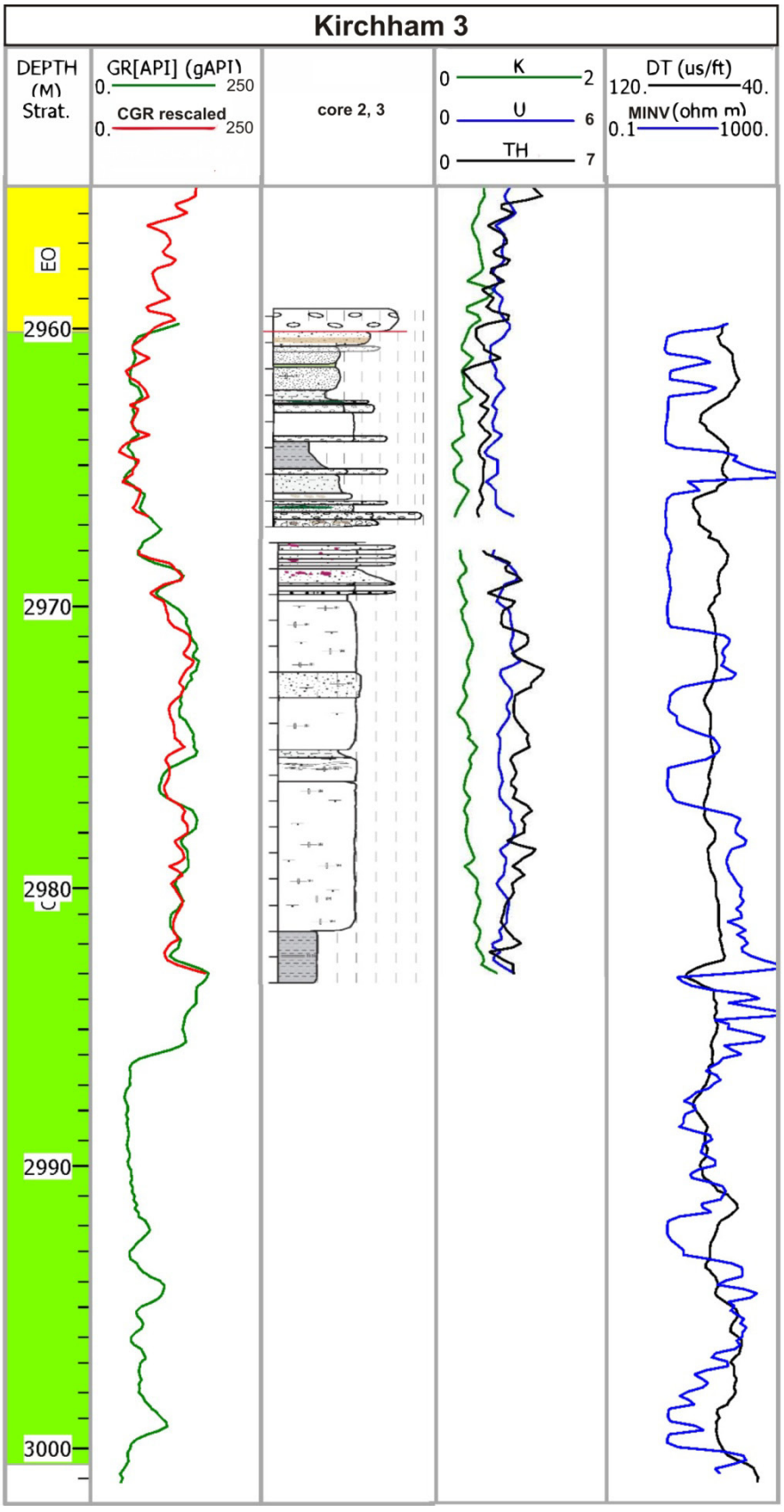

Figure 29: Kirchham 3 well logs and shifted CGR, SCGR logs and core interpretation (Schnitzer).

Table 12: CGR, SCGR and core log depth shift of well Kirchham 3 core 2 and 3.

Core 2 2950-2968 Core recovery 18 m		Core 3 2968-2983.7 Core recovery 15.7 m	
MD [m]	Shift [m]	MD [m]	Shift [m]
2961.132	-0.773	2968.447	-0.330
2961.742	-0.590	2970.124	-0.598
2963.113	-0.605	2972.257	-0.429
2964.79	-0.874	2978.201	-0.932
2965.856	-1.019	2979.115	-0.797
2966.923	-0.909	2982.773	-0.949
		2984.145	-1.348
		2984.297	-1.245
		2984.449	-1.372

Lindach 1

CGR and SCGR logs were measured for cores 6 to 8 from well Lindach 1 (Figure 30). Due to the lack of appropriate well logs, cores could not be depth shifted except core 6 (Table 13).

According to the core boxes 10.5 m out of 17 m were successfully cored. Thus and referring to DT and MINV response core six has been depth shifted to the illustrated position. The available log suite is cut off at base Cenomanian according to geological short profiles.

The K shows a slight upward decrease in its reading from Base to Top Cenomanian. Th and U illustrate almost no variation within the measured interval.

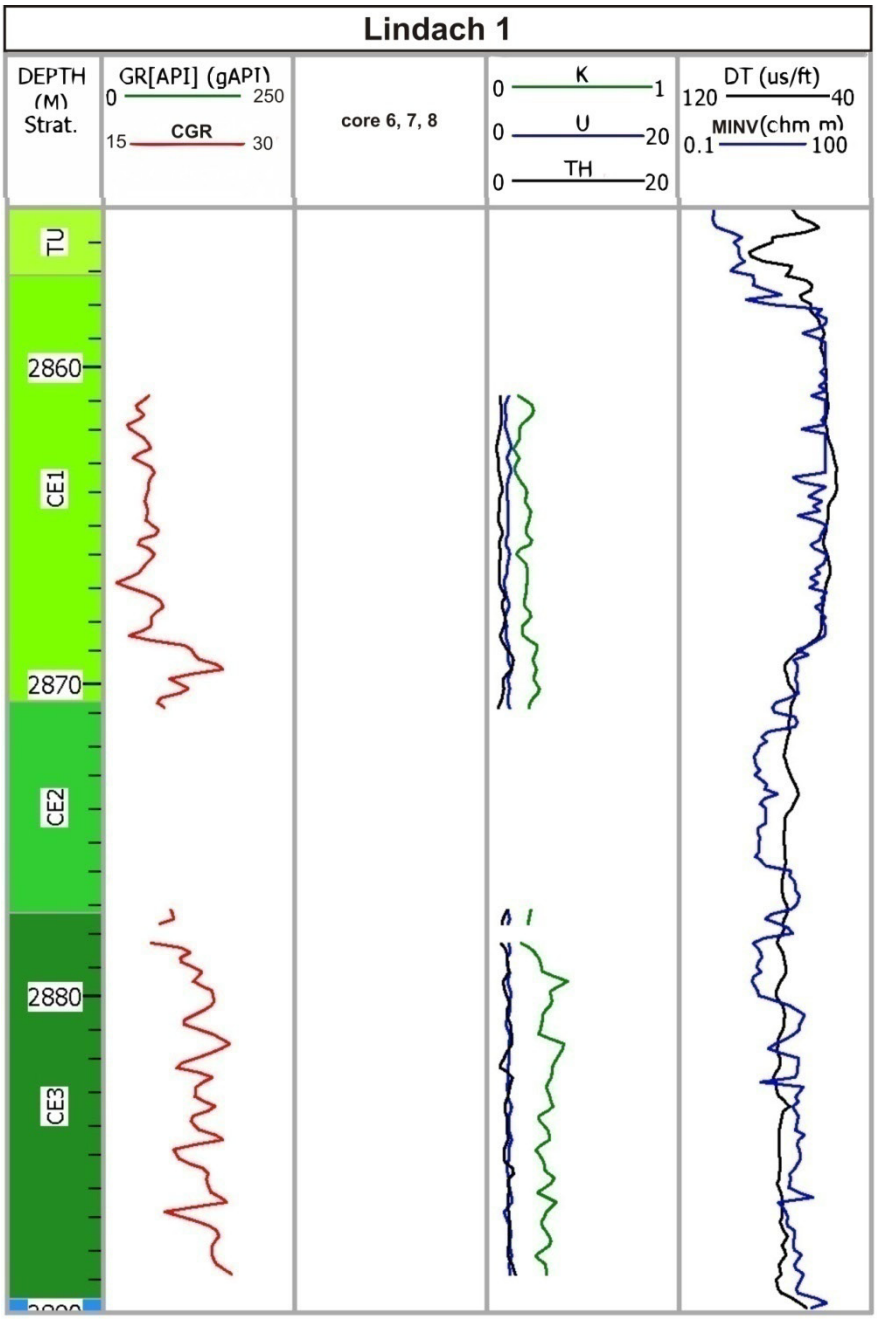

Figure 30: Lindach 1 well logs and shifted CGR and SCGR log.

Table 13: CGR and SCGR log depth shift of well Lindach 1 core 6, 7, 8

Core 6 2860-2877 Core recovery 10.5 m	
MD [m]	Shift [m]
2874.77	-5.904
2875.837	-5.948

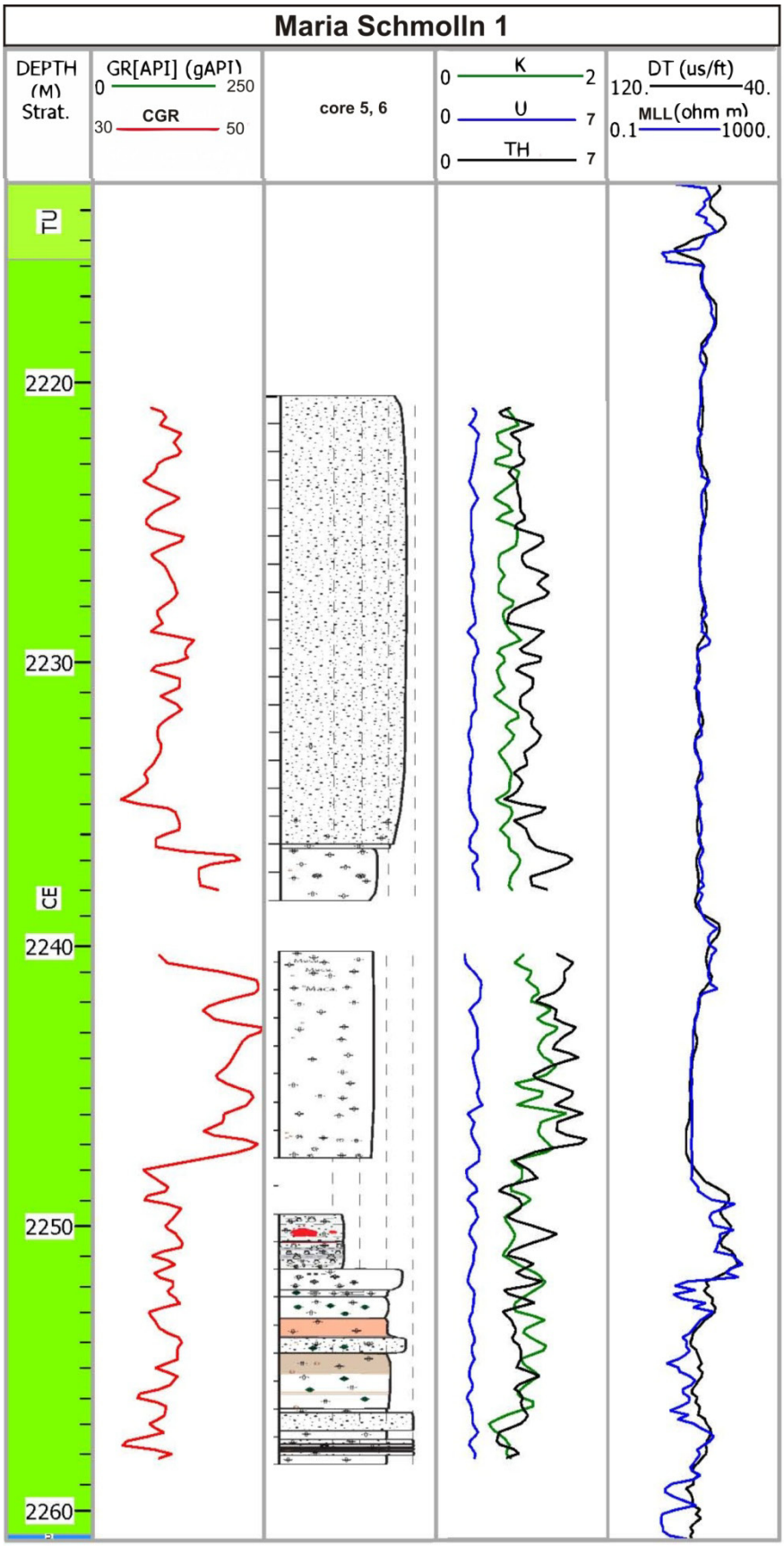

Figure 31: Maria Schmolln 1well logs and shifted CGR, SCGR log and core interpretation (Schnitzer). Apparently 2 core boxes at approximately 2248 m MD have not been interpreted.

Table 14: CGR, SCGR and core log depth shift of well Maria Schmolln 1 core 5 and 6.

Core 5 2221-2239 Core recovery 17.8 m		Core 6 2239-2257 Core recovery 18 m	
MD [m]	Shift [m]	MD [m]	Shift [m]
2224.327	-0.636	2240.938	0.397
2229.661	-0.566		
2237.128	-0.623		

Maria Schmolln 1

Figure 31 illustrates well logs and depth shifted CGR and SCGR logs as well as the depth shifted core description of the well Maria Schmolln 1. Apparently no GR log has been obtained. Therefore, core and SCGR log have been shifted (Table 14) on the basis of the sonic and resistivity log.

The increased CGR values as well as the K response at the base of core 5 and top of core 6 fit very well with the corresponding core interpretation. Hence the increased gamma reading refers to fine grained sandstones, obviously characterized by high glauconite content. The Th log seems to dominate the log response of the CGR log. In any case, the general log response for the Cenomanian of well the Maria Schmolln 1 looks very different compared to most other wells.

Mauern 1

At the well Mauern 1 (Figure 32) only a short Cenomanian interval was cored. It corresponds to a silty to fine grained sandstone, characterized by a upward decrease in its GR log (see also K and Th logs). Although the measured interval is pretty short, the fit between CGR and GR log is very good. Sonic and resistivity logs are similar to those in Maria Schmolln 1. Note the completely different log trend of the GR log compared to the sonic or resistivity log. Both, core interpretation and GR readings suggest a coarsening upward trend. Interestingly, this is not visible in the sonic log.

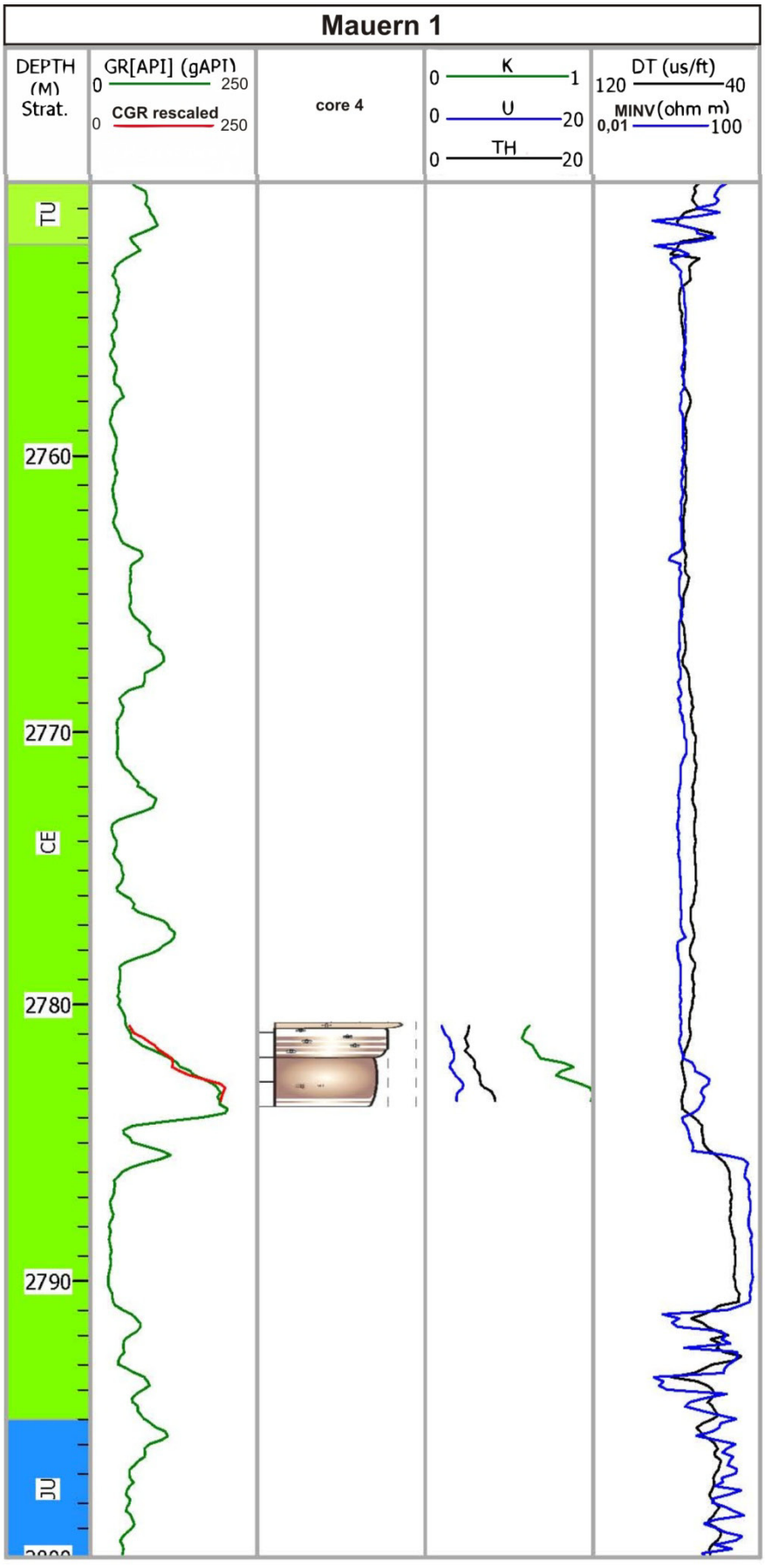

Figure 32: Mauern 1 well logs and shifted CGR, SCGR log and core interpretation (Schnitzer).

Table 15: CGR, SCGR and core log depth shift of well Mauern 1 core 4.

Core 4 2778-2782 Core recovery 3.4 m	
MD [m]	Shift [m]
2778.707	2.159
2780.536	1.661

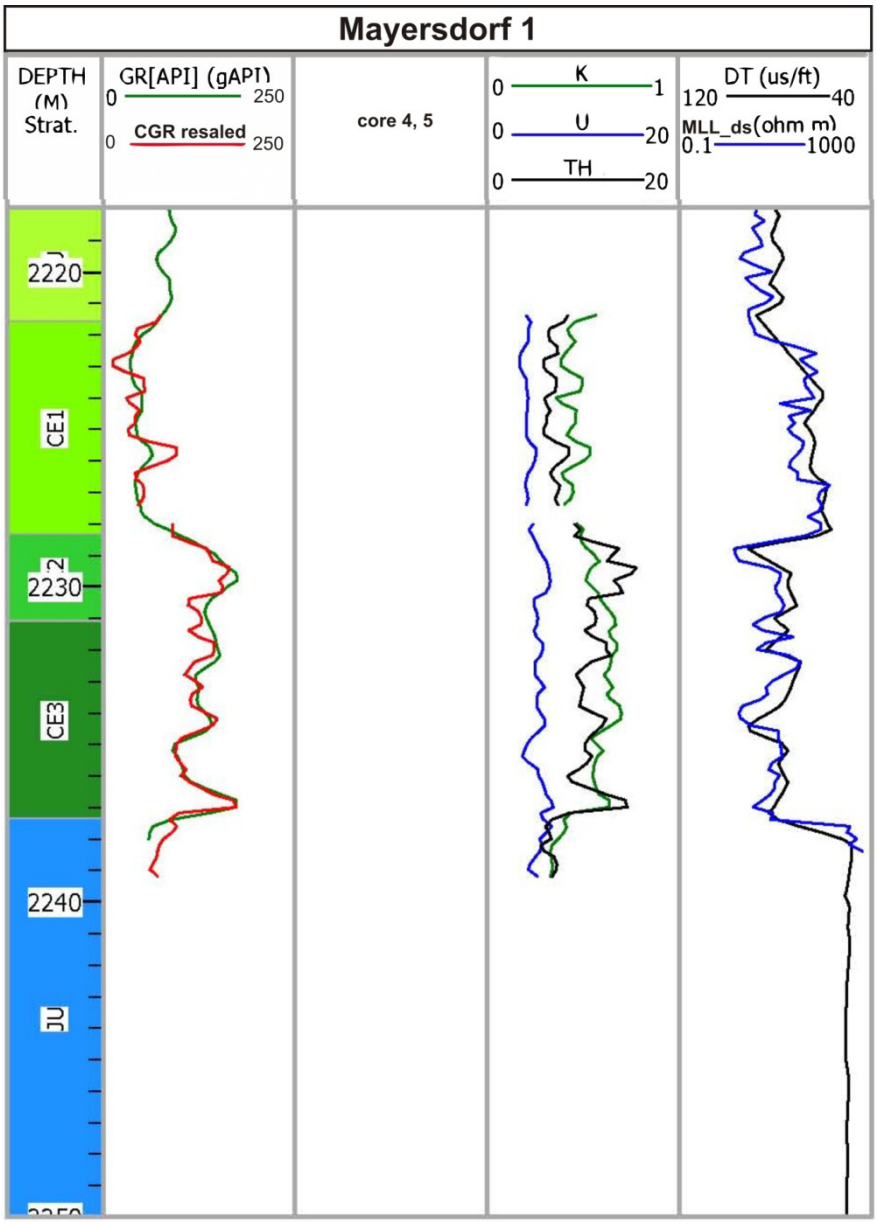

Figure 33: Mayersdorf 1 well logs and shifted CGR, SCGR and MLL log.

Table 16: CGR, SCGR, core and MLL log depth shift of well Mayersdorf 1

Core 4 2224-2230 Core recovery 6 m		Core 5 2230-2242 Core recovery 12 m		MLL
MD [m]	Shift [m]	MD [m]	Shift [m]	Shift [m]
2225.751	-2.915	2232.55	-2.430	0.339
2226.151	-2.675	2234.349	-2.285	
2227.151	-2.754	2236.549	-2.489	
2227.951	-2.581	2237.549	-2.311	
2228.751	-2.357	2238.748	-2.590	

Mayersdorf 1

Core 4 and core 5 of well Mayersdorf 1 (Figure 33) have been shifted upwards by 2 to 3 m relative to the GR log (Table 16) in order to obtain a good fit between the GR and CGR log. The cored interval represents the complete succession of the Cenomanian. It also includes the Jurassic limestones at the base of core 5 and the transition to the Turonian sediments near the top of core 4. Probably the (C)GR log is mainly controlled by Th contents. Together with the K log it decreases upwards from base to top Cenomanian. Especially at base CE3 a considerable Th peak is visible. It might be caused by transgressive sediments rich in (Th-rich) heavy minerals.

Nieder-Thalheim 1

Cores 2, 3, and 4 of well Nieder-Thalheim 1 (Figure 34) have been measured. Based on the flipped sonic log, cores have been shifted upwards by almost 3 m (Table 17). The general fit to the DT log is good. The K response curve suggests, that the CGR trend is mainly controlled by high K contents, which decreases upwards within the Cenomanian section. Below the Cenomanian a thick interval of obviously pre-Cenomanian age appears. On the top it comprises quite low (S)CGR values. The lower pre–Cenomanian refers just to a short cored section, which is characterized by slightly increased K reading. The pre-Cenomanian is underlain by Upper Jurassic limestones. Note the sharp transition between PCE and CE. Base Cenomanian was identified using log correlation profiles (next chapter) and core interpretation. Due to lithological change and a general differing well log response, base Cenomanian has been interpreted at approximately 2191 m MD.

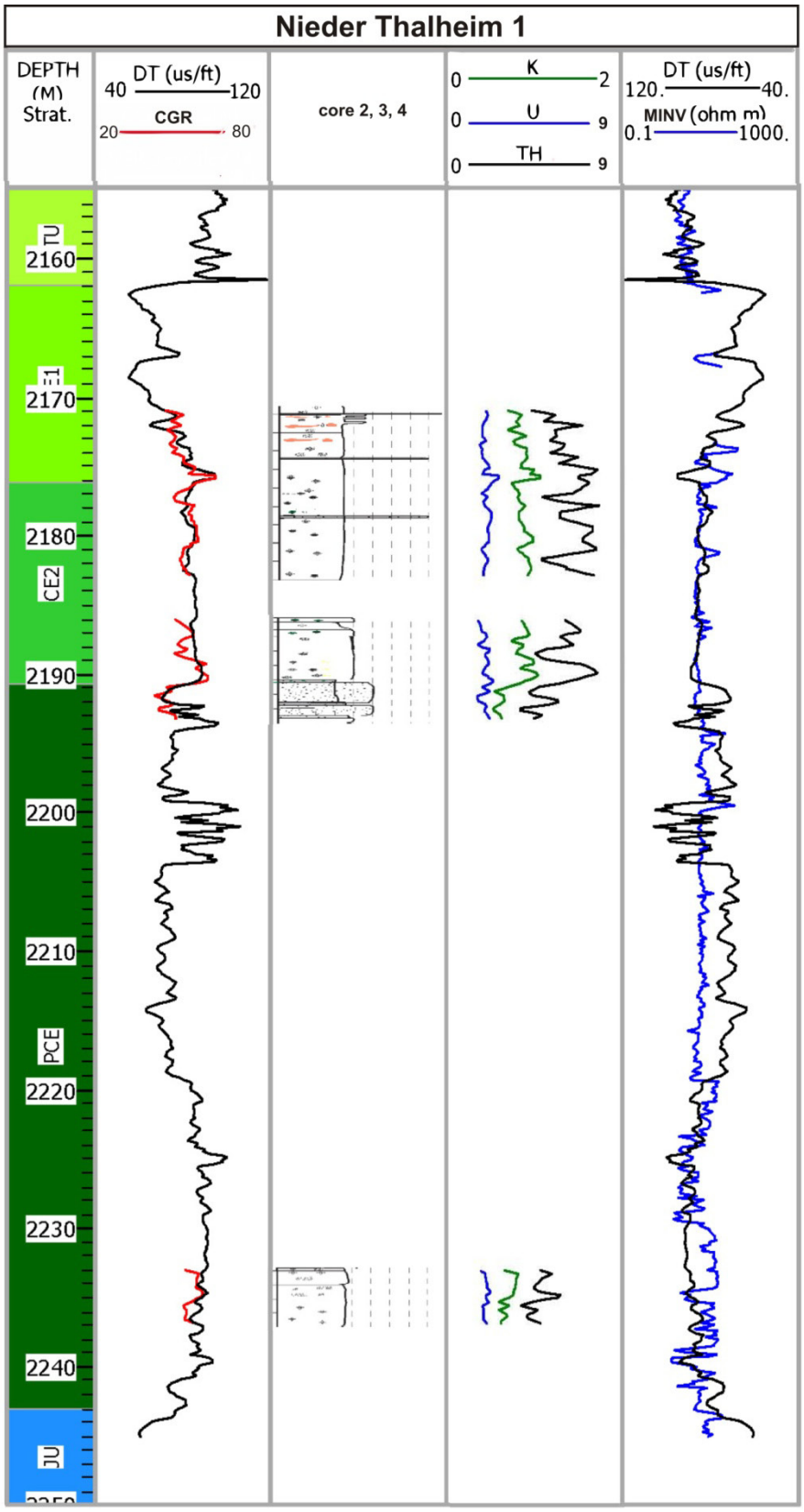

Figure 34: Nieder-Thalheim 1 well logs and shifted CGR, SCGR log and core interpretation (Schnitzer).

Table 17: CGR, SCGR and core log depth shift of well Nieder-Thalheim 1

Core 2 2173-2183.5 Core recovery 9.5 m		Core 3 2183.5-2192 Core recovery 7.3 m		Core 4 2235-2245.5 Core recovery	
MD [m]	Shift [m]	MD [m]	Shift [m]	MD [m]	Shift [m]
2173.425	-2.408	2187.75	2.761	2238.042	-2.913
2176.93	-2.382				
2178.302	-2.679				
2180.588	-2.544				
2181.807	-0.769				
2182.264	-0.510				
2182.721	-0.046				

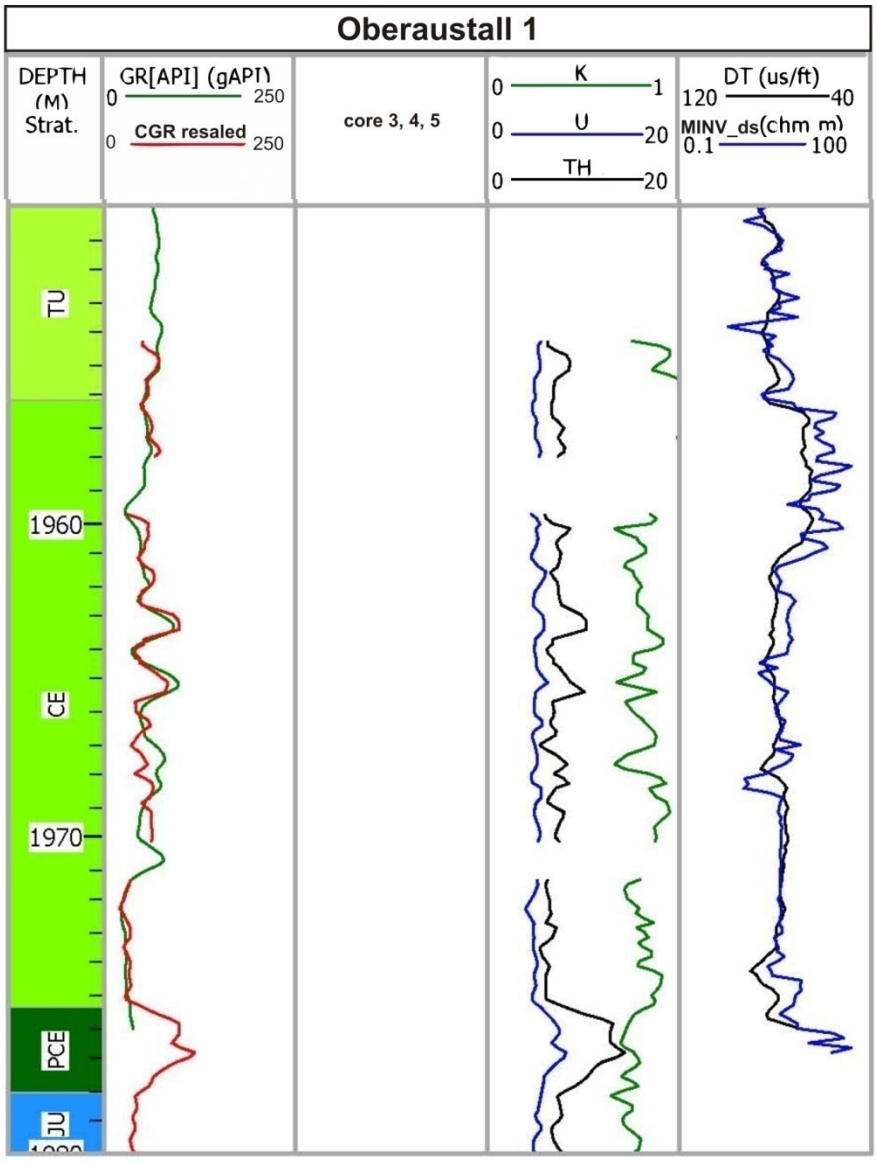

Figure 35: Oberaustall 1 well logs and shifted CGR, SCGR and MINV log.

Oberaustall 1

Figure 35 illustrates the well logs and shifted CGR, SCGR logs of well Oberaustall 1. The general match to the GR log is good. Obviously 2 m of core are missing at approximately 1958 m MD. Furthermore, at 1970 m a short interval is missing. On the basis of the border to the Upper Jurassic limestones the top of the Jurassic formation could be confidentially interpreted. The Jurassic carbonates are overlain by a organic rich layer characterized by a Th peak. By means of the boundary of Cenomanian sandstones to the Turonian marlstones, top Cenomanian could be clearly defined. The CGR log is strongly influenced by the Th log.

Table 18: CGR, SCGR and core log depth shift of well Oberaustall 1 core 3, 4, 5 and MINV log.

Core 3 1952-1956 Core recovery 4.8 m		Core 4 1956-1968.2 Core recovery 12.2 m		Core 5 1968.2-1978.5 Core recovery 10.3 m		MINV
MD [m]	Shift [m]	MD [m]	Shift [m]	MD [m]	Shift [m]	Shift [m]
1952.445	1.963	1956.255	3.543	1969.667	2.814	0.717
1953.512	1.997	1958.389	2.945	1970.581	2.207	
1954.731	1.827	1960.065	2.368	1971.8	1.602	
1955.493	1.448	1960.98	2.528	1974.239	1.415	
1955.646	1.501	1961.285	2.762			
		1961.742	2.842			
		1962.199	2.871			
		1964.79	2.890			
		1966.619	2.418			

Oelling 1

Figure 36 shows the well logs for well Oelling 1 and the interpretation of cores 1 and 2. The cores have been slightly depth shifted (Table 19).

The Cenomanian succession is characterized by a roughly continuous upward increased GR response, mainly driven by the increased K reading. U and Th play a minor role, only at the bottom of the measured interval of core 2 the Th response increases. According to the “geologic short profile” provided by RAG, base Cenomanian (=Top Jurassic) is located at 3002.5 m MD.

The Cenomanian sandstones are overlain by Eocene sandstones. The border is well visible in the well logs.

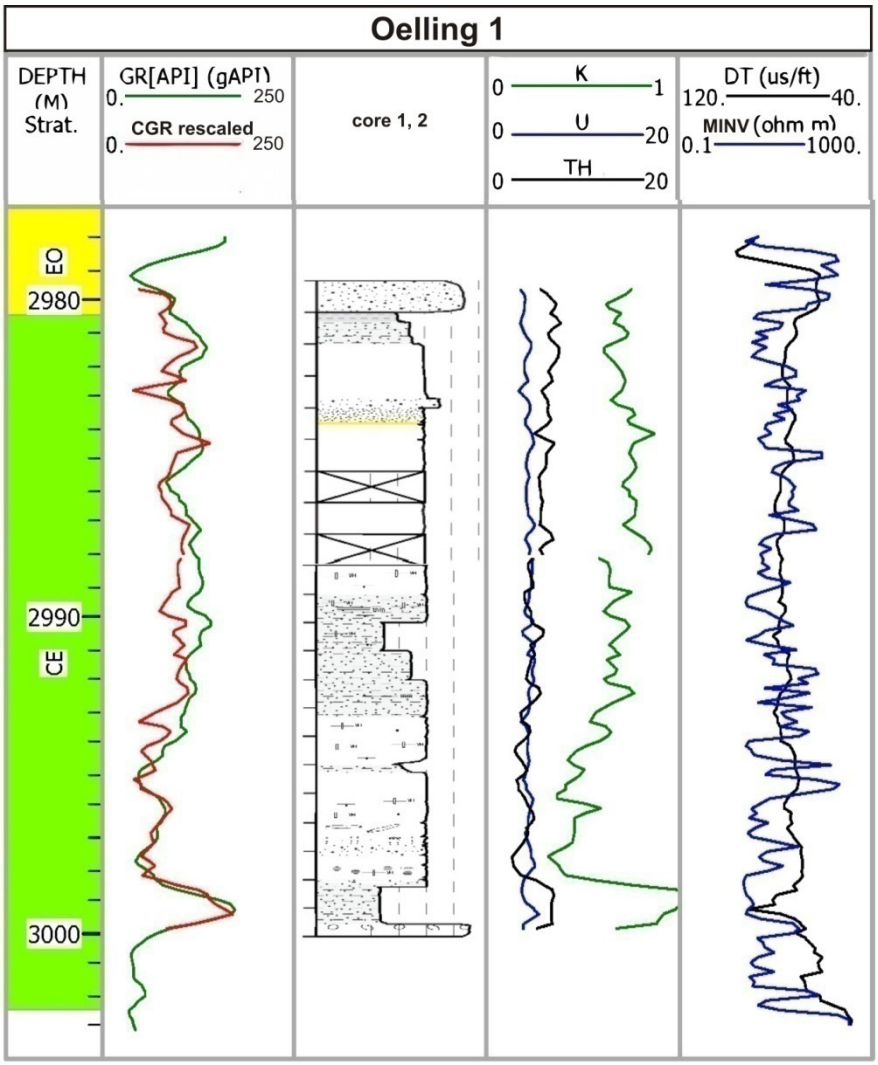

Figure 36: Oelling 1 well logs and shifted CGR, SCGR log and core interpretation.

Table 19: CGR, SCGR and core log depth shift of well Oelling 1 core 1 and 2.

Core 1 2970-2988 Core recovery 18 m		Core 2 2988-3002.5 Core recovery 12.7 m	
MD [m]	Shift [m]	MD [m]	Shift [m]
2979.621	0.284	2988.308	-0.158
2981.298	0.066	2994.252	-0.548
2985.87	0.049	2995.471	-0.616
2986.937	0.364	2996.233	-0.457
		3000.195	-0.786

Redltal 1

Figure 37 illustrates the well logs and depth shifted core interpretations for well Redltal 1. The measured CGR curve matches very well with the obtained GR log. Cores 4, 5 and 6 have been depth shifted according to Table 20.

The CGR reading is mainly dominated by K and Th contents. Core 5 includes at ~2752 m MD a limestone layer, more than 2 m thick, which is easily recognizable in the logs by its low (S)CGR response. The red layer and the marker bed are absent.

The Cenomanian sandstones are overlain by Eocene sandstones comprising high resistivity and low to moderate GR values.

Table 20: CGR, SCGR and core log depth shift of well Redltal 1 core 4, 5 and 6.

Core 4 2742-2760 Core recovery 17.6 m		Core 5 2760-2778 Core recovery 18 m		Core 6 2778-2791 Core recovery 8.8 m	
MD [m]	Shift [m]	MD [m]	Shift [m]	MD [m]	Shift [m]
2744.468	1.248	2762.908	0.179	2778.758	1.460
2745.382	1.588	2765.804	0.815	2779.063	1.488
2746.449	1.698	2766.718	0.694	2779.672	1.364
2747.821	1.555	2772.357	0.557	2780.129	1.086
2748.583	1.637	2773.881	0.773	2780.587	0.859
2750.107	1.586	2776.777	0.513	2781.958	1.202
2750.107	1.586	2777.996	0.783		
2758.489	1.312				

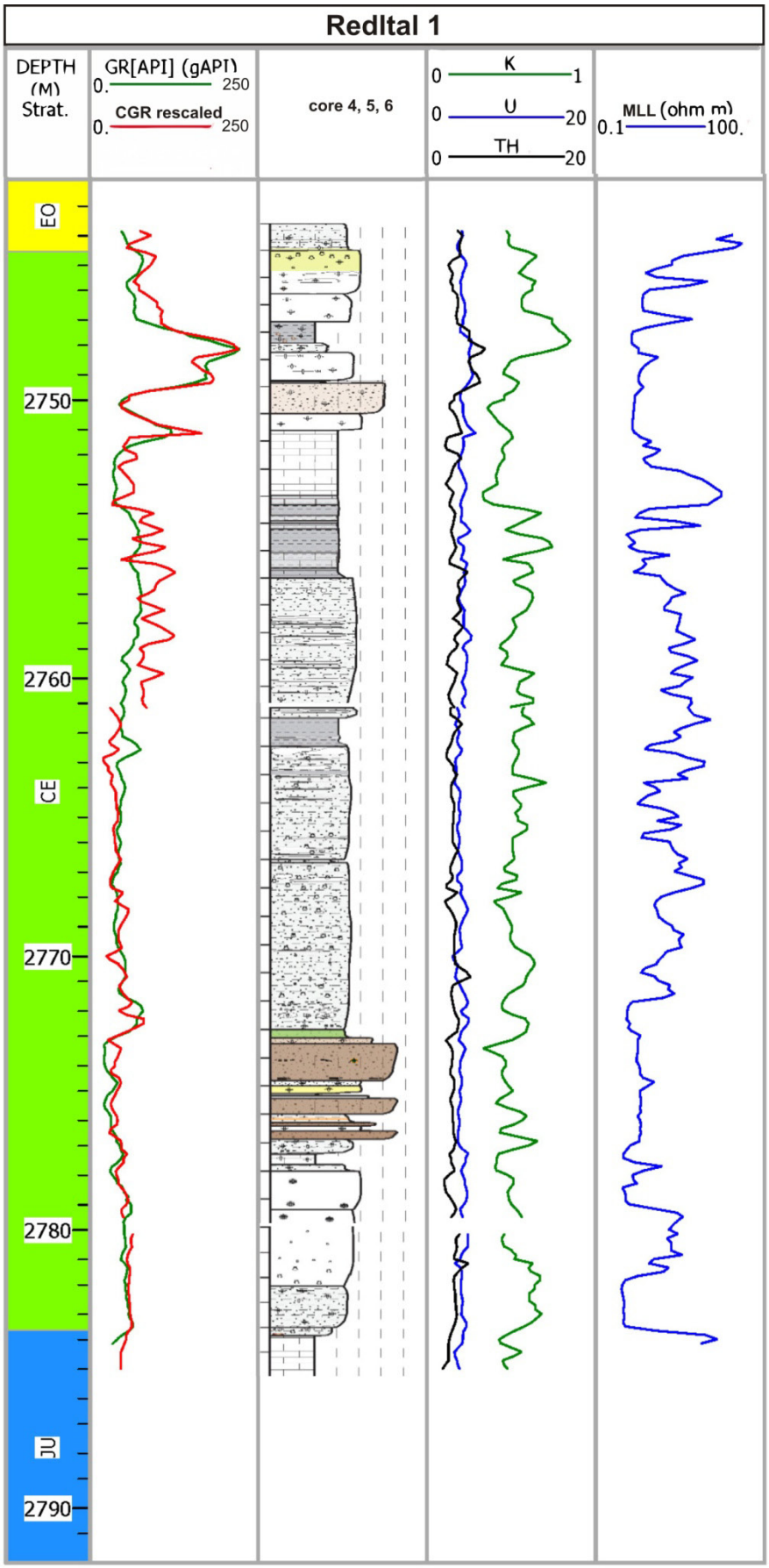

Figure 37: Redltal 1 well logs and shifted CGR, SCGR log and core interpretation (Schnitzer).

Renging 1

Figure 38 illustrates well and core logs for well Renging 1. CGR as well as SCGR logs have been depth shifted according to Table 21. The general fit to the obtained GR log is moderate.

All obtained well logs terminate at base Cenomanian, which refers to Top Jurassic according to geologic short profiles. The SCGR log response suggests that the CGR is dominated by the K contents. The latter decreases upwards from base to top of core 3. Both U and Th have only minor influence on the (S)CGR logs The marker bed at base CE1 is not clearly visible in the DT and resistivity log.

Table 21: CGR, SCGR log depth shift of well Renging 1 core 3.

Core 3 2398-2416 Core recovery 18 m	
MD [m]	Shift [m]
2403.854	-0.828
2406.14	-0.888
2412.541	-1.045
2416.198	-0.838

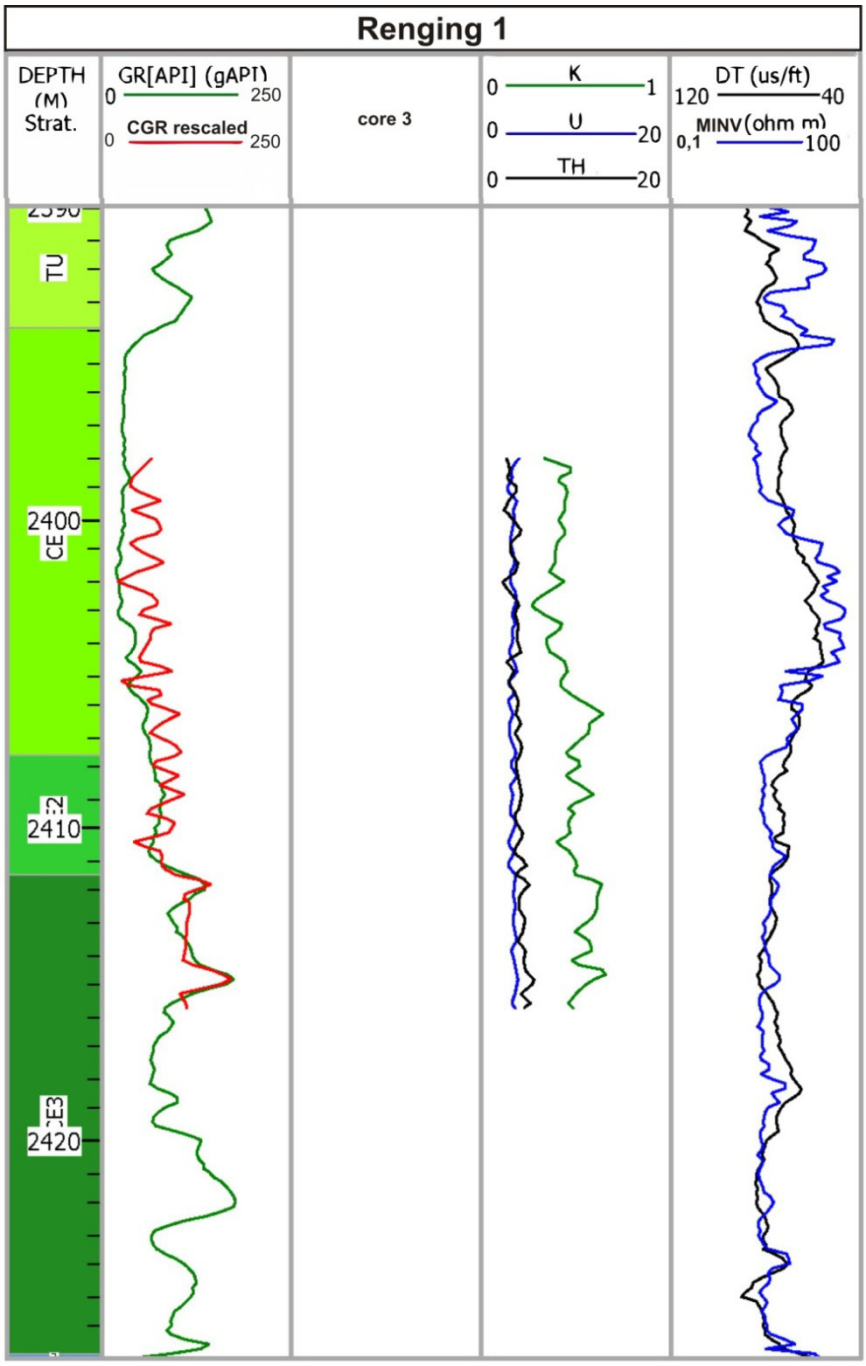

Figure 38: Renging 1 well logs and shifted CGR, SCGR log.

Sattledt 1

Cores 2 and 3 from well Sattledt 1 (Figure 39) have been measured and depth shifted (Table 22). The match to the GR log of core 2 is poor. Because of the absence of well (GR) log data, core 3 could not be depth shifted. The Th as well as the K response is slightly higher in the lower core 3.

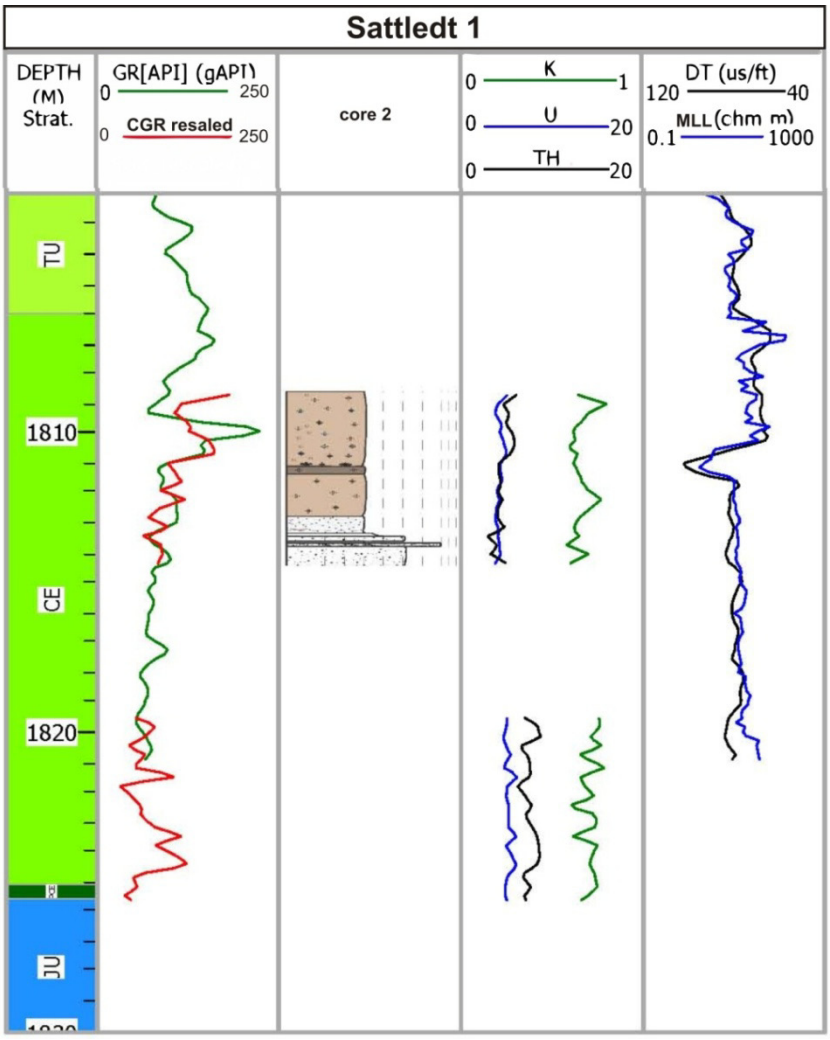

Figure 39: Sattledt 1 well logs and shifted CGR, SCGR logs and core interpretation (Schnitzer).

Table 22: CGR, SCGR and core log depth shift of well Sattledt 1 core 2.

Core 2 1804-1819 Core recovery 7 m	
MD [m]	Shift [m]
1809.646	-0.444
1811.628	-0.762
1814.523	-1.021

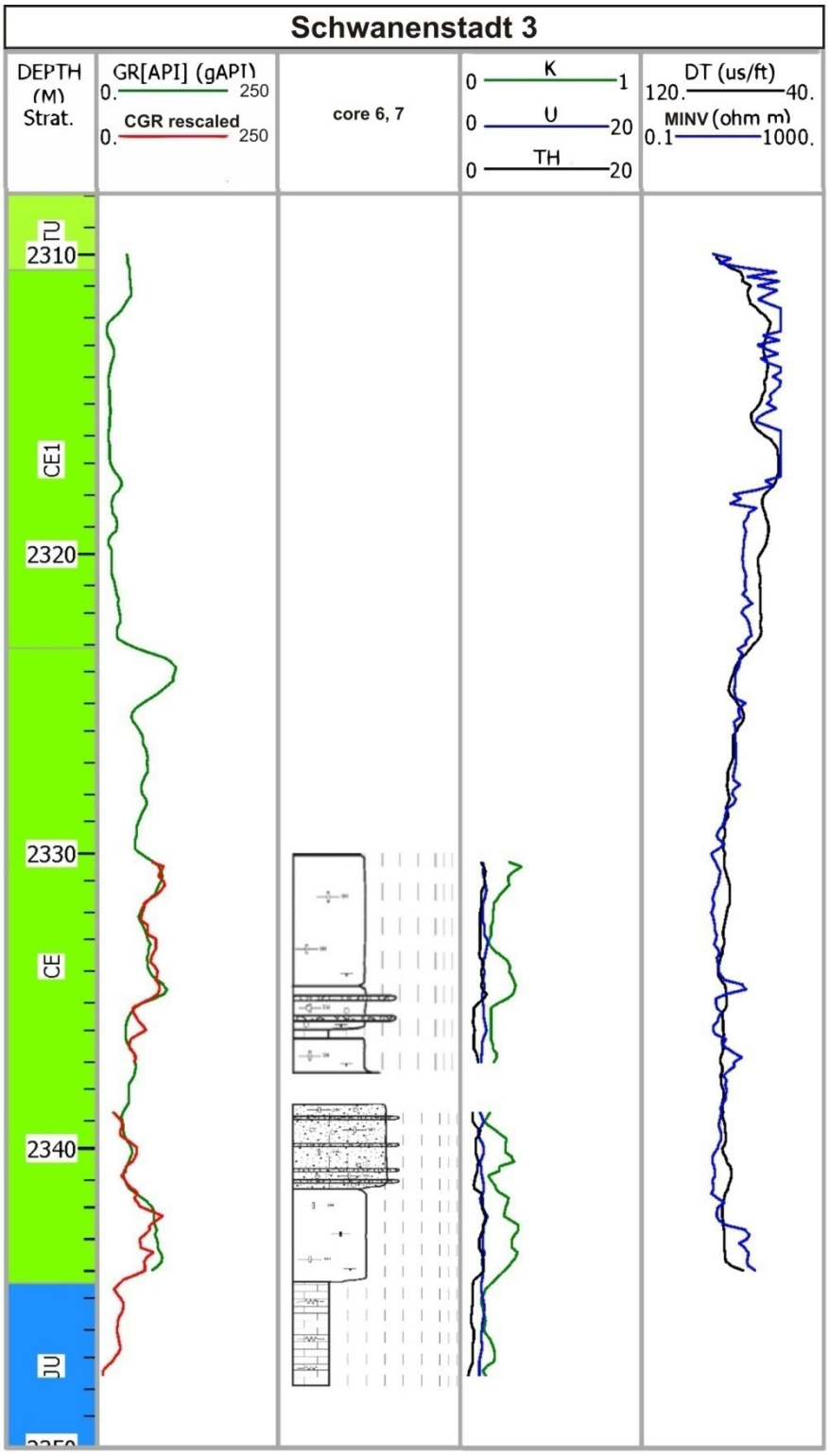

Figure 40: Schwanenstadt 3 well logs and shifted CGR, SCGR logs and core interpretation (Schnitzer).

Schwanenstadt 3

Figure 40 illustrates the facies and well log successions of core 2 and 3 for the well Schwanenstadt 3 covering the lower parts of the Cenomanian. The match to the

obtained GR log is very good. With the border of Jurassic limestones to the Cenomanian sandstones it was possible to define Top Jurassic and to depth shift (Table 23) and clip the CGR exactly to the GR log. The CGR and GR response suggests that most of the radioactive content correspond to the K reading. U and Th play a minor role. Obviously two meters of the core were lost at approximately 2337m MD.

Table 23: CGR, SCGR and core log depth shift of well Schwanenstadt 3 core 6 and7.

Core 6 2329-2339.5 Core recovery 8.3 m		Core 7 2339.5-2349 Core recovery 9.5 m	
MD [m]	Shift [m]	MD [m]	Shift [m]
2329.281	1.027	2340.254	-1.122
2330.653	0.525	2341.169	-1.166
2331.415	0.787	2341.931	-0.828
2331.72	1.429	2342.845	-1.128
2332.482	1.307	2343.455	-1.277
2333.549	1.059	2344.217	-0.964
2335.225	1.302	2345.131	-1.111

Steinhaus N1

For the well Steinhaus N1 (Figure 41) core 2 has been measured, depth shifted (Table 24) and interpreted. Core 2 includes crystalline basement (Bohemian Massif), pre–Cenomanian (Jurassic?) sandstones, intercalated with fine grained and carbonatic layers, and 1 m of the Cenomanian succession. Even though well logs have been cut off at base Cenomanian, the core could be depth shifted to the correct position.

Obviously the K as well as the Th is upward decreasing in the pre–Cenomanian strata. The base of the Cenomanian succession is characterized by a major Th peak. Note also the GR peak in Cenomanian rocks at approximately 1658 m MD.

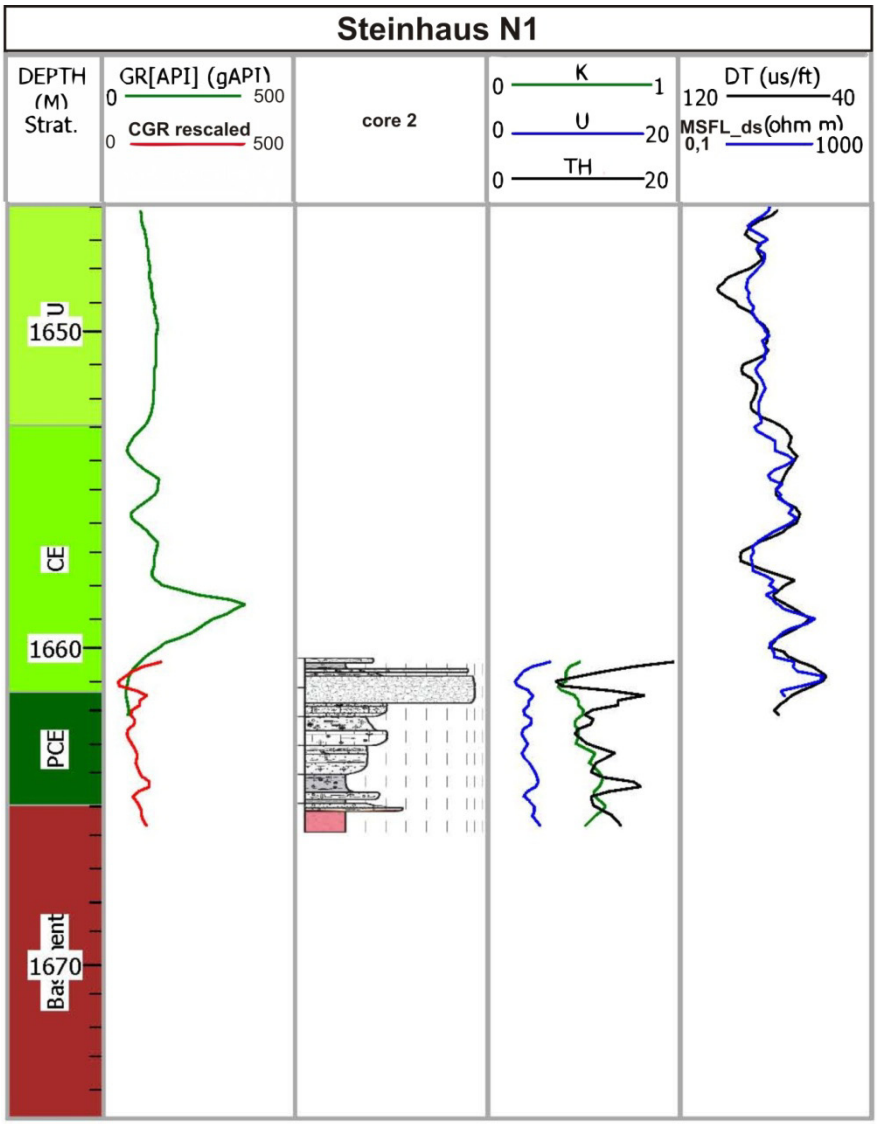

Figure 41: Steinhaus N1 well logs and shifted CGR, SCGR log and core interpretation (Schnitzer).

Table 24: CGR, SCGR and core log depth shift of well Steinhaus N1 core 2.

Core 2 1660-1678 Core recovery 18 m	
MD [m]	Shift [m]
1661.361	-0.177
1661.666	-0.328
1661.971	-0.198

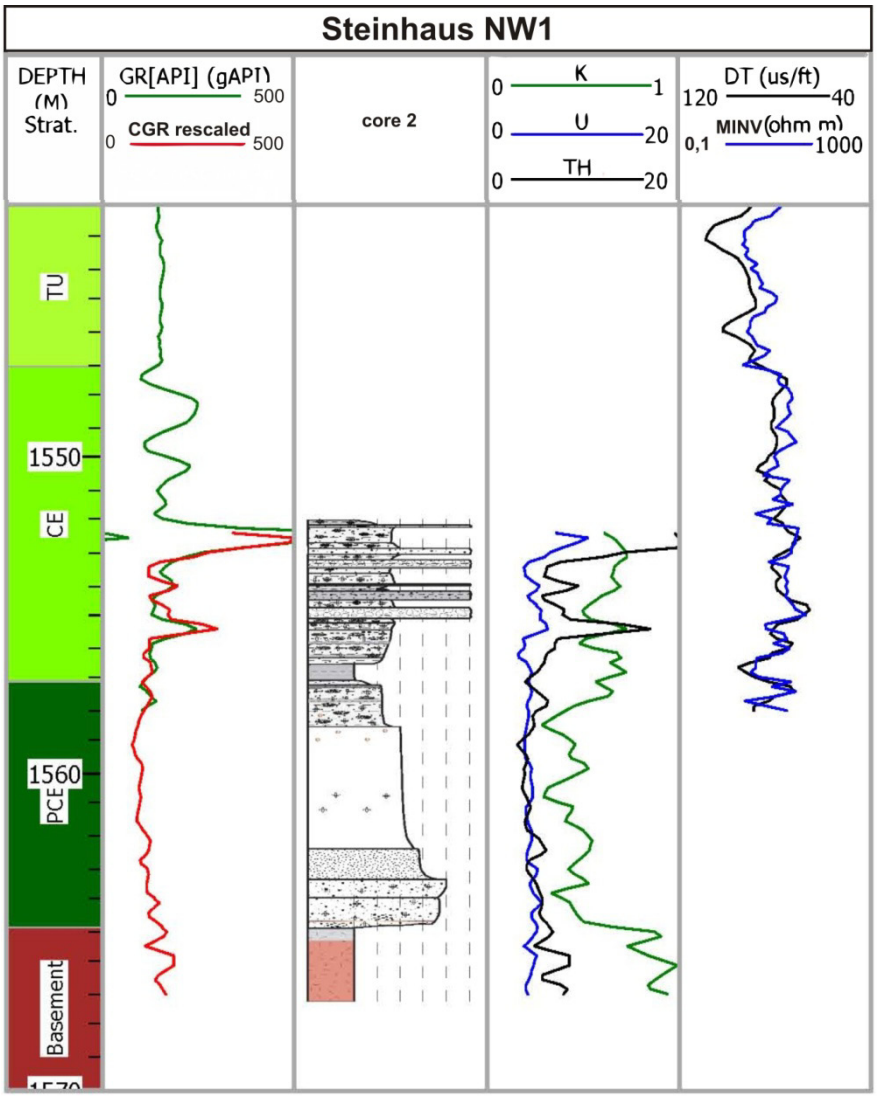

Figure 42: Steinhaus NW1 well logs and shifted CGR, SCGR log and core interpretation (Schnitzer).

Table 25: CGR, SCGR and core log depth shift of well Steinhaus NW1 core 2.

Core 2 1551-1569 Core recovery 19 m	
MD [m]	Shift [m]
1551.633	0.733
1552.852	0.665
1553.157	0.514
1553.309	0.566
1554.833	0.603
1556.662	0.284

Steinhaus NW1

Core 2 from well Steinhaus NW 1 includes crystalline basement, pre–Cenomanian (Jurassic?) and Cenomanian rocks, about 5 m thick (Figure 42). A depth shift according to Table 25 results in a very good fit between GR and CGR in the Cenomanian succession.

The rocks of the Bohemian Massif are characterized by high Potassium readings, while the pre–Cenomanian sediments show lower values. Two Th peaks in fine-medium grained sandstones occur near the base of the Cenomanian.

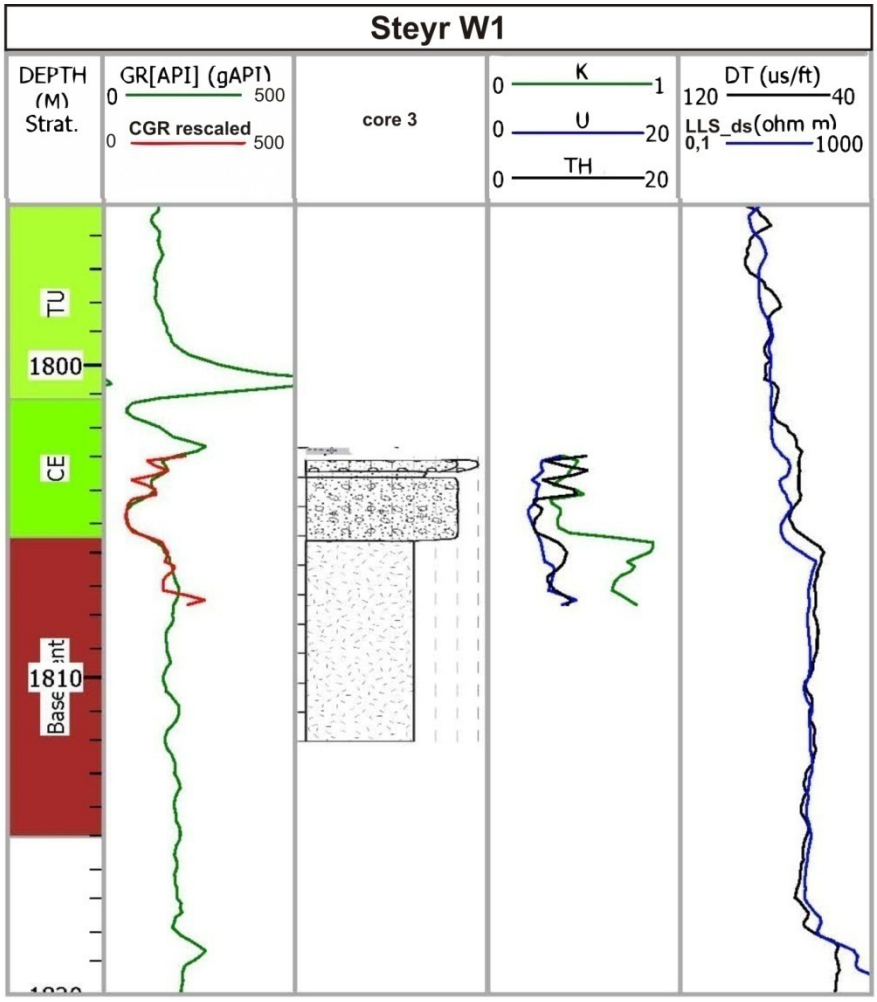

Figure 43: Steyr W1 well logs and shifted CGR, SCGR logs and core interpretation (Schnitzer).

Steyr W1

Figure 43 illustrates well logs of well Steyr W1 together with results from the depth shifted core 3 (Table 26). Core 3 includes crystalline basement rocks, characterized by high K (and slightly elevated Th and U) contents, and a few metres of Cenomanian sandstones. The total thickness of the Cenomanian succession is apparently less than five meters. The core gamma ray match to the obtained GR log is very good.

Table 26: CGR, SCGR and core log depth shift of well Steyr W1 core 2.

Core 3 1802.2-1811.6 Core recovery 9.4 m	
MD [m]	Shift [m]
1802.788	0.638
1803.855	0.236
1805.074	0.194
1807.36	-0.019

Voitsdorf 1

For the well Voitsdorf 1 (Figure 44) five cores have been measured, interpreted and depth shifted (Table 27). The principal match to the obtained GR log is moderate to good. Well logs are obviously cut off at base Cenomanian.

The PCE (Jurassic?) in the Voitsdorf 1 well is characterized by a significant upward decrease in the K log, which apparently acts as dominant source for the total GR log. Both U and Th play a minor role. Referring to geological short profiles Cenomanian sandstones overlay the Jurassic, core interpretation suggest pre-Cenomanian above the Jurassic limestones.

Wendling 1

Cores 3 and 4 from well Wendling 1 (Figure 45) have been measured and depth shifted (Table 28). The CGR has been correlated with the sonic log, due to the missing GR log data. The values are original in [cps] and cannot be directly compared to [API] units.

The border between Jurassic and Cenomanian sediments is clearly evident, comprising a sharp edge with low radioactive content in the Jurassic limestone.

Obtained well logs are cut off at base Cenomanian, which obviously refer to top Jurassic. Estimated CGR is mainly dominated by the reading of the K and Th log. The upward decrease Thorium response is remarkable especially in the lower parts. The general trend of the CGR log reflects an upward decrease from base to top Cenomanian in its total as well as in its spectral reading.

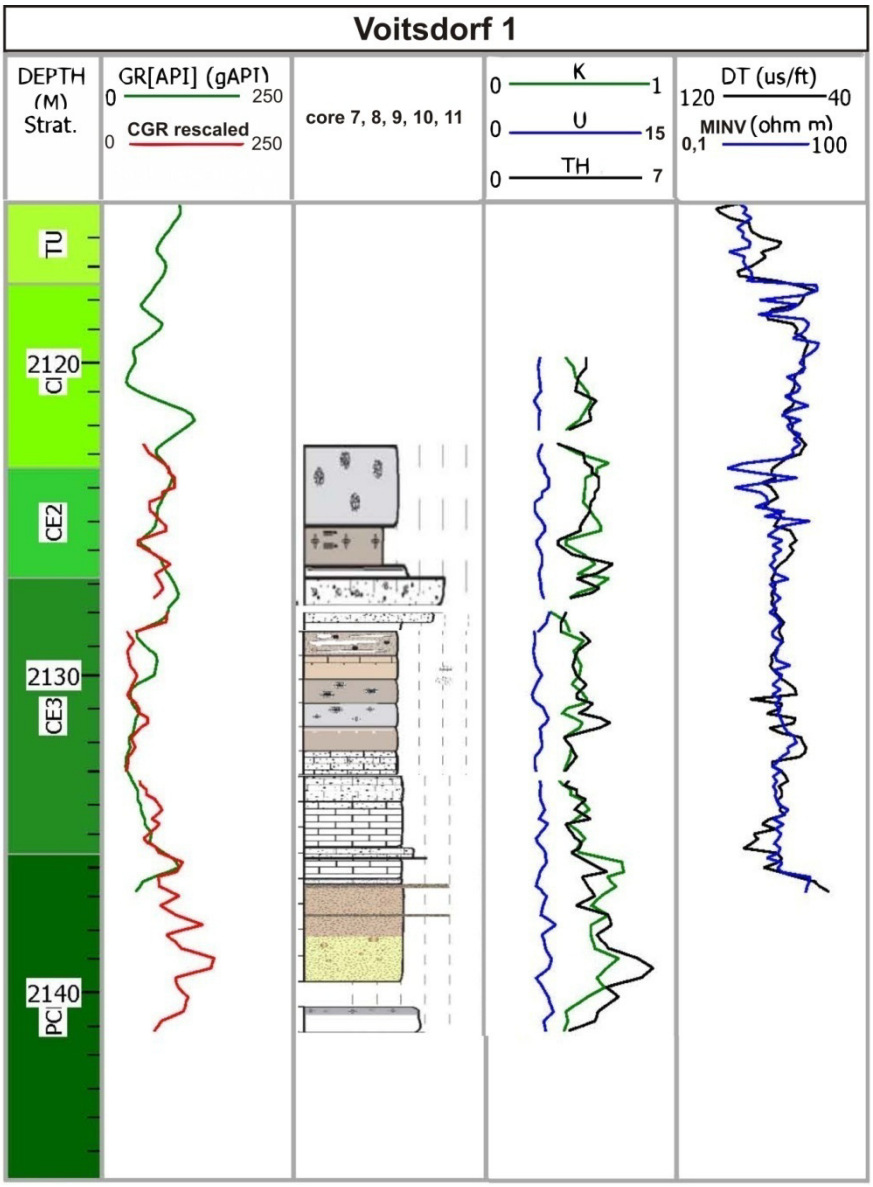

Figure 44: Voitsdorf 1 well logs and shifted CGR, SCGR log and core interpretation (Schnitzer).

Table 27: CGR, SCGR and core log depth shift of well Voitsdorf 1 core 7, 8, 10 and 11.

Core 7 2120-2123 Core recovery 2.65 m		Core 8 2123-2128 Core recovery		Core 10 2129-2135 Core recovery 5.3 m		Core 11 2135-2144 Core recovery 9.3 m	
MD [m]	Shift [m]	MD [m]	Shift [m]	MD [m]	Shift [m]	MD [m]	Shift [m]
2121.714	-0.238	2124	-0.583	2129.182	-0.569	2135.278	-2.390
		2124.305	-0.028	2130.401	-0.559	2137.106	-2.254
		2125.372	0.103	2130.401	-0.559	2138.173	-2.336
		2125.524	0.227	2131.163	-0.554	2138.173	-2.333
		2125.677	0.243	2132.229	-1.114	2138.63	-2.365
		2126.134	0.324	2133.449	-1.212		
		2127.353	0.056				

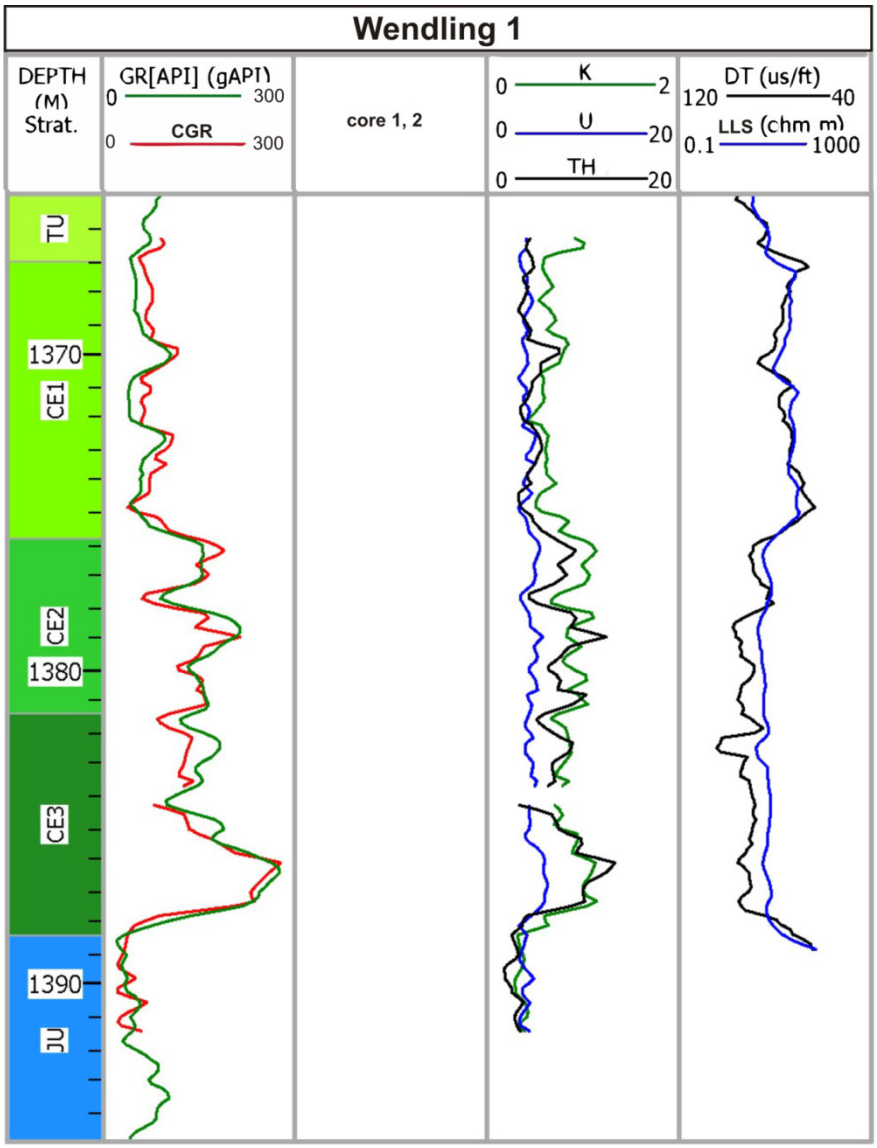

Figure 45: Wendling 1 well logs and shifted CGR, SCGR log.

Table 28: CGR, SCGR log depth shift of well Wendling 1 core 1 and 2.

Core 1 1365-1383 Core recovery 18 m		Core 2 1383-1401 Core recovery	
MD [m]	Shift [m]	MD [m]	Shift [m]
1365.705	1.106	1383.536	0.708
1368.906	1.079	1385.212	0.669
1374.087	0.555	1389.175	0.648
1375.002	0.510	1389.784	0.744
1379.421	0.467		
1381.25	0.301		
1383.536	0.062		

Wolfersberg 1

For the well Wolfersberg 1 core 4 has been measured (Figure 46) and depth shifted (Table 29). One meter is missing in the present study because it was impossible to remove core – box from the rack without destroying it.

The general fit to the GR log is very good. Primarily the K log decreases upward from base to top of the cored interval. The top of core 4 includes the border with the Eocene sandstones.

Table 29: CGR, SCGR log depth shift of well Wolfersberg 1 core 4.

Core 4 2151-2169 Core recovery 18 m	
MD [m]	Shift [m]
2164.69	-1.323
2164.842	-1.470
2166.671	-0.901
2167.128	-0.867
2167.128	-0.858
2167.585	-0.233
2167.738	-0.370
2168.5	-0.334
2168.652	-0.379

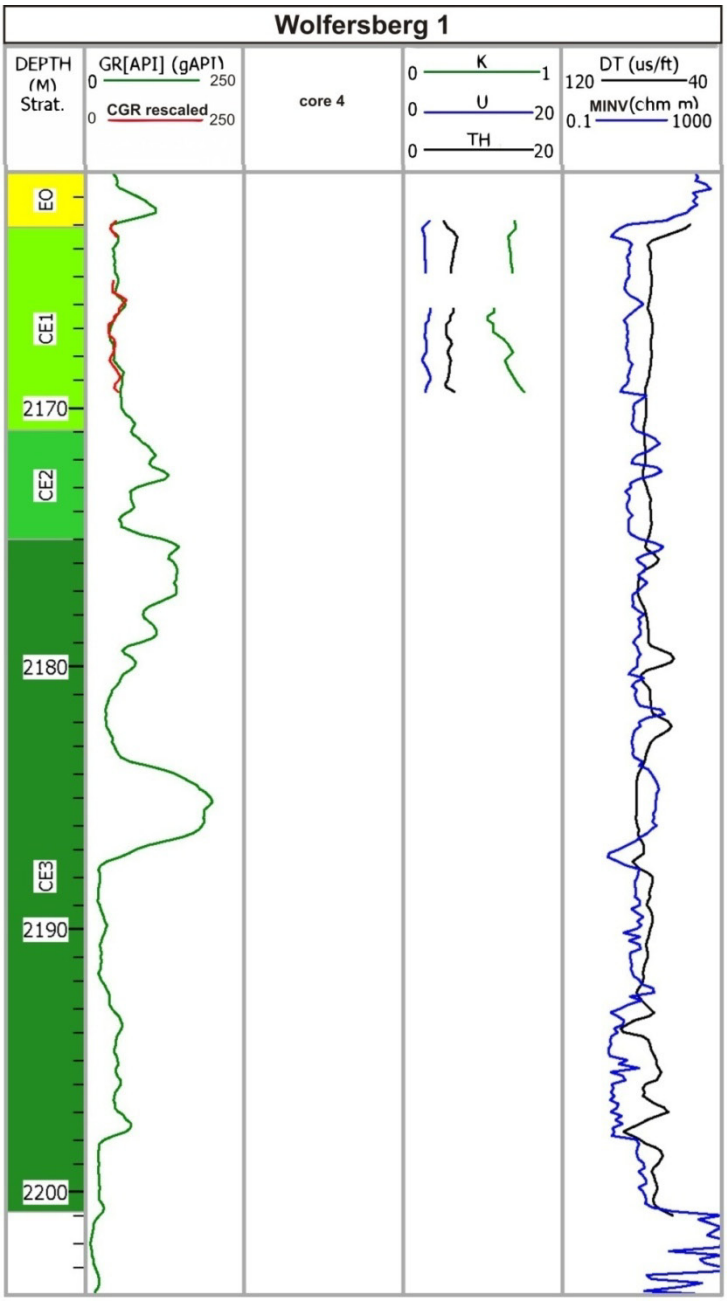

Figure 46: Wolfersberg 1 well logs and shifted CGR, SCGR log.

4.2 Well Log Correlation Profiles

Three NW-SE and three W-E trending log correlation profiles (Figure 47) including Cenomanian strata from 58 wells were created. Based on the Type Log Trattnach 7 and its characteristic log patterns (Figure 48), top and base of the Cenomanian could be identified with certainty. Furthermore the Cenomanian could be subdivided, especially in the area of the Trattnach Field into the subunits CE1, CE2 and CE3 (Nachtmann, 1995). In some wells Cretaceous sediments overlie sandstones, which are either Early Cretaceous ("pre – Cenomanian"; Schutzfels Formation acc. Wilmsen et al., 2010) or Jurrasic in age.

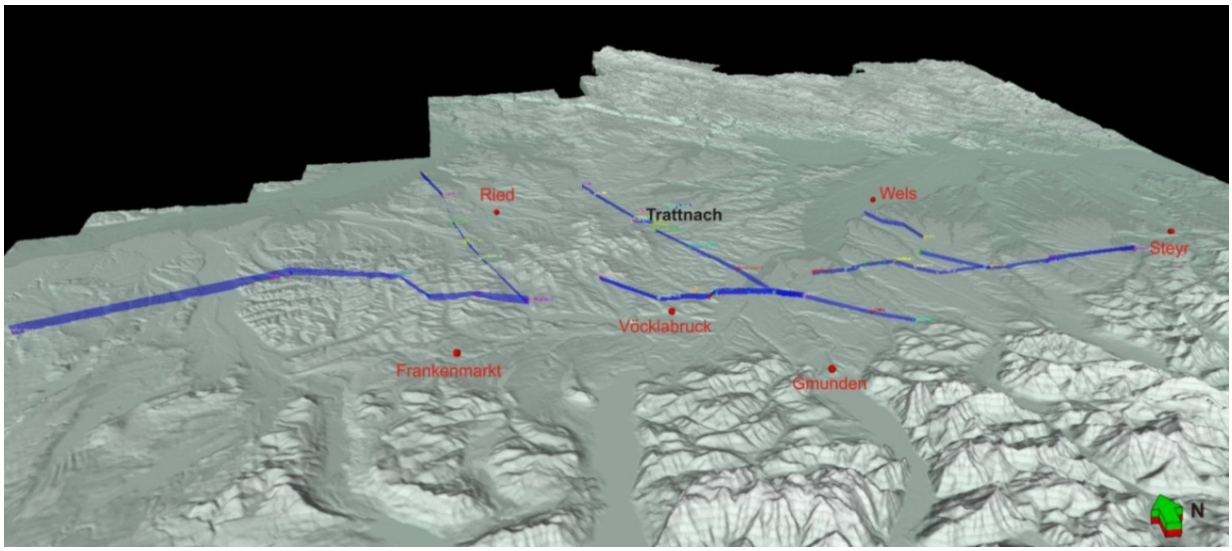

Figure 47: Base map indicating Cenomanian well log correlation profiles in the Upper Austrian Molasse Basin.

With increasing distance from the Trattnach Field, the log signature changes and it gets more and more difficult to distinguish the subunits CE1-CE3. This may be an effect of a change in lithology and or in diagenesis. Furthermore, especially the appearance of glauconite in the Cenomanian sandstones leads to a significant rise of the GR response and may mimic the presence of fine grained rocks.

In order to depth shift and characterize the Cenomanian successions new CGR measurements were successfully incorporated in this study.

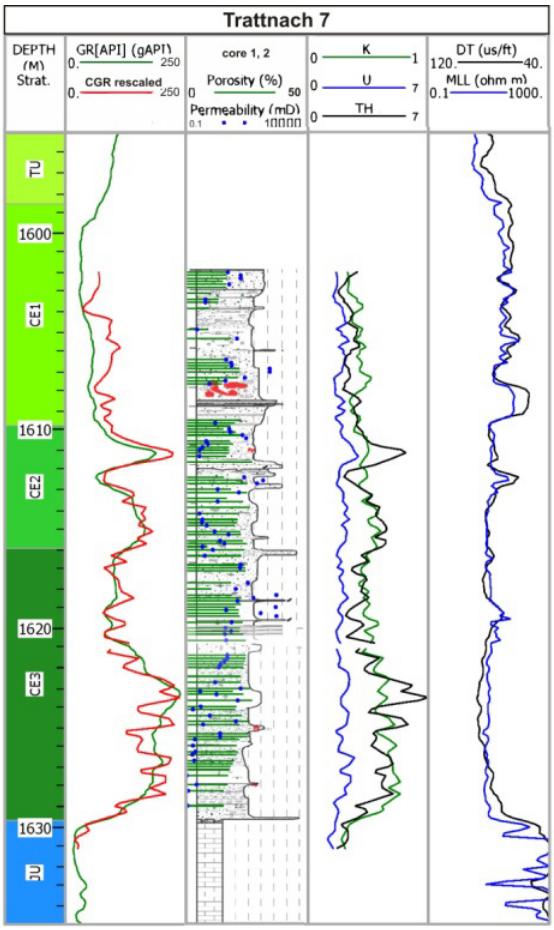

Figure 48: Type well log Trattnach 7 with rescaled and shifted CGR and CSGR curves. The third column includes the core description and also overlain Porosity and Permeability data.

In a second step, a Turonian maximum flooding surface (mfs) was determined and correlated (Figure 49). The mfs belongs to relative sea-level rise and might be accompanied by marine transgression and associated shoreface erosion, which results in a transgressive surface of erosion (Bhattacharya, 1993). The interpreted maximum flooding surface is the indication that the rate of accommodation exceeded the rate of sediment supply.

Figure 49 illustrates a representative north-south well log correlation profile in the Trattnach area referring to Cenomanian, Turonian and in some wells also Jurassic strata.

The mfs could be interpreted along the whole profile. It is defined by a high DT (slow velocity) and GR response reflecting the presence of fine grained sediments. In Figure 49 the yellow-green sections of the GR log refer to the compact and resistant CE1 subunit.

The base of the subunit CE1 is formed by the “marker bed” (Nachtmann, 1995). It is characterized by a very low DT reading and high resistivity in the MLL or MINV log (see red circles).

The interval CE2 is characterized in most cases by two coarsening upward cycles (red arrows) that can be easily correlated in the Trattnach area. Base CE2 refers to a significant peak in the DT and resistivity log and a low GR response. Note the completely different patterns of the GR and DT logs within the subunits CE2 and CE3. The difference is caused by the fact that the GR log is mainly controlled by variations in Th contents and in the amount of glauconite. Thus, in the case of the Cenomanian it must not be used as a grain size indicator. In difference, the DT log probably reflects the degree of cementation.

Base of the well log section illustrates the well log facies successions of the Jurassic limestone. The contact to the Cenomanian referring to the log signature is very sharp. The Upper Jurassic limestone is characterized by high velocities (low DT) and low GR responses. Although there is no obtained GR log for the well Weinberg 1, formation tops could be successfully interpreted. The log trace beneath the Cenomanian is cut off. The GR log in the well Gaspoldshofen 1 below 1780 m MD is obviously incorrect, the signature shows a continuous low response.

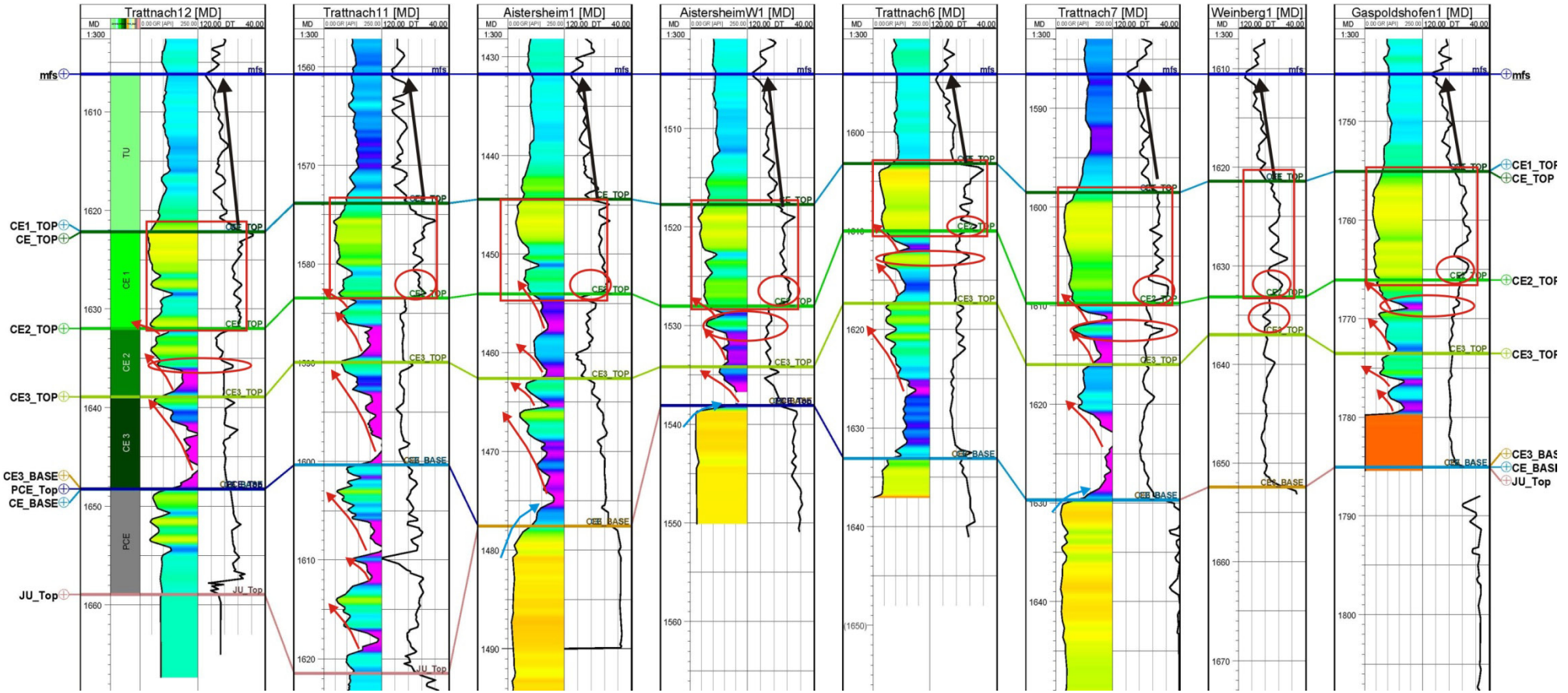

Figure 49: Trattnach N-S well log correlation profile flattened on the maximum flooding surface (blue line). Black arrows describe the fining upward until maximum relative sea level rise. Prominent well log correlation patterns are marked in red.

The well logs of well Trattnach 6 (Figure 50) illustrate a similar log facies succession compared to the logs of Trattnach 7. Compared to Trattnach 7 the marker bed has a typical red color shade and shows an increase in its grain size. The unit below CE3 contains white homogeneous fine to medium grained sandstones and has on the bottom at approximately 1640 m MD a fine grained shaly bed. The K response seems to increase to the bottom of CE3. The sharp contact between Turonian shales and Cenomanian sandstones is concerned to a NW-SE rending fault.

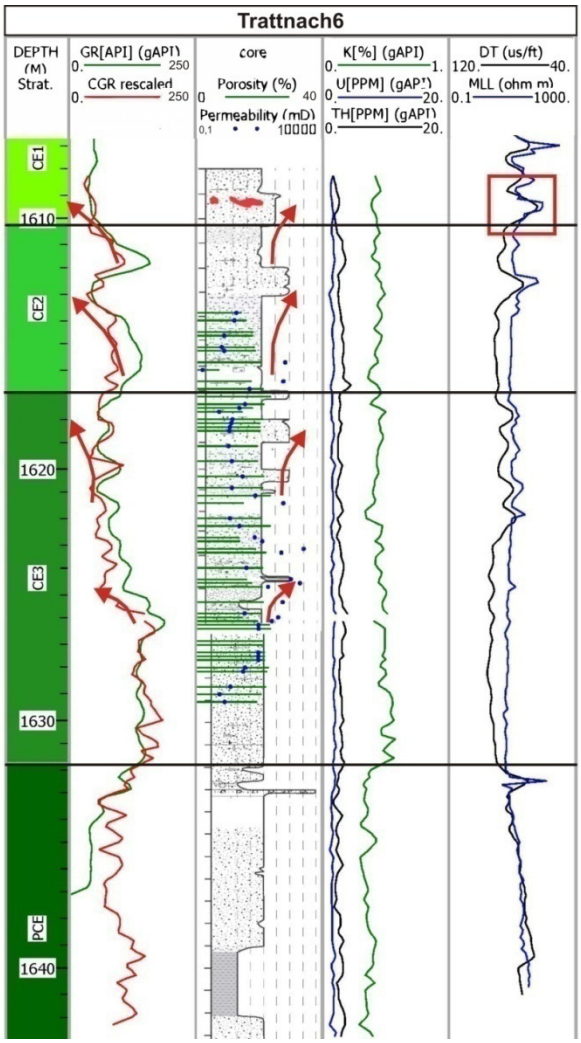

Figure 50: Well Logs of Trattnach 6.

Figure 51 illustrates a cross-section through the Cenomanian cored sandstones with the wells Trattnach 6,7,8 and 12.The well log cross-section is completed with overlain porosity (green) and permeability (blue) data. The cross section is constrained by Top Cenomanian (Top CE1) and Top Jurassic at the base. The cross section clarifies that the marker bed does not necessarily correspond to the red layer. Especially at

the wells Trattnach 8 and Trattnach 12 the red layer appears at shallower positions of the subunit CE1.

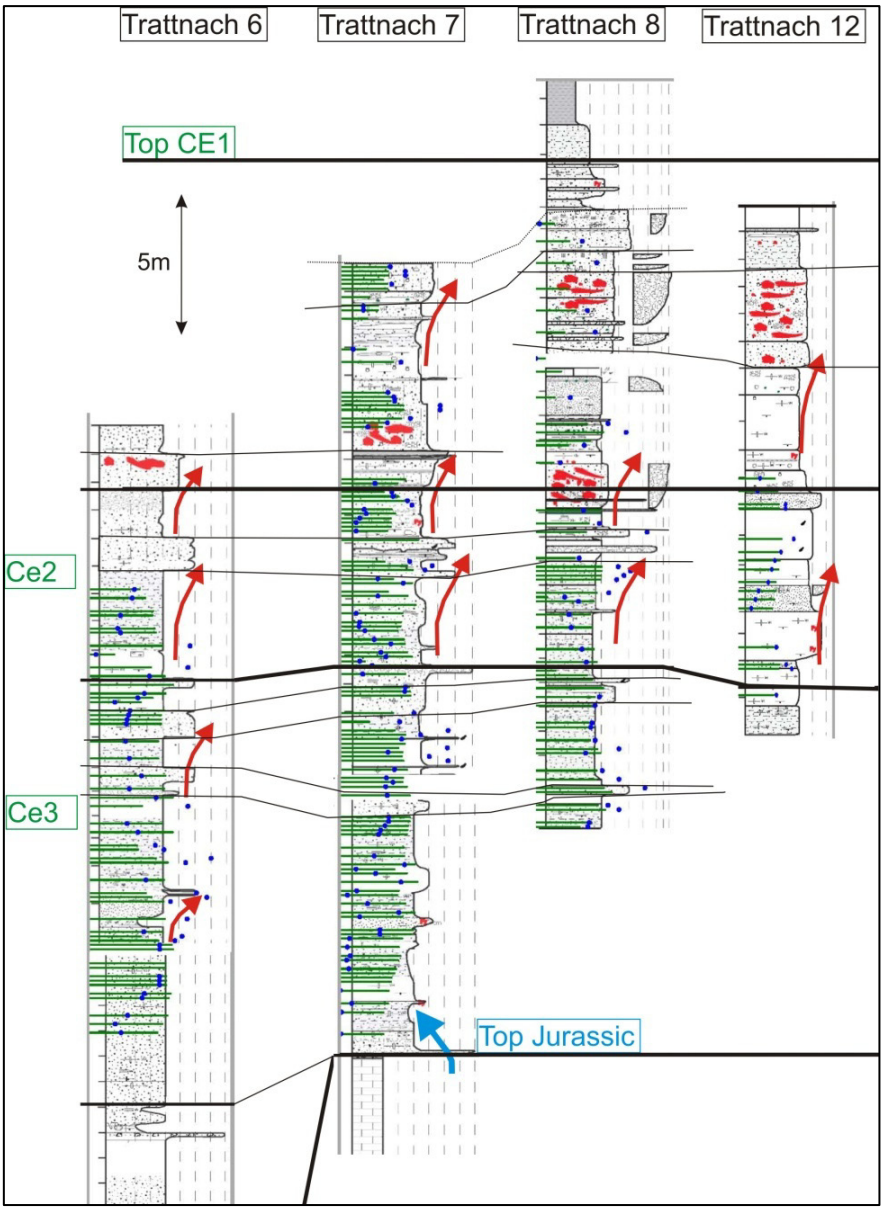

Figure 51: Core-log cross section for the wells Trattnach 6,7,8 and 12 highlighting laterally traceable geometries. Top CE2 has been used as fixed Datum hence it occurs in all cored intervals. Cross section is located in Figure 48. Core descriptions have been provided by Schnitzer.

The NW-SE1 (Figure 52) well log correlation is about 32 km long. The correlation profile is flattened on the maximum flooding surface as fixed datum. At wells Wolfersberg 1 and Hoergersteig 1 the uppermost part of the Cenomanian together with the Turonian marlstones have been eroded in pre-Eocene time. Generally Top / Base Cenomanian can be better interpreted with a combination of DT and MINV or MNOR log because of its high resolution. For the wells Hoergersteig 1 and

Hoergersteig 3 only short sections of logs were obtained. Those intervals look completely different compared to the other wells.

It is not possible to subdivide the Cenomanian, but Top and Base could be interpreted. Anyhow most wells of the NW-SE1 correlation could be successfully interpreted. It seems as if interval CE1 considerably thickens in the northern part and decreases in thickness towards the southern area. The red circles mark another almost homogeneous, obviously sandy interval at the bottom of CE3, which seems to thicken from north to south until well Wolfersberg1. Note also the straight log response of the DT log compared to the GR log at the well Senftenbach 1, Kemating 1 and also Hoergersteig 3.

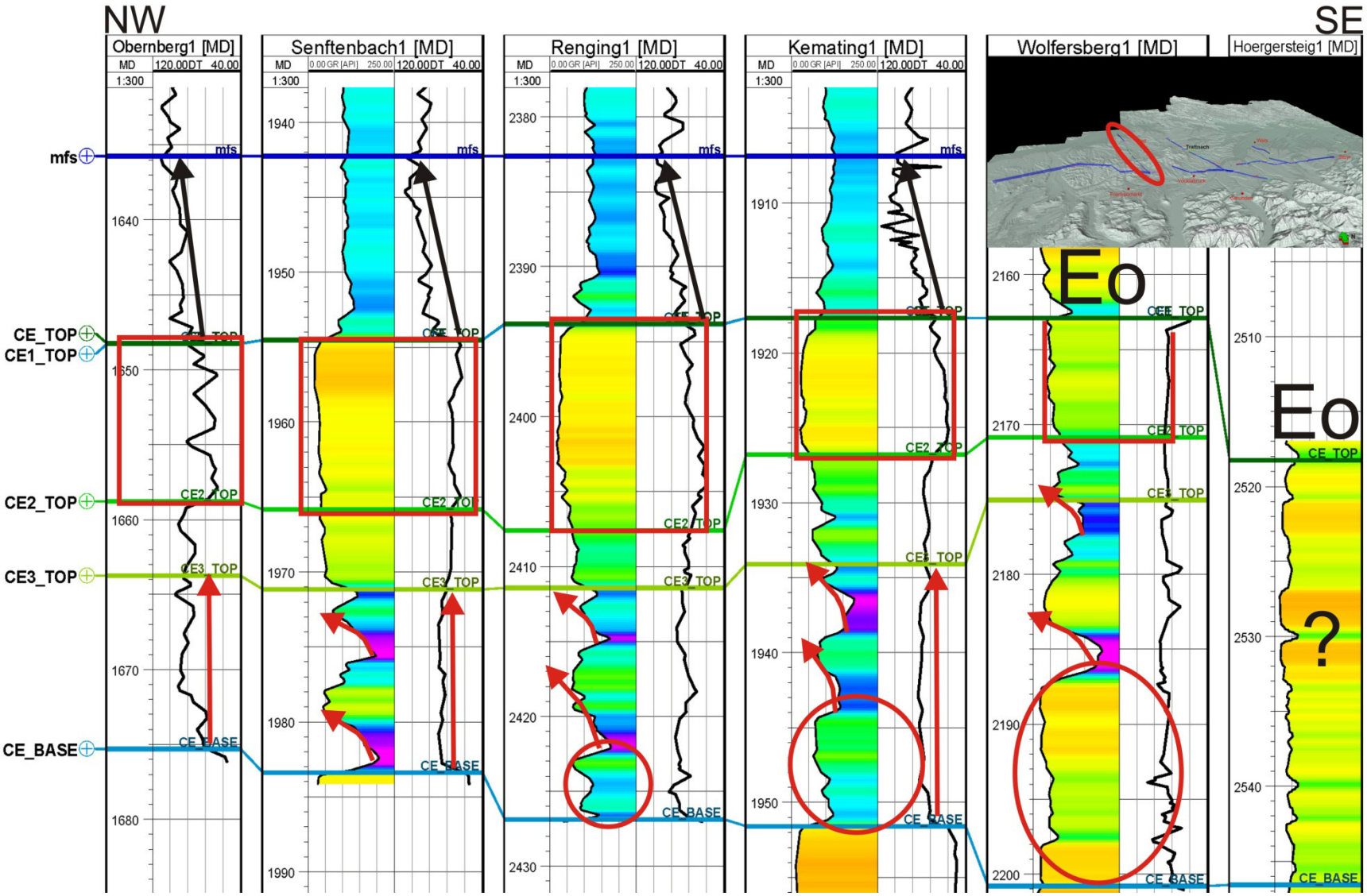

Figure 52: Well Log Correlation Profile NW – SE 1 flattened on the maximum flooding surface.

Figure 53 illustrates the 40 km long NW – SE2 well log correlation profile. Well logs are flattened on the Turonian maximum flooding surface which could be interpreted in every well, where DT and /or GR was available. Note the southward decrease in thickness of the sediment package between the Top Cenomanian and the maximum flooding surface. The logs for the wells Schwanenstadt 3, Oelling 1 and Kirchham 3 were cut at Top Cenomanian.

At Oelling 1 and Kirchham 3 the Turonian shales were eroded. Eocene sandstones overlay the Cenomanian sandstones. Note also here especially in the southern area of the cross-section, the almost flat DT log response. Except for Oelling 1 and Kirchham 3 tops of subunits could be confidentially interpreted and correlated. It seems as if the upper subunits CE1 and eventually CE2 have been eroded for Oelling 1. The GR log response suggests fine grained sediments, shales or mudstones.

Furthermore the well logs for Schwanenstadt 3 are limited to Cenomanian strata. According to geological short profiles the Cenomanian is overlain by Turonian marlstones. The Cenomanian Base for the well Nieder-Thalheim 1 has been corrected and reinterpreted after well log correlation and core interpretation to 2191 m MD. Nevertheless most of the characteristic well log patterns could be successfully interpreted and correlated through the cross-section.

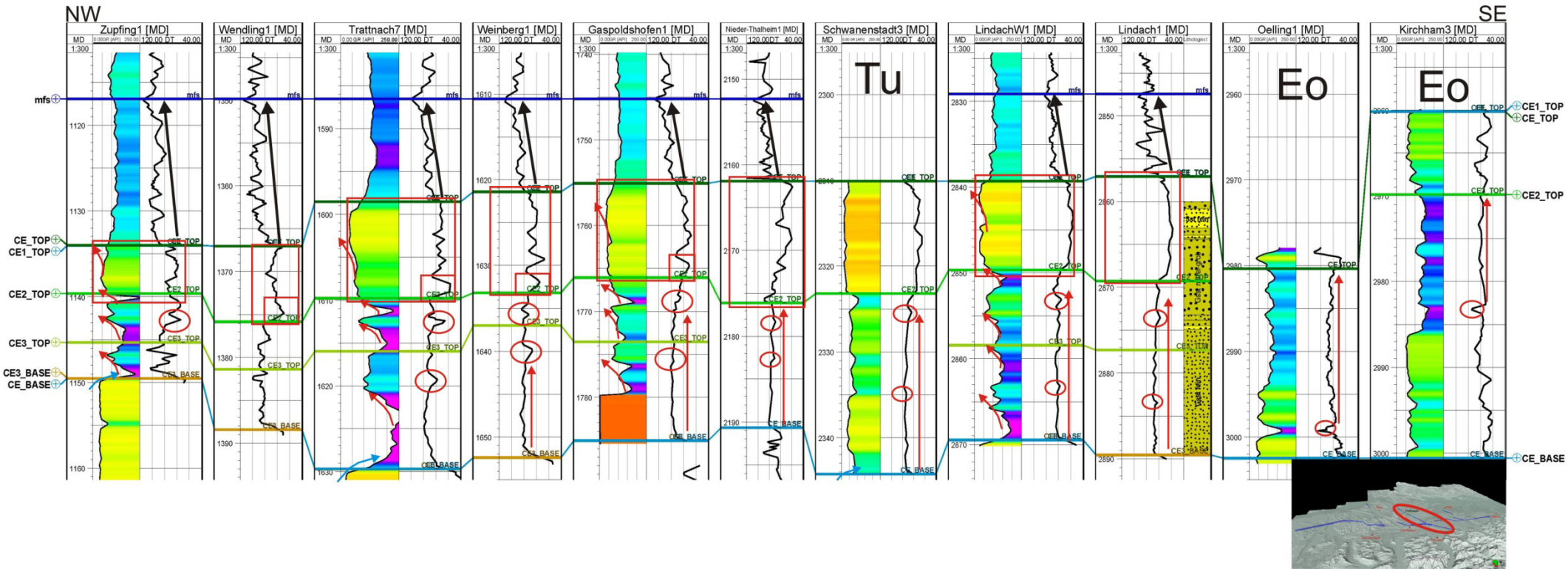

Figure 53: Well Log Correlation Profile NW – SE2 flattened on the maximum flooding surface.

The eastern NW – SE 3 well log correlation profile (Figure 54) extends over a distance of approximately 15 km. All wells except Lichtenegg 2 are flattened on the interpreted maximum flooding surface. In the northern wells Lichtenegg 2, Steinhaus NW1 and Steinhaus N1 the crystalline basement is at shallow depth. Jurassic carbonates are absent. Cenomanian sandstones overlie the cordieritic gneisses of the crystalline basement. The typical Cenomanian thickness of approximately 30 m is considerably reduced to less than 20 m. This may be the result of changes in sediment supply. If the sediment supply at the shoreline is less than the rate of accommodation, very little sediment is preserved in the stratigraphic record. Accommodation is defined as the space available for sedimentation and is interpreted to be a function of eustasy and subsidence (Posamentier & Vail, 1988). It is not possible to divide the Cenomanian strata into the subunits CE1 – CE3 on the basis of the provided well logs. The illustrated Cenomanian base for the well Sattledt 1 refers to the geological short report. For the wells Sattledt 1, Oberaustall 1 and Voitsdorf 37 + 1 the upper CE1 unit may be interpreted and correlated. A subdivision into the lower CE2 and CE3 unit is due to the differing log signature and missing log patterns not realistic.

Note the thickening of Turonian shales below the maximum flooding surface toward the south, compared to the NW-SE2 cross-section (Figure 53)

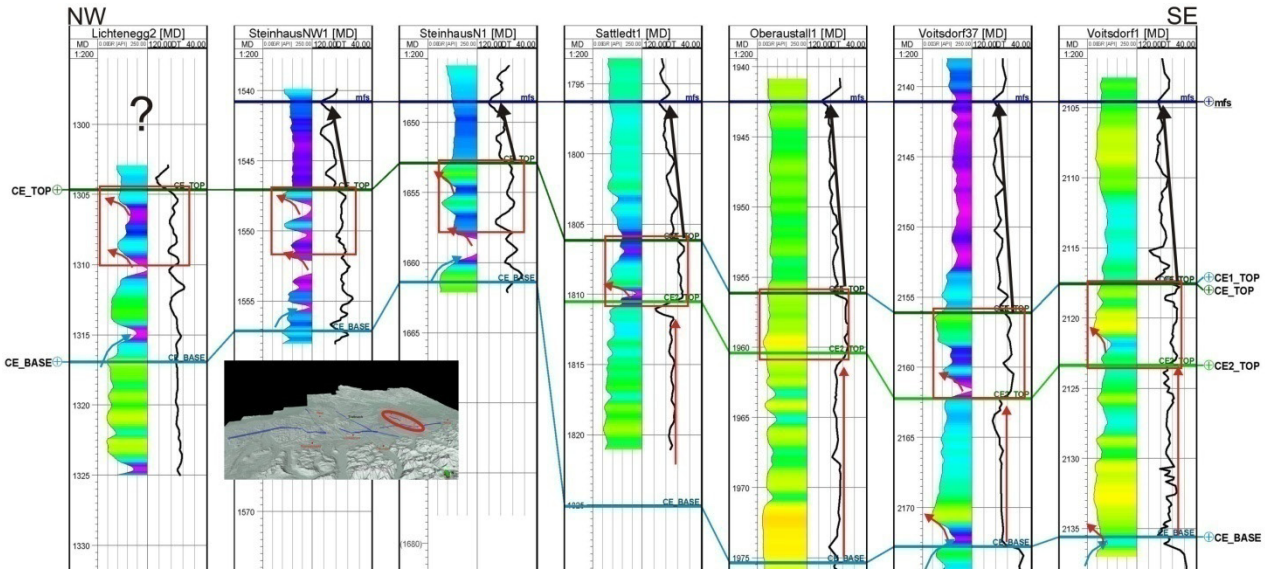

Figure 54: Well Log Correlation Profile NW – SE3 flattened on the maximum flooding surface.

The W - E1 (Figure 55) well log correlation profile illustrates the heterogeneous well log nature of the western part of the study area. The well logs are flattened on base Cenomanian as fixed datum. The red squares mark intervals with similar log signature. The position of Top Cenomanian for the well Perneck 1 follows the geological short profile. Geological short profiles and core interpretations for Perneck 1 and Redltal 1 document that Eocene sediments overlie the Cenomanian sandstones. Equally the well logs for Maria Schmolln 1 and Kohleck 1 illustrate a completely different well log response and do not indicate the typical Cenomanian well log patterns. It is subject of current discussions, which parts may correspond to Cenomanian strata. Especially the huge thickness in the well Mühlberg 1 raises many questions.

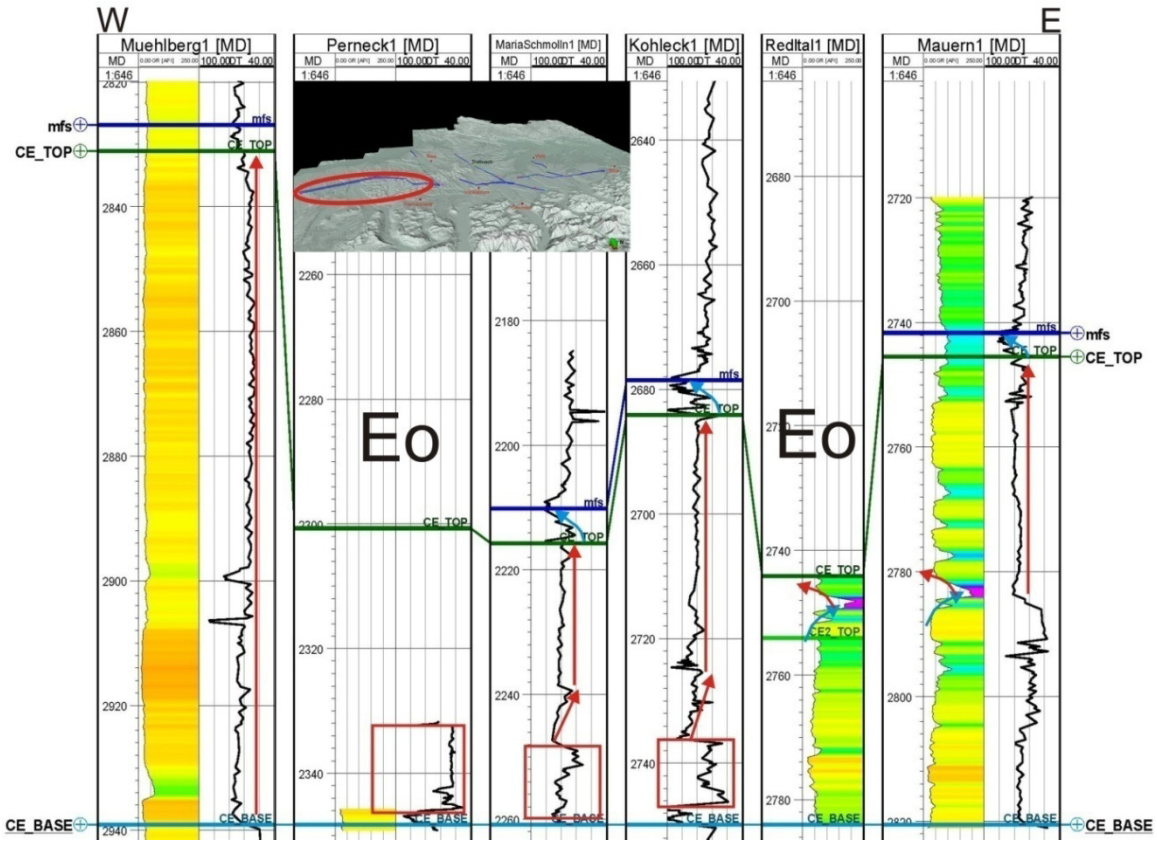

Figure 55: Well Log Correlation Profile W – E1 flattened on base Cenomanian.

The W – E2 (Figure 56) well log correlation profile includes wells, which exhibit typical well log patterns of the Cenomanian sandstone of the Upper Austrian Molasse Basin. The profile extends over a distance of ~18 km. All wells are flattened on the maximum flooding surface. For the well Wegscheid 1 only the resistivity log was applied for interpretation. Using the well logs, all Cenomanian subunits (CE1 – CE3)

can be distinguished. Note the continuous low velocities of the lowermost CE 2 and CE 3 unit compared to the CE1 unit. Additionally the GR log has a completely differing character, which is typical for the study area. The well logs for Desselbrunn 1 are cut off at approximately top Cenomanian.

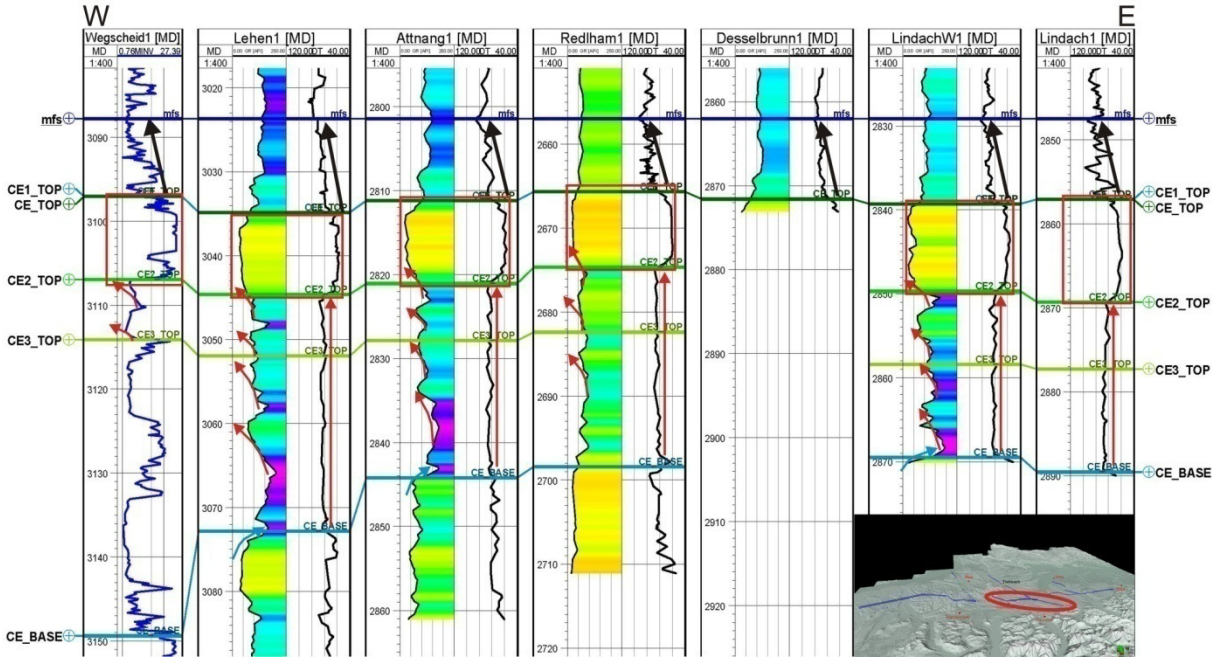

Figure 56: Well Log Correlation Profile W - E2 flattened on the maximum flooding surface.

The W – E3 (Figure 57) well log correlation profile extends over a distance of 44 km. The cross-section is flattened on the maximum flooding surface. The western part of the profile illustrates the typical well log facies of the Cenomanian sandstones. The well logs of Bad Hall 1 and 3 do not allow a confident interpretation of base Cenomanian. The GR well log signature of the well Haidermoos 1 demonstrates a remarkable thickness of the CE 1 unit and is in its log character comparable to Schwanenstadt 3. In Steyr West 1 the Bohemian Massif is in a shallow position and the Cenomanian is only about 4 m thick.

(Because, Bad Hall 1 is characterized by logs with nearly no vertical variation [logging error?], it is not included in Figure 57)

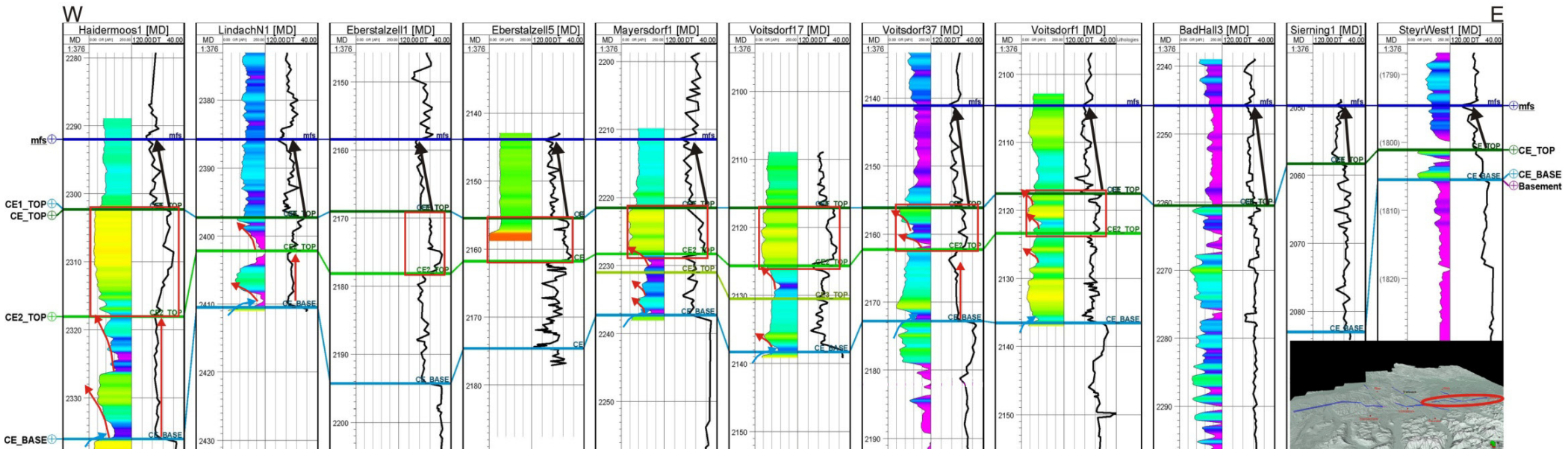

Figure 57: Well Log Correlation Profile W – E flattened on the maximum flooding surface (mfs; where present).

4.3 Facies groups of the study area

The investigation of well log correlation profiles helped to pick and subdivide horizons and to obtain a basic concept of the well log characteristics of the Cenomanian sandstones and their lateral distribution. Nevertheless new questions arose regarding lateral changes in well log facies. Based on similarities, logs are grouped into different log facies groups (Figure 58) in the present section. The GR and DT logs of each group are displayed in the following figures together with digitized core reports (not depth shifted). The nomenclature of the facies groups is based on the geographic position of the wells and relates to consistent log facies patterns. These patterns are discussed in the following section.

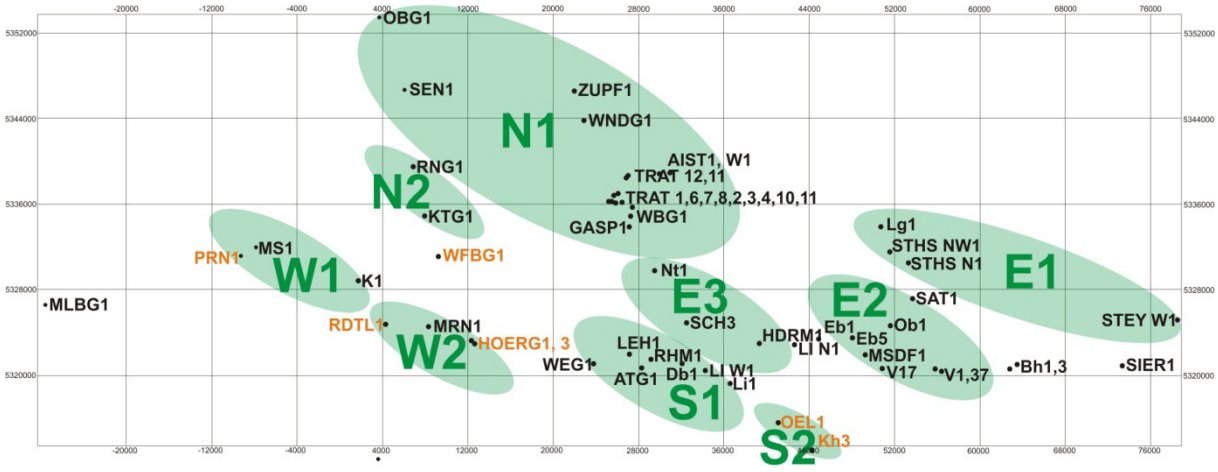

Figure 58: Base Map indicating log facies groups of the study area. The green marked groups relate to the log facies groups. The orange marked wells relate to wells, where the Cenomanian sandstones are overlain by Eocene strata.

Log facies E1

The well log facies group E1 (Figure 59) comprises wells located in the northeastern part of the study area. In the wells Steinhaus N1 and Steinhaus NW1 the Cenomanian sandstones overlie sandstones of at least pre-Cenomanian age. According to the core report those sandstones correspond to Jurassic sandstones. The Cenomanian is characterized by a high GR well log response and variable DT readings. On the basis of prominent GR log peaks, parts of the Cenomanian may be correlated. The thickness is relatively low. A confident subdivision into the CE1 – CE3

units is not possible. Equally for the well Lichtenegg 2 a subdivision is not possible. Additional information for the overlying and underlying formation is missing.

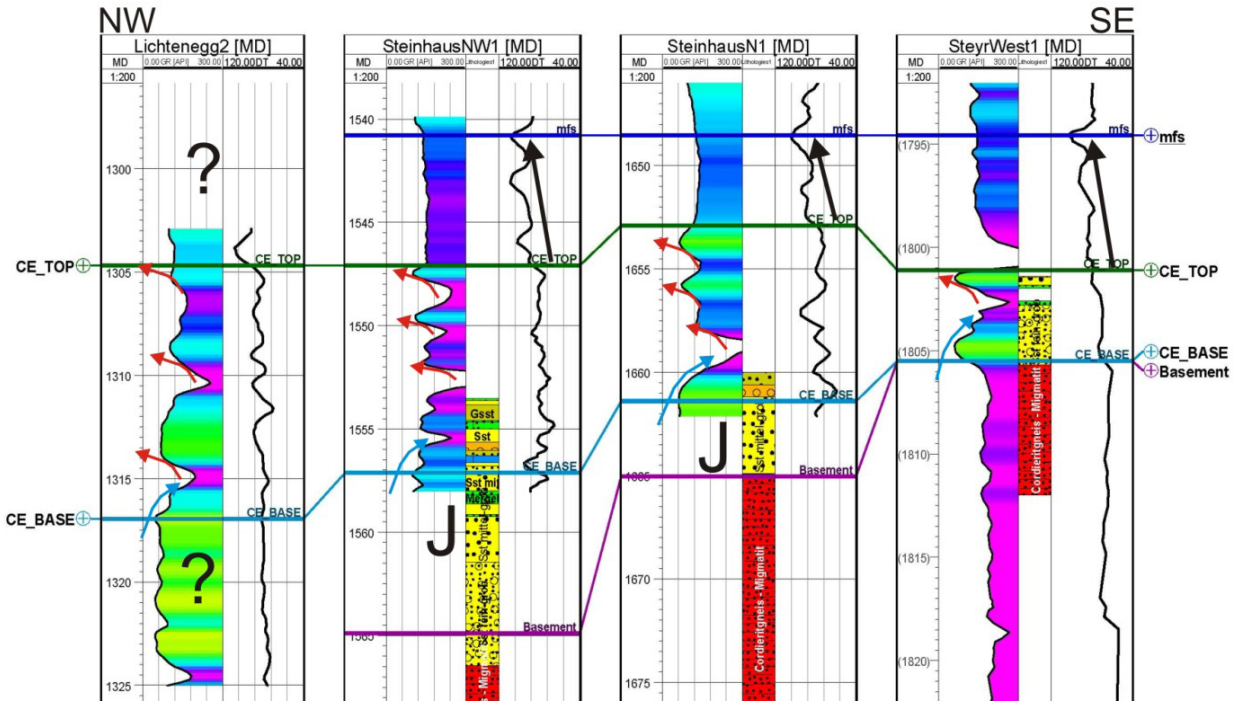

Figure 59: Log facies E1 flattened on the maximum flooding surface.

Log facies E2

Figure 60 illustrates the wells of the E2 facies group. The well logs are flattened on the maximum flooding surface as fixed datum. In all wells the Cenomanian strata is overlain by Upper Jurassic carbonates.

The border to the Cenomanian sandstones may be confidentially interpreted. Velocities of the Jurassic limestones are considerably higher than the Cenomanian sandstones. The CE1 unit occurs in nearly all wells, showing different log signatures. Core reports document fine grained marlstones in the CE1unit as well as in the deeper CE2 and CE3 interval (e.g. Mayersdorf 1). A subdivision of the CE2 and CE3 unit on the basis of well log data is not reliable.

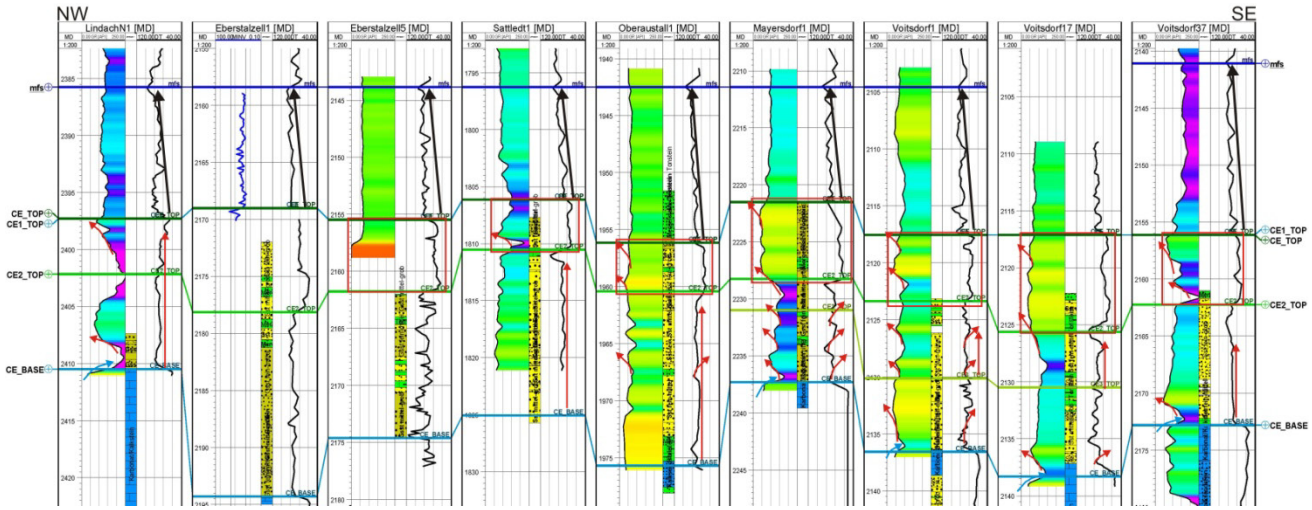

Figure 60: Log facies E2 flattened on the maximum flooding surface.

Log facies E3

Figure 61 illustrates the E3 well log correlation profile. It is characterized by very similar well log patterns of the wells Nieder-Thalheim 1, Schwanenstadt 3 and Haidermoos 1.

The Cenomanian sandstones in the wells Schwanenstadt 3 and Haidermoos 1 directly overly the Upper Jurassic carbonates, while Nieder-Thalheim 1 overlies a thick sequence of pre–Cenomanian sandstones. The sonic log shows a continuous low velocity trend in the CE2 and CE3 unit with a traceable peak (red circle) in the upper section. In contrast to the sonic log the GR log demonstrates a completely differing character with two (pseudo) coarsening upward trends.

Furthermore the CE1 unit illustrates a characteristic DT well log response, which looks like two coarsening upward trends. Core inspection shows that the high velocity peak corresponds to a limestone bed. The GR log looks common for the Cenomanian sandstones, whereas no GR log for Nieder-Thalheim 1 has been provided and the resistivity log is apparently cut off at the upper sections. For all wells except Schwanenstadt 3 a maximum flooding surface has been interpreted in the Turonian marls.

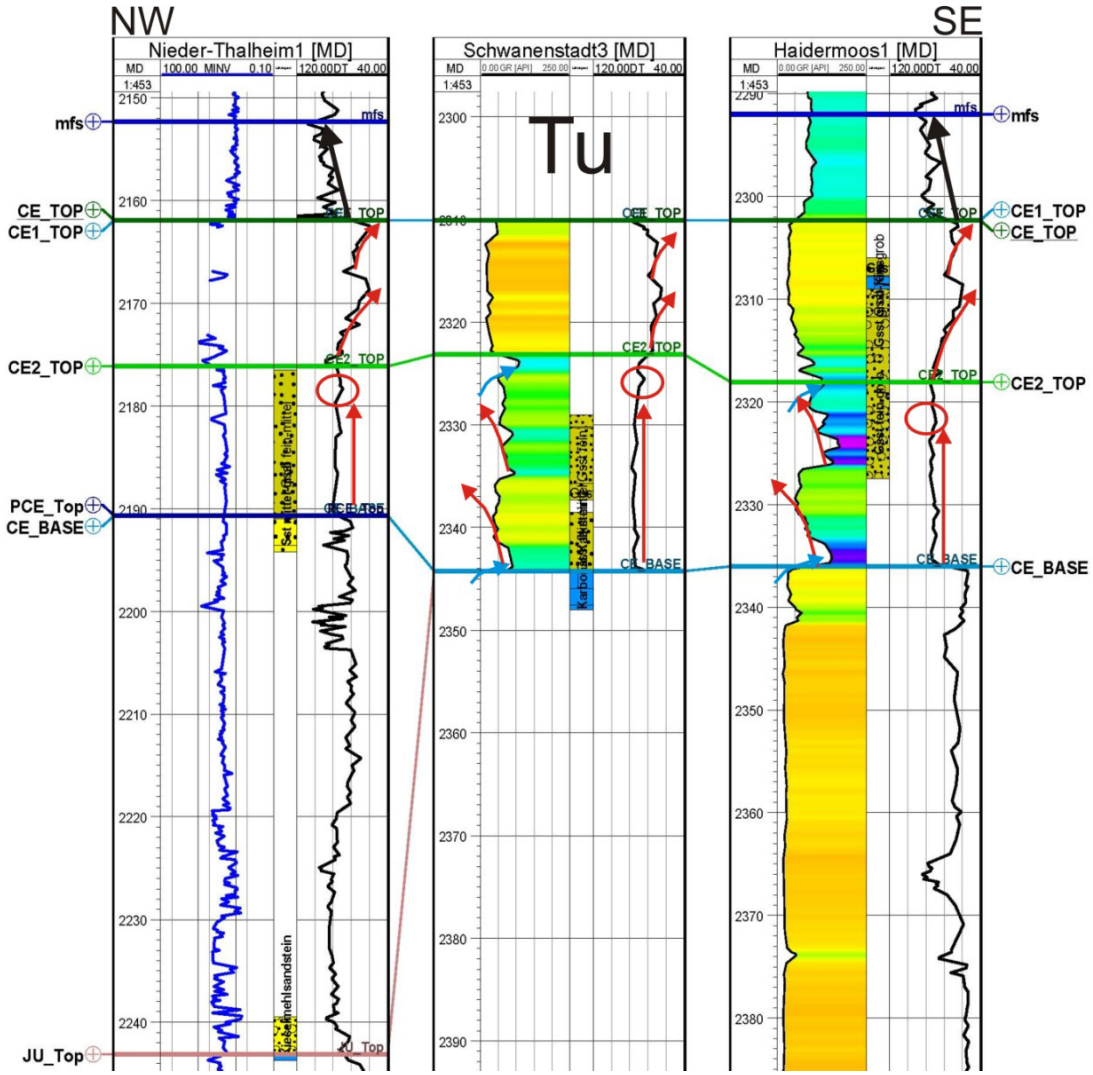

Figure 61: Log facies E3 flattened on top Cenomanian

Log facies N1

The N1 well log correlation profile (Figure 62) covers a majority of the obtained wells. For the Trattnach Field the well Trattnach 7 is exemplarily illustrated. The cross – section is flattened on the maximum flooding surface. The Cenomanian sandstones overly the Upper Jurassic carbonates. The CE2 and CE3 unit shows a characteristic signature in the GR log for most of the wells. However the DT and resistivity log are the most appropriate well logs for the subdivision of the Saal Member into the units CE3 and CE2.

The CE1 unit demonstrates typical high velocity DT log readings, comprising the prominent marker bed for several wells. For the wells Obernberg 1 and Weinberg 1 the marker bed peak corresponds to a calcareous sandstone.

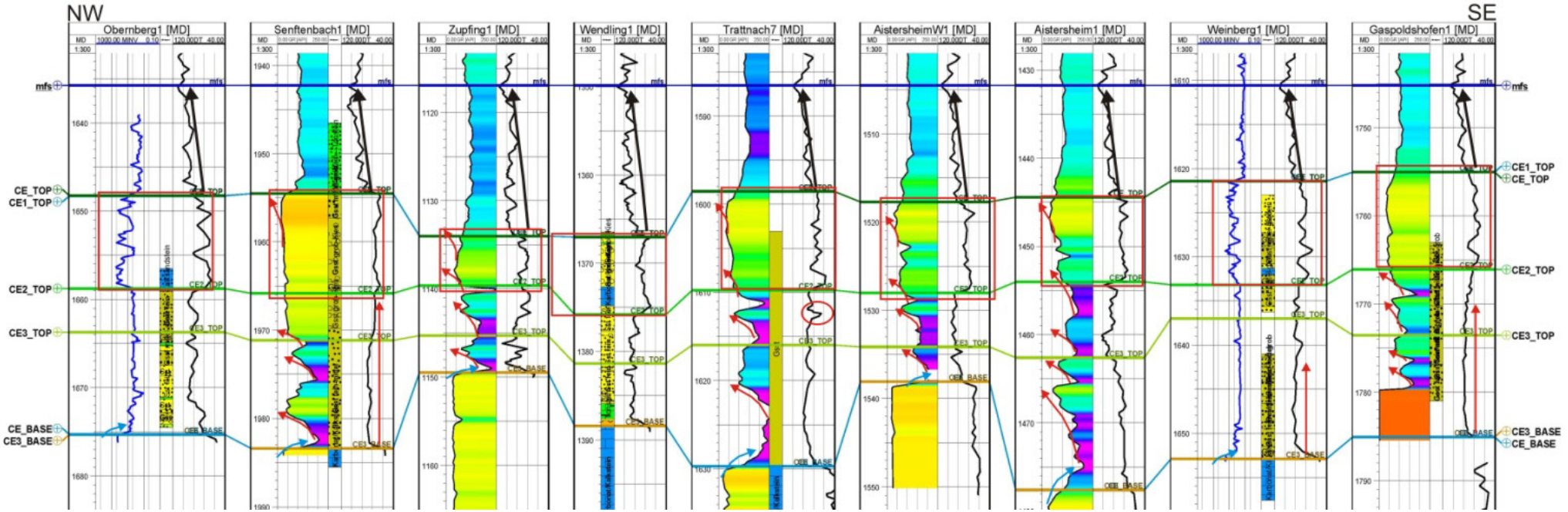

Figure 62: Log facies N1 flattened on the maximum flooding surface.

Log facies N2

The wells Kemating 1 and Renging 1 (Figure 63) demonstrate typical well log patterns for the Cenomanian sandstones. In contrast to facies N1 the base of the Cenomanian sandstones corresponds to a higher GR log response. Both show continuous slow velocity readings in the CE2 and CE3 unit. The GR log in contrast illustrates at least three (pseudo) coarsening upward cycles that can be confidentially correlated.

The CE1 shows typical Cenomanian well log characteristics with a slightly increased thickness particularly at the well Renging 1. Both indicate due to core reports limestone intervals that may correspond to the sections with high velocities.

In both wells the Cenomanian strata is overlain by Turonian marls demonstrating a maximum flooding surface which is used as fixed datum for the correlation profile.

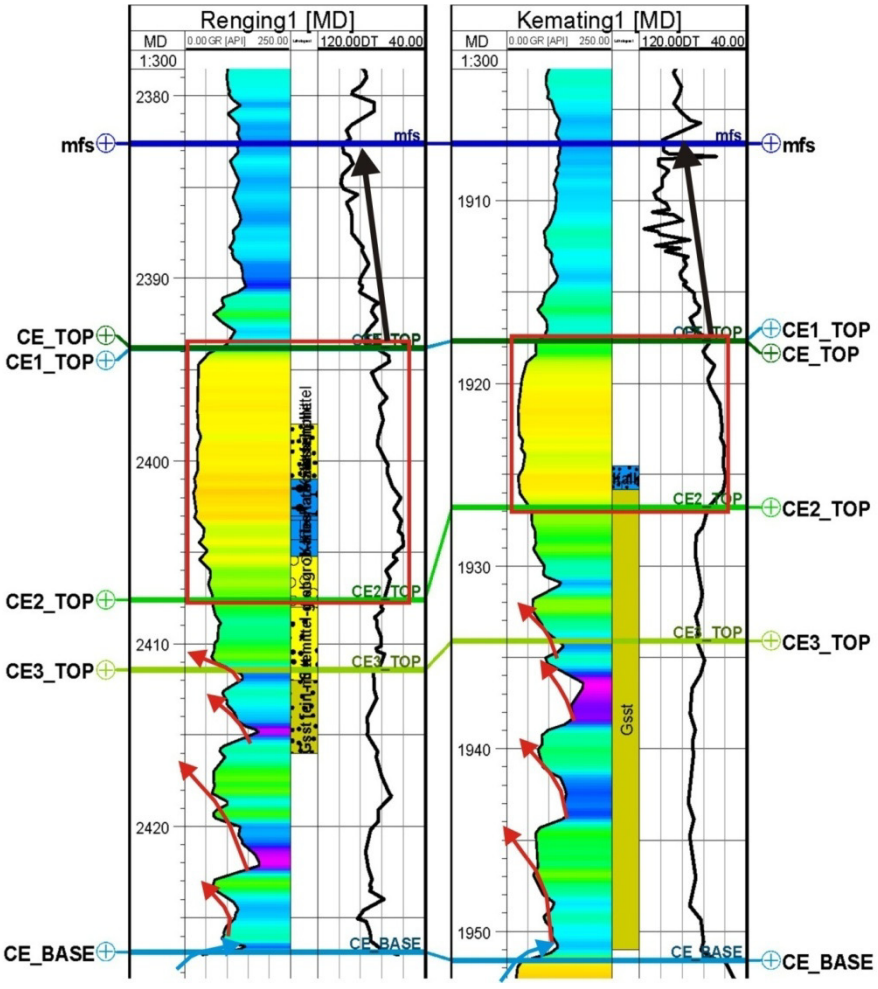

Figure 63: Log facies N2 flattened on the maximum flooding surface.

Log facies S1

The S1 (Figure 64) facies well log correlation profile is flattened on the interpreted maximum flooding surface.

The CE2 and CE3 units illustrate common facies well log patterns for all wells except Wegscheid 1 and Desselbrunn 1. The interpretation of the Cenomanian strata for Wegscheid 1 is constrained on the shallow MINV resistivity log, which hinders a reliable interpretation of base Cenomanian. Thus the picked base should be regarded with caution. No well log exist below top Cenomanian for the well Desselbrunn 1. Lindach 1 can be confidentially correlated on the basis of the provided sonic log to the nearby Lindach W1 well.

The CE1 unit has the common high velocity and resistivity signature with average thicknesses of about 20 meters for this well section. The GR log comprises constantly low values.

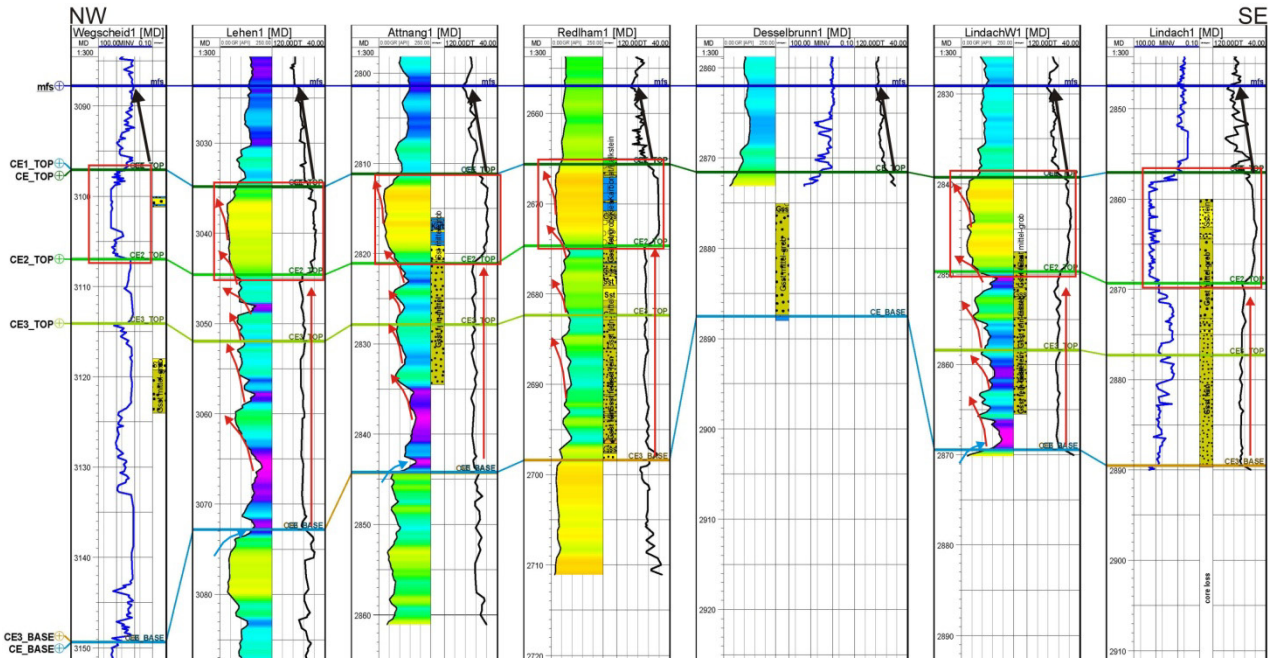

Figure 64: Log facies S1 flattened on the maximum flooding surface.

Log facies S2

The S2 correlation profile (Figure 65) illustrates two wells near the southern margin of the study area. The well logs are flattened on base Cenomanian. In both wells Eocene sandstones directly overlie the Cenomanian sandstones. The Turonian

marlstones are apparently eroded. Consequently the CE1 unit is absent in the Oelling 1 well and parts of it are missing at the Kirchham 3 well.

However the CE2 and CE3 unit show an uncommon well log response for the lower sections. Especially the low GR response for the Kirchham 3 well is untypical for the lower CE3 unit.

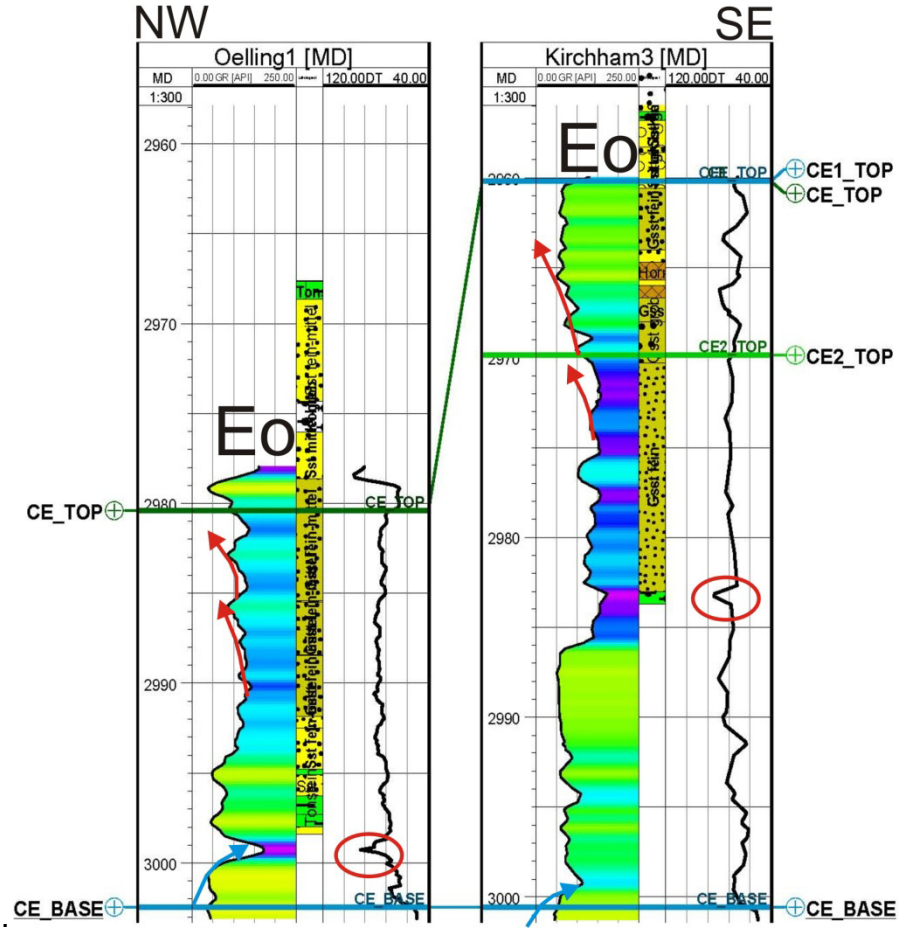

Figure 65: Log facies S2 flattened on base Cenomanian (digitized RAG core reports are not depth shifted).

Log facies W1

The well logs for the W1 facies group are not illustrated in this section due to the lack of appropriate well log data. The logs are characterized by a differing log response (Figure 55) compared to the W2 logs (Figure 66). Additional information is necessary for a reliable interpretation.

Log facies W2

Figure 66 illustrates the facies well log successions and core descriptions for wells Redltal 1 and Hoergersteig 1 + 3. The well logs are flattened on the Cenomanian base. Well logs are cut off at the boundaries with Jurassic and Eocene sediments.

All wells demonstrate a different log facies compared to the standard-facies encountered in the Trattnach area. The GR log is the only log that is present in all wells. It is characterized by a continuous low GR response except a peak in the upper section that corresponds to a siltstone interval.

Based on the provided well log data, a subdivision into the CE1, CE2 and CE3 unit is impossible.

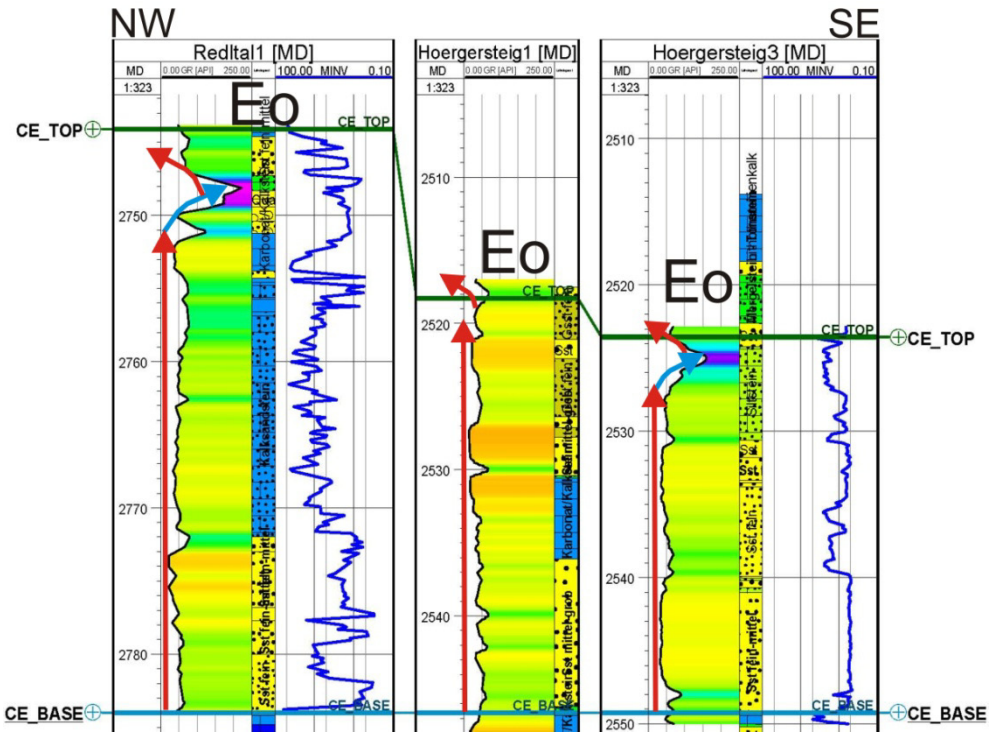

Figure 66: Log facies W2 flattened on base Cenomanian (digitized RAG core reports are not depth shifted).

4.4 Thickness maps

The investigation of well log correlation profiles is an appropriate method for identifying and correlating formations and their subunits. In order to get an idea of the lateral extent of the Saal Member (CE3, CE2) and Bad Abbach Member (CE1) as well as the unit from Top Cenomanian upwards to the maximum flooding surface, thickness maps were constructed.

Interpreted thicknesses of respective members were used as input data. Wells with reduced thickness of individual members due to faults or erosive events were excluded in the thickness map.

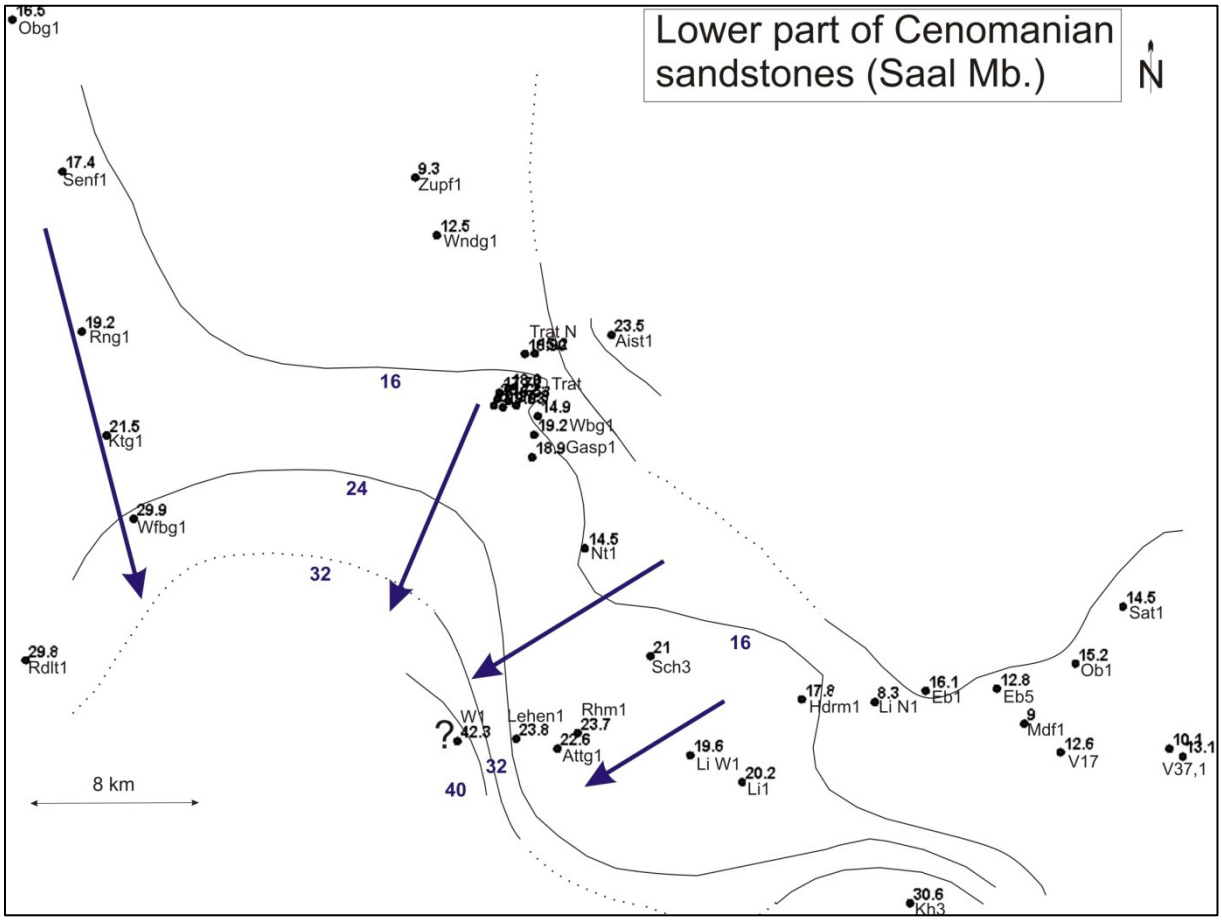

Figure 67: Hand-contoured map of the thickness of the Saal Mameber (CE3 + CE2) constrained by shown wells. Blue arrows mark the direction of thickness increase, while the blue marked values correspond to the contour lines in [m].

Figure 67 illustrates thickness variations of the CE2 and CE3 unit in the study area. It demonstrates a basinward thickness increase from NE to SW. This confirms the transgressive character of the lower part of the marine glauconitic Cenomanian

sandstone (“Saal Mb.”). The thickness varies between 10 and 40 m, showing particularly in the north (Zupfing 1, Wendling 1) and in the east (Voitsdorf Field) the lowermost values. The Wegscheid 1 well shows a remarkable high thickness for the Saal Member. The interpreted thickness should be regarded with cautiousness due to the lack of appropriate well log data which considerably reduces a reliable interpretation.

The thickness variation of the Bad Abbach Member (CE1, Figure 68) illustrates a similar trend compared to the Saal Member. Also the CE1 unit shows a thickness increase from NE to SW. In contrast to the Saal Member thicknesses vary between 5 and 15 m. The wells in the western area were not included in the interpretation, because either of their eroded CE1 unit or their differing log response. Based on the well logs it is not certain if those indeed relate to the Bad Abbach Member.

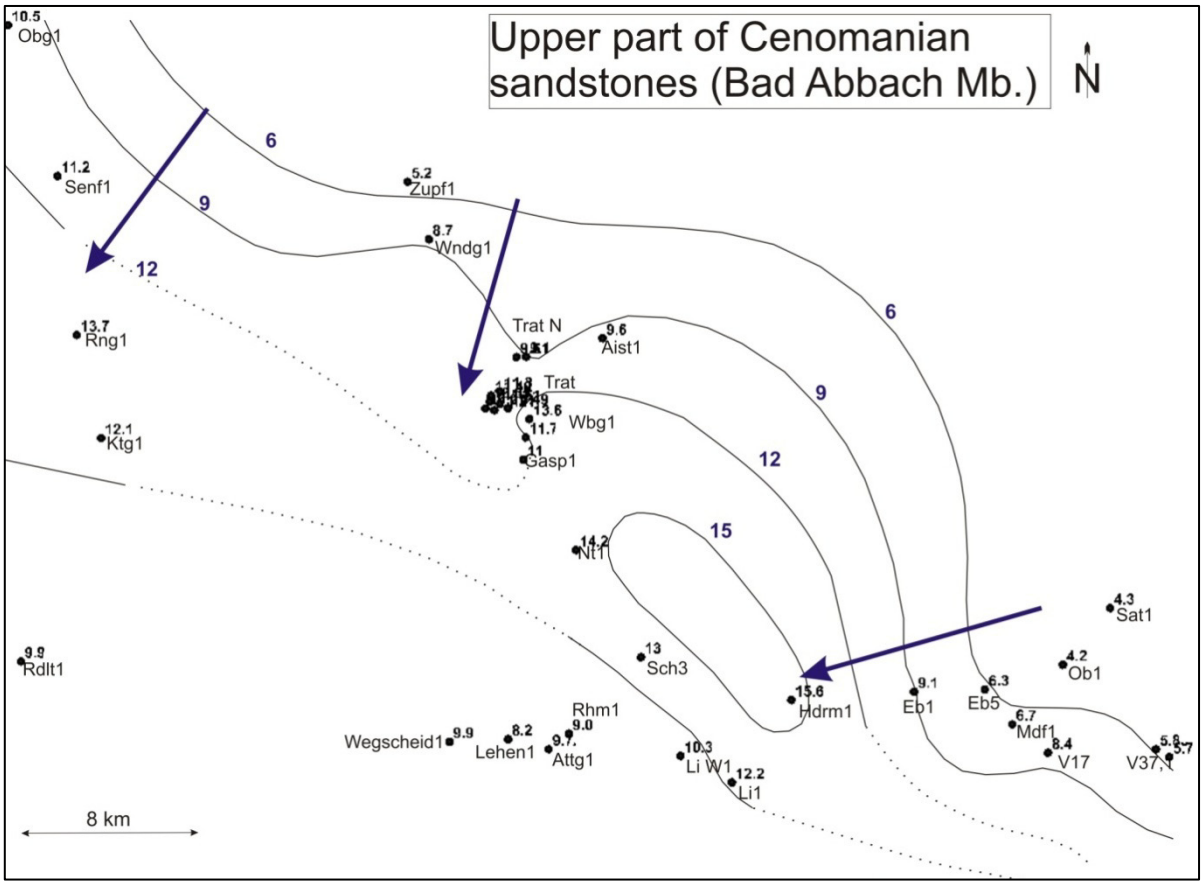

Figure 68: Hand-contoured map of the thickness of the Bad Abbach Member (CE1) constrained by indicated wells. Blue arrows mark the direction of thickness increase, while the blue marked values correspond to the contour lines.

In Figure 69 the thickness of the interval between Top Cenomanian sandstone (Top CE1) and the maximum flooding surface is shown. Similar to the Bad Abbach member the interval decreases in its thickness in southwestern direction. The figure shows a remarkable thickness increase from SW to NE with thicknesses ranging from 4 to 16 m. In the eastern part of the study area thicknesses are generally decreased but slightly rise from NE to SW.

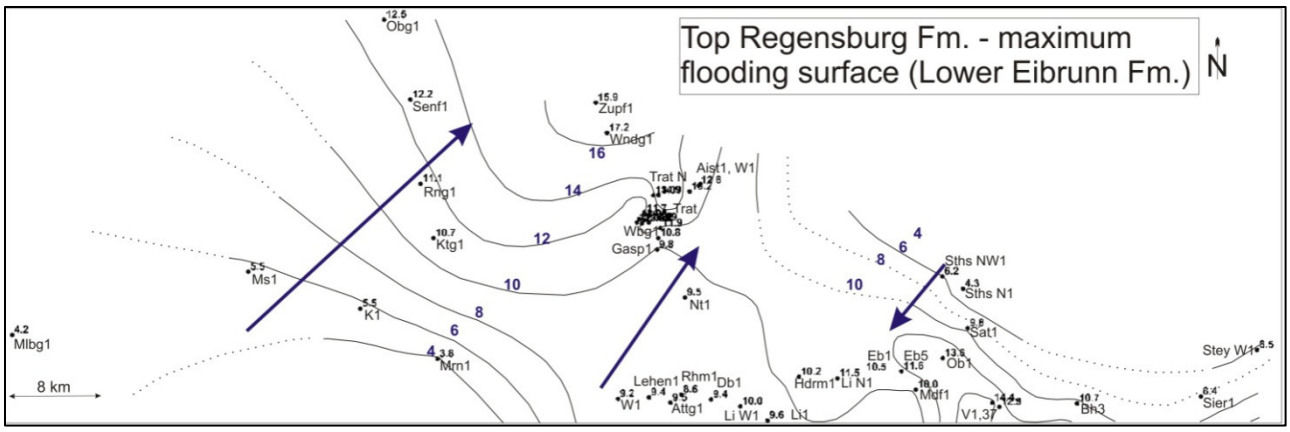

Figure 69: Hand-contoured map of the interval between Top Regensburg Fm. (top CE1) and the Lower Turonian Maximum Flooding Surface (Lower Eibrunn Fm.). Blue arrows mark the direction of thickness increase, while the blue marked values correspond to the contour lines.

5 Conclusion

The Cenomanian sandstones of the Upper Austrian Molasse Basin have been correlated and interpreted on the basis of well logs provided by Rohöl-Aufsuchungs AG (RAG). A subdivision into the Saal and Bad Abbach Member according to Niebuhr et al., 2009 has been accomplished. A maximum flooding surface in the Turonian marls has been interpreted and correlated for all wells. Additional total and spectral core gamma measurements on 30 respective wells complete the initial framework.

The lowermost Cenomanian strata corresponds to the Saal Member which is part of the Regensburg Formation. The lithostratigraphy comprises high energetic glauconitic sandstones deposited in a shallow marine environment. The provided gamma ray logs for this section demonstrate considerably increased values which apparently do not relate to the sonic responses. The result of the estimated spectral gamma measurements clarifies that the dominant amount of radioactive content primarily corresponds to Potassium and Thorium isotopes. Consequently the common link as grain size indicator has only restricted validity for the Upper Austrian Cenomanian sandstones since a majority of the Potassium relates to the high glauconite content. The high Thorium reading may relate to terrestrial sediments or heavy minerals. The sonic log is characterized by low velocities and often shows a continuous log response with low variability.

The investigated thickness map highlights a basinward thickness increase from NE to SW. The average thickness varies between 10 and 40 m. The Saal Member is in its thickness considerably decreased in the eastern area, where the crystalline basement of the Bohemian Massif is in its structurally almost highest position of the study area. A reasonable subdivision of the Saal Member in the western area, based on provided well logs is not possible, due to the highly differing log signature.

The Saal Member is overlain by lower energetic fine–silty, often calcareous sandstones of the Bad Abbach Member. Especially in the area of the Trattnach Field the prominent marker bed separates the Saal Member from the Bad Abbach Member, which was interpreted with the sonic or resistivity log. In contrast to the Saal Member the Bad Abbach Member is characterized by very low gamma log readings

and high velocities. The intervals comprising the highest velocities correspond to well cemented sandstones.

Similar to the Saal Member also the Bad Abbach Member illustrates a basinward thickness increase from NE to SW, showing thicknesses between 10 and 15 m. The Bad Abbach Member is in the southwestern area directly overlain by Eocene sandstones and often partly eroded.

The uppermost Cenomanian to Lower Turonian sediments correspond to the marlstones of the Eibrunn Formation. The succession is characterized by high gamma responses and very low velocities and were successfully interpreted and correlated for all wells in the study area.

The results demonstrate a remarkable thickness increase from SE to NW with thicknesses between 4 and 15 m from top Cenomanian to the maximum flooding surface. The main center of deposition is trending from NW to SE.

6 References

6.1 List of references

Andeweg, B., & Cloetingh, S. (1998). Flexure and unflexure of the North Alpine German-Austrian Molasse Basin: constraints from forward tectonic modelling. In A. Mascle, C. Puigdefabregas, H. P. Luterbacher, & M. Fernandez (eds.), Cenozoic Foreland Basins of Western Europe. Geological Society Special Publication, 134, 403-422.

Bachmann, G., Müller, M., & Weggen, K. (1987). Evolution of the Molasse Basin (Germany, Switzerland). Tectonophysics, 137, 77-92.

Bhattacharya, J. (1993). The expression and interpretation of marine flooding surfaces and erosional surfaces in core; examples from the Upper Cretaceous Dunvegan Formation, Alberta foreland basin, Canada. In H. Posamentier, C. Summerhayes, B. Haq, & P. Allen (eds.), Sequence Stratigraphy and Facies Associations. International Association of Sedimentologists, Special Publications, 18, 125-160.

Cant, D. (1992). Subsurface facies analysis. In R. G. Walker, & N. P. James, Facies Models: Response to Sea Level Change. Geological Association of Canada, GeoText, 1, 27-45.

De Ruig, J., & Hubbard, S. M. (2006). Seismic facies and reservoir characteristics of a deep-marine channel belt in the Molasse foreland basin, Puchkirchen Formation, Austria. AAPG Bulletin, 90, 735-752.

De Ruig, M. J. (2003). Deep Marine Sedimentation and Gas Reservoir Distribution in Upper Austria. Oil Gas European Magazine, 2, 64-73.

Fricke, S., & Schön, J. (1999). Praktische Bohrlochgeophysik, Enke, 254 pp.

Fuchs, G., & Matura, A. (1980). Die Böhmische Masse in Österreich. In R. Oberhauser, Der geologische Aufbau Österreichs. Vienna, Springer, 121-143.

Genser, J., Cloethingh, S. A., & Neubauer, F. (2007). Late orogenic rebound and oblique Alpine convergence: New constraints from subsidence analysis of the Austrian Molasse Basin. Global and Planetary Change, 58, 214-223.

Gratzer, R., Bechtel, A., Sachsenhofer, R. F., Linzer, H. -G., Reischenbacher, D., & Schulz, H. -M. (2011). Oil - oil and oil - source rock correlations in the Alpine Foreland Basin of Austria: Insights from biomarker and stable carbon isotope studies. Marine and Petroleum Geology, 28, 1171-1186.

Kley, J., & Voigt, T. (2008). Late Cretaceous intraplate thrusting in Central Europe: Effect of Africa-Iberia-Europe, not Alpine collision. Geology, 36, 839-842.

Kollmann, K. (1977). Die Öl- und Gasexploration der Molassezone Oberösterreichs und Salzburgs aus regionalgeologischer Sicht. Erdöl Erdgas Zeitschrift International Edition (Oil and Gas European Magazine), 93, 36-49.

Malzer, O., Rögl, F., Seifert, P., Wagner, L., Wessely, G., & Brix, F. (1993). Die Molassezone und deren Untergrund. In F. Brix, & O. Schultz (eds.), Erdöl und Erdgas in Österreich. Vienna: Naturhistorisches Museum Vienna and F. Berger, 281-358.

Nachtmann, W. (1995). Fault - Bounded Structures as Hydrocarbon Traps in the Upper Austrian Molasse Basin, Austria. Geolog. Paläont. Mitt. Innsbruck, 20, 221-230 .

Nachtmann, W. (1995). The Cenomanian beneath the upper Austrian Molasse basin - a reservoir - geological study. Zentralblatt für Geologie und Paläontologie, 1, 271-282 .

Nachtmann, W., & Wagner, L. R. (1987). Mesozoic and Early Tertiary evolution of the Alpine Foreland in Upper Austria and Slazburg, Austria. In A. Ziegler (ed.), Compressional Intra Plate Deformations in the Alpine Foreland, Tectonophysics, 137, 61-76.

Niebuhr, B., Pürner, T., & Wilmsen, M. (2009). Lithostratigraphie der außeralpinen Kreide Bayerns. Schriftenreihe der deutschen Gesellschaft für Geowissenschaften, 65, 7-58 .

Posamentier, H. W., & Vail, P. R. (1988). Eustatic controls on clastic deposition II - sequence and systems tract models. In C. K. Wilgus, B. S. Hastings, C. G. Kendall,

H. W. Possamentier, C. A. Ross, & J. C. Van Wagoner (eds.), Sea-level Changes: An Integrated Approach. Special Publication Society Economic Mineralogists Paleontologists Tulsa, 42, 125-154.

Posamentier, H. W., Jervey, M. T., & Vail, P. R. (1988). Eustatic controls on clastic deposition I - conceptual framework. In C. K. Wilgus, B. S. Hastings, C. G. Kendall, H. W. Possamentier, C. A. Ross, & J. C. Van Wagoner (eds.), Sea-level Changes: An Integrated Approach. Special Publication Society Economic Mineralogists Paleontologists Tulsa, 42, 109-124.

Roeder, B., & Bachmann, G. H. (1996). Evolution, structure and petroleum geology of the German Molasse Basin. In P. Ziegler, & F. Horvath (eds.), Peri-Tethys Memoir 2: Structure and Prospects of Alpine Basins and Forelands, Memoires Museum National d'Histoire Naturelle, Paris, 170, 263-284.

Sachsenhofer, R. F., Gratzer, R., Tschelaut, W., & Bechtel, A. (2006). Characterisation of non-producible oil in Eocene reservoir sandstones (Bad Hall Nord field, Alpine Foreland Basin, Austria). Marine and Petroleum Geology, 23, 1-15.

Sachsenhofer, R. F., Leitner, B., Linzer, H. G., Bechtel, A., Coric, S., Gratzer, R., et al. (2010). Deposition, Erosion and Hydrocarbon Source Potential of the Oligocene Eggerding Formation (Molasse Basin, Austria). Austrian Journal of Earth Sciences, 103, 76-99.

Schlumberger. (1996). Introduction to Openhole Logging Services, Schlumberger Educational Services.

Schulz, H.-M., Bechtel, A., Rainer, T., Sachsenhofer, R. F., & Struck, U. (2004). Paleoceanography of the western Central Paratethys during nannoplankton zone NP 23-the Dynow Marlstone in the Austrian Molasse Basin. Geologica Carpathica, 55, 311-323 .

Schulz, H.-M., Sachsenhofer, R. F., Bechtel, A., Polesny, H., & Wagner, L. (2002). The origin of hydrocarbon source rocks in the Austrian Molasse Basin (Eocene-Oligocene transition). Marine and Petroleum Geology, 19, 683-709.

Serra, O. & Serra, L. (2004). Well Logging. Vol. 1, Data Acquisition and Applications, Editions Technip, 688 pp.

Sissingh, W. (1997). Tectonostratigraphy of the North Alpine Foreland Basin: correlation of Tertiary depositional cycles and orogenic phases. Tectonophysics, 282, 223-256.

Steininger, F. F., Wessely, G., Rögl, F., & Wagner, L. (1988). Tertiary sedimentary history and tectonic evolution of the Eastern Alpine Foredeep. Giornale di Geologia, ser. 3°, 48, 285-297 .

Van Wagoner, J. C., Mitchum, R. M., Campion, R. M., & Rahmanian, V. D. (1990). Siliciclastic sequence stratigraphy in well logs, cores and outcrops: concepts for high - resolution correlation of time and facies. AAPG Methods in Exploration, 7, 55.

Veron, J. (2005). The Alpine Molasse Basin – Review of Petroleum Geology and Remaining Potential. Bulletin angewandte Geologie, 10, 75-86.

Wagner, L. R. (1996). Stratigraphy and hydrocarbons in the Upper Austrian Molasse Foredeep (active margin). In G. Wessely, & W. Liebl (eds.), Oil and Gas in the Alpidic Thrustbelts and Basins of Central and Eastern Europe, EAGE Special Publications, 5, 217-235.

Wagner, L. R. (1998). Tectono-stratigraphy and hydrocarbons in the Molasse Foredeep of Salzburg, Upper and Lower Austria. In A. Mascle, C. Puigdefàbregas, & H. P. Luterbacher (eds.), Cenozoic Foreland Basins of Western Europe. Geological Society London Special Publications, 134, 339-369.

Wagner, L. R., & Wessely, G. (1993). Molassezone Österreichs - Relief und Tektonik des Untergrundes. In F. Brix, & O. Schultz (eds.), Erdöl und Erdgas in Österreich. Vienna: Naturhistorisches Museum Vienna and F. Berger, 147-179.

Wallbrecher, E., Brandmayr, M., Handler, R., Loitzenbauer, J., & Dallmeyer, J. D. (1996). Konjugierte Scherzonen in der südlichen Böhmischen Masse. In H. Egger, T. Hofmann, & C. Rupp (eds.), Ein Querschnitt durch die Geologie Oberösterreichs, Exkursionsführer der Österreichischen Geologischen Gesellschaft, Wien, 12-28.

Wessely, G., Schreiber, O. S., & Fuchs, R. (1981). Lithofazies und Mikrostratigraphie der Mittel- und Oberkreide des Molasseuntergrundes im östlichen Oberösterreich. Jahrbuch Geologische Bundesanstalt, 124, 175-281.

Wilmsen, M., & Niebuhr, B. (n.d.). On the age of the Upper Cretaceous transgression between Regensburg and Neuburg an der Donau (Bavaria, southern Germany). N. Jb. Geolog. Paläont., 256, 267-278.

Wilmsen, M., Niebuhr, B., Chellouche, P., Pürner, T., & Kling, M. (2010). Facies pattern and sea-level dynamics of the early Late Cretaceous transgression: a case study from the lower Danubian Cretaceous Group (Bavaria, southern Germany), 56, 483-507.

Ziegler, P. A. (1987). Late Cretacceous and Cenozoic intra-plate compressional deformation in the Alpine foreland - a geodynamic model. Tectonophysics, 137, 389-402.

Ziegler, P. A. (1990). Geological Atlas of Western and Central Europe, 2nd ed. Shell Intern. Petrol. Maatschappij B.V, Den Haag, 239 pp.

Ziegler, P. A., Cloething, S., & Van Wees, J.-D. (1995). Dynamics of intra-plate compressional deformation: the Alpine Foreland and other examples. Tectonophysics, 252, 7-59.

6.2 List of figures

Figure 1: Geographic overview of the study area indicating position of the investigated wells. 8
Figure 2: Geologic map of the Molasse Basin in upper Austria indicating well positions (black squares) (modified after Sachsenhofer et al., 2010). 9
Figure 3: Geologic map of the Molasse Basin in Upper Austria indicating pre-Tertiary faults and the Central Swell Zone (modified after Nachtmann & Wagner, 1987) 11
Figure 4: Kinematic evolution in central Europe from Upper Cretaceous to Neogene times (after Kley & Voigt, 2008)..... 12
Figure 5: Geological cross-section indicating tectonic elements through the Austrian Molasse Basin (modified after Wagner 1996, De Ruig, 2006). 13
Figure 6: Schematic stratigraphic column illustrating the Mesozoic and Paleozoic sedimentary record of the western and eastern Upper Austrian Molasse Basin (modified after Malzer, 1993). 15
Figure 7: Pre-Cenozoic subcrop map in the Alpine Foredeep (modified after Wagner, 1998). 17
Figure 8: Paleogeography of the Cenomanian - Turonian in Central Europe (after Ziegler, 1990) with indication of the depositional area. 18
Figure 9: Stratigraphy of the Cenozoic sedimentary record in the Upper Austrian Molasse (modified after Wagner, 1998). 20
Figure 10: Gamma ray emission spectra of radioactive elements (after Serra 2004)..... 24
Figure 11: Sonic log device (tool with two receivers), illustrating the principle for measuring the interval time (after Serra, 2004)..... 26
Figure 12: Microlaterolog measurement principle (left) and hydraulic pad (right) (after Schlumberger, Serra, 2004) 28
Figure 13: Microspherically focused logsonde (left) including pad and caliper arms, distribution (middle) and electrode arrangement device (right) (after Serra, 2004) 29
Figure 14: Example of a lithology recorded by S. Schnitzer. 29
Figure 15: Gamma Surveyor (GF Instruments)..... 32
Figure 16: Example of rescaled and depth shifted core gamma log (Wendling 1). Red line: core gamma log (CGR); green line: well gamma log (GR). First column: original CGR and GR log, second column: CGR log after rescaling, third column: rescaled and depth shifted (squeezed) CGR log. 33
Figure 17: Example for SGR log rescaling for well Trattnach 7. 34
Figure 18: Base map indicating wells (marked in green) that have been measured with the Gamma Surveyor..... 35
Figure 19: Trattnach 6 well logs and shifted CGR, SCGR logs and core interpretation. Porosity (green) and permeability (blue) data overlie in the third column the core interpretation (Schnitzer). 37
Figure 20: Trattnach 7 well logs and shifted CGR, SCGR logs and core interpretation. Porosity (green) and permeability (blue) data overlay in the third column the core interpretation (Schnitzer). 39
Figure 21: Trattnach 8 well logs and shifted CGR, SCGR logs and core interpretation. Porosity (green) and permeability (blue) data overlay in the third column the core interpretation (Schnitzer). 41

Figure 22: Trattnach 1well logs and shifted CGR, SCGR logs and porosity and permeability data. Porosity (green) and permeability (blue) data are illustrated in the third column. 43
Figure 23: Trattnach 12 well logs and shifted CGR, SCGR logs and core interpretation. Porosity (green lines) and permeability (blue points) data overlay in the third column the core interpretation (Schnitzer)..... 45
Figure 24: Desselbrunn 1 well logs and core interpretation (Schnitzer). 47
Figure 25: Eberstalzell 1 well logs and shifted CGR, SCGR and core interpretation (Schnitzer)..... 48
Figure 26: Haidermoos 1 well logs and shifted CGR, SCGR and core interpretation (Schnitzer). 50
Figure 27: Hoergersteig 1 well logs and shifted CGR and SCGR logs. 52
Figure 28: Kemating 1 well logs and shifted CGR, SCGR logs and core interpretation (Schnitzer)..... 54
Figure 29: Kirchham 3 well logs and shifted CGR, SCGR logs and core interpretation (Schnitzer)..... 56
Figure 30: Lindach 1 well logs and shifted CGR and SCGR log. 58
Figure 31: Maria Schmolln 1well logs and shifted CGR, SCGR log and core interpretation (Schnitzer). Apparently 2 core boxes at approximately 2248 m MD have not been interpreted. 59
Figure 32: Mauern 1 well logs and shifted CGR, SCGR log and core interpretation (Schnitzer). 61
Figure 33: Mayersdorf 1 well logs and shifted CGR, SCGR and MLL log. 62
Figure 34: Nieder-Thalheim 1 well logs and shifted CGR, SCGR log and core interpretation (Schnitzer)..... 64
Figure 35: Oberaustall 1 well logs and shifted CGR, SCGR and MINV log. 65
Figure 36: Oelling 1 well logs and shifted CGR, SCGR log and core interpretation. 67
Figure 37: Redltal 1 well logs and shifted CGR, SCGR log and core interpretation (Schnitzer). 69
Figure 38: Renging 1 well logs and shifted CGR, SCGR log. 71
Figure 39: Sattledt 1 well logs and shifted CGR, SCGR logs and core interpretation (Schnitzer)..... 72
Figure 40: Schwanenstadt 3 well logs and shifted CGR, SCGR logs and core interpretation (Schnitzer)..... 73
Figure 41: Steinhaus N1 well logs and shifted CGR, SCGR log and core interpretation (Schnitzer). .. 75
Figure 42: Steinhaus NW1 well logs and shifted CGR, SCGR log and core interpretation (Schnitzer).76
Figure 43: Steyr W1 well logs and shifted CGR, SCGR logs and core interpretation (Schnitzer). 77
Figure 44: Voitsdorf 1 well logs and shifted CGR, SCGR log and core interpretation (Schnitzer). 79
Figure 45: Wendling 1 well logs and shifted CGR, SCGR log. 80
Figure 46: Wolfersberg 1 well logs and shifted CGR, SCGR log. 82
Figure 47: Base map indicating Cenomanian well log correlation profiles in the Upper Austrian Molasse Basin..... 83
Figure 48: Type well log Trattnach 7 with rescaled and shifted CGR and CSGR curves. The third column includes the core description and also overlain Porosity and Permeability data. 84
Figure 49: Trattnach N-S well log correlation profile flattened on the maximum flooding surface (blue line). Black arrows describe the fining upward until maximum relative sea level rise. Prominent well log correlation patterns are marked in red..... 86
Figure 50: Well Logs of Trattnach 6. 87

Figure 51: Core-log cross section for the wells Trattnach 6,7,8 and 12 highlighting laterally traceable geometries. Top CE2 has been used as fixed Datum hence it occurs in all cored intervals. Cross section is located in Figure 48. Core descriptions have been provided by Schnitzer. 88
Figure 52: Well Log Correlation Profile NW – SE 1 flattened on the maximum flooding surface. 90
Figure 53: Well Log Correlation Profile NW – SE2 flattened on the maximum flooding surface. 92
Figure 54: Well Log Correlation Profile NW – SE3 flattened on the maximum flooding surface. 93
Figure 55: Well Log Correlation Profile W – E1 flattened on base Cenomanian. 94
Figure 56: Well Log Correlation Profile W - E2 flattened on the maximum flooding surface. 95
Figure 57: Well Log Correlation Profile W – E flattened on the maximum flooding surface (mfs; where present). 96
Figure 58: Base Map indicating log facies groups of the study area. The green marked groups relate to wells, where the Cenomanian sandstones are overlain by Turonian sediments. The orange areas mark wells, where the Cenomanian sandstones are overlain by Eocene strata. 97
Figure 59: Log facies E1 flattened on the maximum flooding surface. 98
Figure 60: Log facies E2 flattened on the maximum flooding surface. 99
Figure 61: Log facies E3 flattened on top Cenomanian 100
Figure 62: Log facies N1 flattened on the maximum flooding surface. 101
Figure 63: Log facies N2 flattened on the maximum flooding surface. 102
Figure 64: Log facies S1 flattened on the maximum flooding surface. 103
Figure 65: Log facies S2 flattened on base Cenomanian (digitized RAG core reports are not depth shifted). 104
Figure 66: Log facies W2 flattened on base Cenomanian (digitized RAG core reports are not depth shifted). 105
Figure 67: Hand-contoured map of the thickness of the Saal Mameber (CE3 + CE2) constrained by shown wells. Blue arrows mark the direction of thickness increase, while the blue marked values correspond to the contour lines in [m]..... 106
Figure 68: Hand-contoured map of the thickness of the Bad Abbach Member (CE1) constrained by indicated wells. Blue arrows mark the direction of thickness increase, while the blue marked values correspond to the contour lines. 107
Figure 69: Hand-contoured map of the interval between Top Regensburg Fm. (top CE1) and the Lower Turonian Maximum Flooding Surface (Lower Eibrunn Fm.). Blue arrows mark the direction of thickness increase, while the blue marked values correspond to the contour lines. 108

6.3 List of tables

Table 1: List of the most important well logs available for the study area. Stated depths refer to measured depth in meters. Boxes marked with x document, that the log trace is not limited to the Upper Cretaceous. 22
Table 2: Wells for which RAG provided geological short profiles and/or completion logs 30
Table 3: CGR, SCGR and core log depth shift of well Trattnach 6 core 1 and 2. 38
Table 4: CGR, SCGR and core log depth shift of well Trattnach 7 core 1 and 2. 40
Table 5: CGR, SCGR and core log depth shift of well Trattnach 8 core 1 and 2. 42
Table 6: CGR and SCGR log depth shift of well Trattnach 1 core2. 44
Table 7: CGR, SCGR and core log depth shift of well Trattnach 12 core 1. 46
Table 8: CGR, SCGR and core log depth shift for well Eberstalzell 1 core 4 and 5. 48
Table 9: CGR, SCGR and core log depth shift for well Haidermoos 1 core 5 and 6. 51
Table 10: CGR and SCGR log depth shift for well Hoergersteig 1 core 2, 3 and 4. 53
Table 11: CGR, SCGR and core log depth shift for well Kemating 1 core 5 and 6. 55
Table 12: CGR, SCGR and core log depth shift of well Kirchham 3 core 2 and 3. 57
Table 13: CGR and SCGR log depth shift of well Lindach 1 core 6, 7, 8 58
Table 14: CGR, SCGR and core log depth shift of well Maria Schmolln 1 core 5 and 6. 60
Table 15: CGR, SCGR and core log depth shift of well Mauern 1 core 4. 62
Table 16: CGR, SCGR, core and MLL log depth shift of well Mayersdorf 1 63
Table 17: CGR, SCGR and core log depth shift of well Nieder Thalheim 1 65
Table 18: CGR, SCGR and core log depth shift of well Oberaustall 1 core 3, 4, 5 and MINV log. 66
Table 19: CGR, SCGR and core log depth shift of well Oelling 1 core 1 and 2. 67
Table 20: CGR, SCGR and core log depth shift of well Redltal 1 core 4, 5 and 6. 68
Table 21: CGR, SCGR log depth shift of well Renging 1 core 3. 70
Table 22: CGR, SCGR and core log depth shift of well Sattledt 1 core 2. 72
Table 23: CGR, SCGR and core log depth shift of well Schwanenstadt 3 core 6 and7. 74
Table 24: CGR, SCGR and core log depth shift of well Steinhaus N1 core 2. 75
Table 25: CGR, SCGR and core log depth shift of well Steinhaus NW1 core 2. 76
Table 26: CGR, SCGR and core log depth shift of well Steyr W1 core 2. 78
Table 27: CGR, SCGR and core log depth shift of well Voitsdorf 1 core 7, 8, 10 and 11. 80
Table 28: CGR, SCGR log depth shift of well Wendling 1 core 1 and 2. 81
Table 29: CGR, SCGR log depth shift of well Wolfersberg 1 core 4. 81